U.S. DEPARTMENT OF
ENERGY

PNNL-19122

Prepared for the U.S. Department of Energy
under Contract DE-AC05-76RL01830

Review of Potential Candidate Stabilization Technologies for Liquid and Solid Secondary Waste Streams

EM Pierce	RJ Serne	W Um
SV Mattigod	JP Icenhower	NP Qafoku
JH Westsik, Jr.	RD Scheele	

January 2010

Pacific Northwest
NATIONAL LABORATORY

Proudly Operated by Battelle Since 1965

DISCLAIMER

PACIFIC NORTHWEST NATIONAL LABORATORY
operated by
BATTELLE MEMORIAL INSTITUTE
for the
UNITED STATES DEPARTMENT OF ENERGY
under Contract DE-AC05-76RL01830

Printed in the United States of America

Available to DOE and DOE contractors from the
Office of Scientific and Technical Information,
P.O. Box 62, Oak Ridge, TN 37831-0062;
ph: (865) 576-8401
fax: (865) 576-5728
email: reports@adonis.osti.gov
Available to the public from the National Technical Information Service,
U.S. Department of Commerce, 5285 Port Royal Rd., Springfield, VA 22161
ph: (800) 553-6847
fax: (703) 605-6900
email: orders@ntis.fedworld.gov

online ordering: http://www.ntis.gov/ordering.htm

PNNL-19122

Review of Potential Candidate Stabilization Technologies for Liquid and Solid Secondary Waste Streams

EM Pierce
SV Mattigod
JH Westsik, Jr.
RJ Serne
JP Icenhower
RD Scheele
W Um
NP Qafoku

January 2010

Prepared for
the U.S. Department of Energy
under Contract DE-AC05-76RL01830

Pacific Northwest National Laboratory
Richland, Washington 99352

Executive Summary

Pacific Northwest National Laboratory has initiated a waste-form testing program to support the long-term durability evaluation of a waste form for secondary wastes generated from the treatment and immobilization of Hanford radioactive tank wastes. The purpose of the work discussed in this report is to identify candidate stabilization technologies and getters that have the potential to successfully treat the secondary waste stream liquid effluent, mainly from off-gas scrubbers and spent solids, produced by the Hanford Tank Waste Treatment and Immobilization Plant (WTP). Down-selection to the most promising stabilization processes/waste forms is needed to support the design of a solidification treatment unit (STU) to be added to the Effluent Treatment Facility (ETF). To support key decision processes, an initial screening of the secondary liquid waste forms must be completed by February 2010. Later, more comprehensive and longer term performance testing will be conducted, following the guidance provided by the secondary waste-form selection, development, and performance evaluation roadmap. The resulting waste form will be compliant to regulations and performance criteria and will lead to cost-effective disposal of the secondary wastes.

This report starts with a brief review of some of the most commonly used solidification formulations that would be candidates for secondary liquid waste streams. In this review, the available data on performance are discussed, and some preliminary recommendations are provided for materials that should undergo additional screening testing. We also 1) discuss options for disposal of WTP secondary solid waste streams, 2) provide a brief overview of standard regulatory test methods used for measuring contaminant leachability and waste-form physical strength (with emphasis on the U.S. Environmental Protection Agency's [EPA's] new methods as a screening tool for comparing waste solidification materials of interest), and 3) provide an overview of factors that must be considered in long-term performance testing, including state-of-the-art characterization tools that can provide the data needed to technically defend predictive modeling simulations of long-term material behavior. The long-term waste-form testing and solid and leachate characterization must be robust enough to effectively predict material performance in the Integrated Disposal Facility over the 10,000-year period of performance for the engineered system.

The solidification technologies for liquid waste streams include cement/grout, containerized Cast Stone, phosphate-bonded ceramics, alkali-aluminosilicate geopolymers, hydroceramics, L-TEM, and fluidized-bed steam reforming (FBSR). In addition to these, other mature technologies and two compounds, namely goethite and sodalite (that are still being developed), that show considerable promise as waste forms or getters are also discussed. It is our recommendation, based upon the available literature, that Cast Stone, chemically bonded phosphate ceramics (Ceramicrete), alkali-aluminosilicate geopolymers (Duralith), and FSBR should be considered for further testing and evaluation for the baseline addition of an STU with the ETF evaporator. The FBSR product in an encapsulation matrix is another viable waste form that warrants further testing and evaluation. Recent results on the performance of the FBSR process with simulated secondary waste indicate that the higher processing temperature does not impact the capability of the FBSR product to incorporate Cs, Re (chemical analogue for ^{99}Tc), and ^{129}I in the matrix. For geothite and sodalite, we recommend that these materials continue being evaluated either as a waste form or getter with separate applied research funding from the U.S. Department of Energy Office of Environmental Management's Office of Engineering and Technology in FY10. For proprietary materials, such as L-TEM, we recommend that a process be developed to solicit additional information from industry through a Request for Information process.

Low-temperature alkali-aluminosilicate hydroceramics do not appear to be a viable waste form for the liquid secondary wastes. The challenge for hydroceramics is associated with obtaining the needed physical strength for a disposal system without having to process the material at high temperatures. The first step in the process of forming the hydroceramic material consists of mixing the liquid waste with metakaolin and/or a reducing agent and calcining the mixture at 500 to 700°C (Bao et al. 2004, 2005). Calcination at these temperatures would volatilize ^{99}Tc or ^{129}I, thereby reducing the concentration of these contaminants in the waste form and creating yet another waste stream for treatment. Similar reasons exclude vitrification as a suitable waste form to sequester ^{99}Tc or ^{129}I.

Getters have been deployed in two modes to immobilize and retard contaminant release. In this report, we provide a detailed comparison of the sorption capacity (K_d) for various getters for iodide (in some cases also iodate) and for pertechnetate. Based on existing test data, the most promising getters that need additional evaluation include layered bismuth hydroxides, argentite, silver-impregnated carbon, and Ag-zeolites as iodide and iodate getters. Goethite, sodalite, nanoporous tin phosphates, Sn(II) treated apatite, nano zero-valent iron, and ground-blast-furnace slag (BFS) were identified as Tc getters. The BFS is part of the base mix for both Savannah River Site Saltstone and Hanford Cast Stone cementitious formulations.

In addition to stabilization options for the liquid waste stream, WTP is expected to produce several solid wastes that are also a part of the secondary waste stream. The solid wastes considered most hazardous and challenging for disposal include sulfur-impregnated activated carbon that is to be used for controlling gaseous mercury emissions, ^{137}Cs-laden spent ion exchange resin (resorcinol-formaldehyde resin), and reduced-silver mordenite (Ag^0Z) to control ^{129}I emissions from the WTP. Several options appear suitable for disposal of WTP’s mercury-containing activated carbon waste. These options are direct disposal without treatment, solidification or stabilization in Portland cement, and encapsulation in chemically bonded phosphate ceramic. Disposal of silver mordenite (Ag^0Z) is extremely challenging because of the mixture of both silver and ^{129}I. Four methods of stabilizing the material have been discussed in the literature: 1) a sintered metal and ceramic, 2) a glass, 3) iodo-apatites and 4) cements. Currently, it is unclear which of these three options represents the most suitable choices for disposal. For spent ion exchange resins, direct disposal in either steel canisters or within high-integrity containers that are placed within concrete boxes is a suitable disposal path.

Specific test methods to screen candidate liquid stabilization options are needed, and they need to provide a framework to 1) rapidly assess material performance, 2) provide some indication of the dominant release mechanism for specific contaminants of concern, 3) evaluate the strengths and weaknesses of a variety of materials (placing each material on a level playing field), and 4) gain regulatory acceptance by drawing on standard test methods approved by the regulatory community. To address these test needs, four draft test protocols being developed for EPA will be used to screen each of the down-selected stabilization technologies. These results, coupled with geochemical modeling and with targeted chemical and solid phase characterization to identify pre- and post-test solid phases, should further narrow the set of candidate waste forms for investigation.

After completing the down-select process, the next phase of the waste-form testing program for selected stabilization technologies is performance testing in support of the Integrated Disposal Facility performance assessment. Performance testing provides model parameters that explain the key processes in contaminant release, in some cases accelerating the weathering process to obtain the data needed in a practical time frame. These experiments must provide the parameters needed for the model(s) so that

calculations yield credible performance and contaminant release results for various geological conditions over ~10,000 years. In this report, we provide a brief overview of performance testing and discuss the characterization techniques that can be used to identify and describe the processes controlling waste-form weathering or other mechanisms of contaminant release.

Acronyms and Abbreviations

AA	atomic absorption (spectroscopy)
ANS	American Nuclear Society
ANSI	American National Standards Institute
ASTM	American Society for Testing and Materials
BET	Brunauer-Emmett-Teller
BFS	blast furnace slag
CBPC	chemically bonded phosphate ceramic
CCD	charge-coupled device
CCS	Containerized Cast Stone
CD	Critical Decision
CEC	Cation Exchange Capacity
COC	contaminants of concern
C-S-H	hydrous calcium and silica-rich gel
DI	de-ionized (water)
DOE	U.S. Department of Energy
Ecology	Washington State Department of Ecology
EDA	ethylene di-amine
EDS	energy dispersive spectrometry
EM	U.S. Department of Energy Office of Environmental Management
EPA	Environmental Protection Agency
ETF	Effluent Treatment Facility
EXAFS	extended X-ray absorption fine structure
FBSR	fluidized-bed steam reformation
FTIR	Fourier transform infrared spectroscopy
FY	fiscal year
HEPA	high-efficiency particulate air
HF	hydrogen fluoride
HIC	high-integrity container
HLW	high-level waste
HSAB	hard and soft acid and base
IC	ion chromatography
ICP-AES	inductively coupled plasma-atomic emission spectroscopy
ICP-MS	inductively coupled plasma-mass spectroscopy
ICP-OES	inductively coupled plasma-optical emission spectroscopy

IDF	Integrated Disposal Facility
ILAW	immobilized low-activity waste
INEEL	Idaho National Engineering and Environmental Laboratory
IZA	International Zeolite Association
KOH	potassium hydroxide
LAW	low-activity waste
LBH	layered bismuth hydroxides
LBNL	Lawrence Berkeley National Laboratory
LDH	layered double hydroxide
LERF	Liquid Effluent Retention Facility
LI	Leachability Index
LLW	low-level waste
MAS	magic-angle spinning
MDL	minimum detection limit
MKP	MgO and KH_2PO_4
MS	mass spectroscopy
NMR	nuclear magnetic resonance
NRC	U.S. Nuclear Regulatory Commission
OE&T	Office of Engineering and Technology (Department of Energy)
OPC	ordinary Portland cement
ORP	US Department of Energy Office of River Protection
PCT	product consistency test
PNNL	Pacific Northwest National Laboratory
PUF	pressurized unsaturated flow apparatus
PUREX	plutonium uranium extraction
PZC	point of zero charge
RCRA	Resource Conservation and Recovery Act
RS	Raman spectroscopy
S/S	stabilization and solidification
SAMMS	self-assembled monolayers on meso-porous silica
SAXS	small-angle X-ray scattering
SBW	sodium-bearing waste
SEM	scanning electron microscopy
SPFT	single-pass flow-through
SRNL	Savannah River National Laboratory
SRS	Savannah River Site

SSRL	Stanford Synchrotron Radiation Laboratory
STEM	scanning transmission electron microscopy
STU	Solidification Treatment Unit
TCLP	Toxicity Characteristics Leaching Procedure
TEM	transmission electron microscopy
THOR	Thermal Organic Reduction
TRU	transuranic
UTS	Universal Treatment Standard
VSI	vertical scanning interferometry
WRPS	Washington River Protection Solutions, LLC
WTP	Hanford Tank Waste Treatment and Immobilization Plant
XANES	X-ray absorption near-edge spectroscopy
XAS	X-ray absorption spectroscopy
XMT	X-ray micro tomography
XPS	X-ray photoelectron spectroscopy
XRD	X-ray diffraction
XRF	X-ray fluorescence

Contents

Figures

Tables

1.0 Introduction

The federal facilities located on the Hanford Site in southeastern Washington State have been used extensively by the U.S. government to produce nuclear materials for the U.S. strategic defense arsenal. Currently, the Hanford Site is under the stewardship of the U.S. Department of Energy (DOE) Office of Environmental Management (EM). A large inventory of radioactive and mixed waste, resulting from the production of nuclear materials, has accumulated, mainly in 177 underground single- and double-shell tanks located in the central plateau of the Hanford Site (Mann 2002). The DOE EM Office of River Protection (ORP) is proceeding with plans to permanently dispose of the liquid and solid wastes contained in the tanks. Pacific Northwest National Laboratory (PNNL)(a) was contracted to initiate a waste-form testing program to support the evaluation of the long-term durability of a waste form for the solidification of secondary wastes generated from the treatment and immobilization of Hanford radioactive tank wastes.

1.1 Overview—Disposal of Hanford Tank Wastes

Under the Office of River Protection (ORP) Hanford tank waste disposal plans, liquid and solid wastes will first be retrieved from the tanks and transferred to preprocessing facilities at the Hanford Tank Waste Treatment and Immobilization Plant (WTP). In the pretreatment facility, the sludges (insoluble material) will be washed and the liquids processed to generate a high-level waste (HLW) fraction and a low-activity waste (LAW) fraction. The HLW fraction will contain the bulk of the radionuclides, in particular the actinides. The low-activity fraction will contain predominately inactive sodium and aluminum from LAW processing and ^{99}Tc as the major radionuclide. Both waste streams will be converted to glass at vitrification facilities in the WTP. The LAW fraction is destined to be disposed of on the Hanford Site in the Integrated Disposal Facility (IDF) (Ecology et al. 1989) and the HLW fraction will be transferred to a proposed HLW repository, previously Yucca Mountain. In addition to the vitrified HLW and immobilized LAW (ILAW) glass, the waste processing steps being implemented at WTP will generate secondary wastes that must be processed, stabilized, and disposed of in IDF.

The secondary wastes that will be generated from processing tank wastes include routine solid wastes and liquid process effluents. Because ^{99}Tc and ^{129}I will volatilize when exposed to the high processing temperatures used to produce glass, the solid and liquid secondary waste streams are expected to contain a portion of the total technetium (^{99}Tc) and iodine (^{129}I) inventory. Solid wastes from the waste treatment facilities may include failed equipment, decontamination wastes, high-efficiency particulate air (HEPA) filters, carbon absorption beds, silver mordenite iodine sorbent beds, and spent ion-exchange resin. Liquid wastes may include process condensates and scrubber and/or off-gas treatment liquids from the thermal waste treatment processes. After packaging, the solid secondary wastes will be sent to the IDF for disposal. The liquid-effluent secondary wastes will be sent to the Effluent Treatment Facility (ETF) for further treatment and disposal, either as treated liquid effluents under the ETF State Wastewater Discharge Permit or as solidified liquid effluents under the Dangerous Waste Permit for disposal at the IDF.

(a) Pacific Northwest National Laboratory is operated for the U.S. Department of Energy by Battelle under Contract DE-AC05-76RL01830.

The ETF is a Resource Conservation and Recovery Act (RCRA)-permitted multi-waste treatment and storage unit that can accept dangerous, low-level, and mixed wastewaters for treatment. The ETF receives liquid effluents from cleanup projects on the Hanford Site, which are disposed of after being treated. Currently, ETF supports the 242-A Evaporator, Mixed Waste Burial Trench, and Environmental Restoration Disposal Facility leachates, groundwater treatment projects, and other decontamination and decommissioning projects. The liquid effluents are treated to remove toxic metals, radionuclides, and ammonia and to destroy organic compounds. Plans are to increase the capacity of ETF to process the increased volume of secondary wastes when the WTP begins waste treatment and immobilization operations (Koci 2005). A Solidification Treatment Unit (STU) will be added to the ETF to provide the needed additional capacity. The current baseline calls for solidification of the ETF evaporator concentrate in a cement-based waste form. The cement will be cast into 4-ft × 4-ft × 4-ft cubes for curing, storage, and disposal.

Washington River Protection Solutions (WRPS) has been chartered to move forward with the design and construction of the STU for ETF. The STU needs to be operational by 2018 to receive secondary liquid wastes from the WTP. The schedule of activities requires Critical Decision 0 (CD0) in early 2010, CD1 on the approach by mid-2011, and CD3 to authorize construction by 2014/2015. There will be a formal decision on the waste form for the secondary liquid wastes, including agreement with the Washington State Department of Ecology (Ecology), by 2012. To support CD0, an initial screening of the secondary liquid waste forms must be completed by February 2010.

Significant uncertainties are associated with the processing of these secondary wastes, and in 2008, the DOE Office of Engineering and Technology (OE&T) sponsored a meeting to develop a roadmap to outline the steps necessary to design the secondary waste forms. At the highest level, the secondary waste roadmap includes elements addressing regulatory and performance requirements, waste composition, preliminary waste-form screening, waste-form development, process design and support, and validation. The regulatory and performance requirements activity will provide the secondary waste-form performance requirements. The waste-composition activity will provide workable ranges of secondary waste compositions and formulations for simulants and surrogates. Preliminary waste-form screening will identify candidate waste forms for immobilizing the secondary wastes. The waste-form development activity will mature the waste forms, leading to a selected waste form(s) with a defensible understanding of the long-term release rate and input into the critical decision process for a secondary waste treatment process and/or facility. The process and design support activity will provide a reliable process flowsheet and input to support a robust facility design. The validation effort will confirm that the selected waste form meets regulatory requirements. The final outcome of the implementation of the secondary waste roadmap is the compliant, effective, timely, and cost-effective disposal of the secondary wastes.

1.2 Purpose and Scope

The purpose of PNNL's work documented in this report is to identify candidate stabilization technologies and getters that have the potential to successfully treat liquid effluent and spent solids produced by the WTP as part of the secondary waste stream. One additional objective of the work reported here is to identify existing gaps in the data needed to support a decision-making process to identify a subset of the candidate waste forms that are most promising and that should be moved forward for future development and performance testing. In addition to describing the stabilization of the liquid and solid waste streams, we also 1) discuss options for treating the solid waste streams and potential disposal pathways, 2) provide a brief overview of standard regulatory test methods, highlighting the U.S. Environmental Protection Agency's (EPA's) new methods as a screening tool for each of the waste-solidification materials of interest, and 3) provide an overview of factors that must be considered when it comes to performance testing and the state-of-the-art science tools that can be used to provide the defense-in-depth needed to address key uncertainties. Simulations that are robust enough to effectively predict material performance in the IDF performance assessment need to be conducted. The waste-form testing program needs to be developed over fiscal year 2010, and the performance baseline needs to be changed as needed to reflect the emerging program details.

1.3 Report Contents and Organization

The ensuing sections of this report document a literature review conducted to identify candidate waste forms and data on those waste forms to support a screening and selection process for a waste form for the solidification of secondary wastes generated from the WTP. Sections 2.0 and 3.0 describe liquid and solid waste-form options, respectively. Section 4.0 describes stabilization technology regulatory and screening tests, i.e., regulatory test methods performed to provide data for screening potential secondary waste-stabilization technologies. Section 5.0 describes 1) performance testing related to the quantification of the rate and extent of element or contaminant release from secondary waste forms and 2) characterization techniques that can be used for leachate solution and solid sample analyses of secondary wastes forms. Relevant technologies for waste-form analysis and characterization are described in Appendix A.

2.0 Liquid Waste Stabilization Options

Several candidate waste forms, getters, and waste-form/getter combinations can be used to stabilize the secondary liquid waste being produced by WTP. These include cement/grouts, chemically bonded phosphate ceramics, alkali aluminosilicate hydroceramic, alkali-aluminosilicate geopolymers, geothite, L-TEM, and sodalite as described in the following sections.

2.1 Waste Forms

Table 2.1 provides a list of binders that are or have been used to stabilize and solidify wastes (Spence and Shi 2005). The reader is directed to Spence and Shi's book for details on the various waste forms listed. The literature review conducted here focuses on recent work with direct relevance to the secondary wastes from the WTP. The information discussed in this section is not intended to be exhaustive, but rather provides a brief overview of candidate stabilization materials and identifies the performance data, if any, that currently exist for each waste-form type. Each of the materials discussed are at different levels along the technology maturation pathway, and as a result, the amount of available information for each technology varies.

Table 2.1. Binders Used for Stabilization and Solidification (Spence and Shi 2005)

Inorganic Binder Systems	Organic Binder Systems
Portland cement	Bitumen
Portland slag cement	Urea formaldehyde
Portland pozzolan cement	Polybutadiene
Portland cement-silicate system	Polyester
Polymer-modified cement	Epoxy
Masonry cement	Polyethylene
Lime-pozzolan cement	
Calcium aluminate cement	
Alkali-activated slag cement	
Alkali-activated pozzolan cement	
Phosphates	
Gypsum	
Sulfur polymer cement	
Alkali silicate minerals	

2.1.1 Cement and/or Grout

According to Spence and Shi (2005), stabilization and solidification with cements is the most widely used method for treating hazardous wastes. Cements also have the advantage that their chemistry can be easily modified to include getters for the hazardous-waste constituents to further reduce their mobility. Few anthropogenic materials have undergone scientific scrutiny comparable to that of cement and grout. Types of cementitious materials have been used since antiquity, especially in the era of the Roman Empire, and because of their commonplace use in time and space, a great deal of data on the physical and chemical durability of the materials has been recorded. Numerous review articles and more focused papers have been written, and the following summary is abstracted from selected sources (Lukens et al. 2003, Pabalan et al. 2009, Young et al. 1995).

Grout consists mainly of calcium, aluminum, and silicon oxides produced during high-temperature heating of impure limestone or marble. The high temperature results in partial melting of the material, with the glassy portion designated as “clinker.” The clinker is cooled, crushed, and mixed with other reactive materials (e.g., clay, gypsum, and pozzolans). When the dry material is “slaked” with water, the bonds of the original material break and re-form to stabilize new compounds that are typically hydrous. The chemical reactions are strongly exothermic in character (i.e., they liberate heat), causing the material to heat up. Volume changes accompany the heating, although not all of the resulting swelling is temperature induced. As the grout sets, a group of characteristic phases forms. The cardinal phases include portlandite ($Ca(OH)_2$), ettringite ($Ca_6Al_2(SO_4)_3(OH)_{12}{\bullet}26H_2O$), and a hydrous calcium and silica-rich gel called C-S-H. Both portlandite and ettringite are rarely found in nature and are manifested mainly in unusual contact with metamorphosed impure limestones or shallow to extrusive igneous rocks. Portlandite has been studied for decades, and a fairly detailed set of information has been collected on this phase. In contrast to the well-studied portlandite, the properties of ettringite are less well known. The formation of ettringite is essential because its presence prevents the rapid heating and setting of grout. Without the formation of ettringite, any excess water added to the cement powder would boil because of the vigor of the chemical reaction. The “glue” that binds together the crystalline phases of the grout is the C-S-H gel. Defining the composition and structure of C-S-H has been difficult because it is amorphous to nano-crystalline in its properties with some attendant variability in chemistry and the nature of the associated water. Roughly speaking, the formation of C-S-H is due to the following reaction:

$$2CaSiO_5 + 7H_2O \rightleftarrows 3CaO{\bullet}2SiO_2{\bullet}4H_2O + 3Ca\ \ OH\ \ _2 + 174\ \text{kJ} \qquad (1.1)$$

Examining the C-S-H phase with scanning electron microscopy (SEM) or X-ray diffraction (XRD) methods reveals that the structure is mainly amorphous, except for some thin flakes or dendrils and fibrils (Diamond and Kjellsen 2006). Recent neutron-scattering experiments showed that the water molecules are bound in a variety of different ways, but no clear consensus emerged regarding the state of “typical” water. The hydrous and amorphous nature of the C-S-H phase renders it reactive, and the gel continues to react with other phases in grout over many years.

The amorphous structure and chemical variability of the C-S-H phase renders it difficult to characterize thermodynamically. Therefore, defining the thermodynamic stability of cement/grout is difficult. The stability of portlandite, in contrast, is well-known with respect to calcite and dolomite, with a favorable free-energy of formation of carbonate minerals because of the reaction between portlandite and atmospheric or dissolved CO_2. Degradation of grout through carbonation is a major mechanism that affects cement performance, as discussed further below.

Radioactive elements added to grout typically do not partition into the typical grout phases. For example, ^{99}Tc, ^{129}I, and ^{137}Cs are thought to reside in the space between solid phases, but ^{90}Sr can substitute for calcium in the various calcium-rich minerals and C-S-H gel. Accordingly, the former elements are more vulnerable to release into aqueous solutions that may enter into the waste form from outside of the disposal system, causing them to be more easily leached (Bao et al. 2005). For this reason, many investigators suggest that mechanisms governing the release of radionuclide elements from grout are rate-limited by their diffusion through interconnected pores in the grout.

A large body of work has been conducted on the physical and chemical durability of cement, and the interested reader is directed to the review conducted by Pabalan et al. (2009a). More pertinent to the present work is the mobility of anionic contaminants like ^{99}Tc within the grouted waste form. This problem was thoroughly examined by Lukens and co-workers at Lawrence-Berkeley National Laboratory (LBNL) (Lukens et al. 2003). Because the mobility of ^{99}Tc depends so strongly upon its oxidation state—mobile as oxidized $Tc(VII)O_4^-$ and relatively immobile as reduced $Tc(IV)O_2$—Lukens et al. (2003, 2005) used a grout recipe that included reducing agents. Reduced sulfur species in blast furnace slag were ground and mixed into the grout with the objective that Tc(VII) would be reduced—and stay reduced—in the cement over a long period of time. Soluble ^{99}Tc was added to the slurry during hydration of the cement-clinker powder and, after curing and drying, the hardened waste form was exposed to air. The research team subjected the hardened waste forms, both before and after exposure to air, to high-energy X-rays at the synchrotron facility at Stanford Synchrotron Radiation Laboratory (SSRL). Near-edge spectra (X-ray absorption near-edge spectroscopy, or XANES) were used to determine the valence of ^{99}Tc. They found that initially, the reducing agents in the grout caused Tc(VII) to be reduced to Tc(IV). However, after only a few months of exposure to air, the XANES data indicated rapid re-oxidation of Tc(IV) to Tc(VII) within the small (a few to 10 mm on a side) rectangular specimens. They concluded that adding reducing agents to the grout formulation had little long-lasting positive effect on maintaining a reducing environment for ^{99}Tc. The very high surface-area-to-volume ratio of the specimens afforded rapid ingress of oxygen to the interior of the specimens. Scientists at Savannah River National Laboratory (SRNL) (Kaplan 2003, Kaplan et al. 2005) have argued that oxygen ingress into the large Saltstone monoliths being produced at the Savannah River Site (SRS) to dispose of their LAW will be much more limited, such that reduced ^{99}Tc [Tc(IV)] will not be substantially re-oxidized for up to 10 000 years. More discussion of the assumptions used in the predictive modeling and more experiments on air re-oxidation are warranted.

2.1.1.1 Containerized Cast Stone

The Cast Stone (Figure 2.1) waste form was developed at the CH2M Hill Hanford Group Inc. to solidify numerous waste streams, including secondary waste generated at the Hanford Site (Lockrem 2005b, Cooke et al. 2003, Lockrem et al. 2003, Lockrem et al. 2008, Cooke and Lockrem 2005, Cooke et al. 2006a, 2006b, 2006c, 2006d; Duncan et al. 2009, Duncan and Burke 2008, Clark et al. 2005, Silsbee et al. 2005, Clark et al. 2006, Cooke et al. 2007, Cooke et al. 2009).(a) Cast Stone is a cementitious waste form that consists of a mixture of Class F fly ash, Grade 120 blast furnace slag (BFS), and Type I and II Portland cement. After conducting screening tests on four different formulations, two of the formulations were selected for further testing. The compositions of these two formulations are provided in Table 2.2.

(a) ES Aromi and KD Boomer. 2003a. "The Application of the Incidental Waste Requirements to Cast Stone & Steam Reforming." Memo to RJ Schepens 7-14-2003, CH2M-0302577, CH2M Hill, Richland, Washington.

ES Aromi and RE Raymond. 2003b. "Final Test Reports for Bulk Vitrification & Cast Stone Technologies Demonstrations for Treatment & Disposal of K Basin Sludge." Memo to RJ Schepens., 12-22-2009. CH2M-0304811, CH2M Hill, Richland, Washington.

Figure 2.1. Picture of a Cast Stone Monolith (Cooke et al. 2009)

Cast Stone has also been tested with various getters as a waste form for treating the Basin 43 waste stream of the Liquid Effluent Retention Facility (LERF) that is concentrated to achieve 28.9% solids (Duncan et al. 2008, Cooke et al. 2009). The getters tested with this waste form included bone char, bone ash, bone black, synthetic apatites, iron powder, iron phosphate, tin apatites, and two resins (Cooke et al. 2009, Lockrem 2005b). Each getter was added to the solid mix (10% by mass), except that only 1% by mass of tin apatite (previously loaded with Tc) was incorporated in to the mix. The getters (with oxidation reduction potential adjustment) with the best ANSI 16.1 leach performance were two of the resins and tin apatite. Among these getters, tin apatite exhibited the highest leach index (LI = 12.7 for Tc), indicating that it was more effective in Tc sequestration as compared to all other getters that were tested (Duncan et al. 2008; Cooke et al. 2009).

Table 2.2. Dry Reagent Compositions Used in Cast Stone

Ingredient	DRF2 (wt %)	DRF4 (wt %)
Portland Cement Type I, II	8	20
Fly Ash Class F	45	66
Blast Furnace Slag, Grade 120	47	--
Attapulgite clay	--	14

The two dry reagent formulations were tested with a LAW simulant at waste loadings ranging from 8.2 to 24.2% by weight. The results of tests conducted on the Cast Stone monoliths are shown in Table 2.3. The data indicated that Cast Stone made from the DRF2 mix met both the U.S. Nuclear Regulatory Commission (NRC) (1991) and the Washington State Administrative Code Land Disposal (WAC 2000b) regulatory requirements. This waste form also appeared to perform well when subjected to other waste-form property tests, such as volume reduction, bleed water percentage, hydraulic conductivity, thermal transmission, curing heat evolution, and the evolution of gases (toxic and explosive).

Cast Stone has also been tested as a waste form for the disposal of iodine-rich caustic wastes from the Hanford site (Lockrem 2005a). Cast Stone was tested as both a baseline waste form (containing spiked I) and with getters such as silver zeolite, silver mordenite, a calcium phosphate (Will Form), and bone char (Cosmic Black #7). The results showed that the leachability index (LI) (as per ANSI/ANS16.1) for iodine in the baseline waste form ranged from 10 to 9.1. The leaching increased (lower LI) with increasing iodine loading in Cast Stone. The presence of Ag-bearing getters in Cast Stone noticeably decreased iodine and silver leachability. However, the calcium phosphate getters appeared to increase the leaching of I, possibly due to increased porosity of Cast Stone (Lockrem 2008).

These data indicate that Cast Stone is a cementitious monolithic waste form that has been developed and tested to specifically solidify the liquid effluents entering the LERF, including the WTP off-gas scrubber waste stream. Based on the demonstrated performance of Cast Stone, this waste form needs to be included in further evaluation.

Table 2.3. Performance Evaluation of Cast Stone (Lockrem et al. 2005b)

No	Parameter	Test Method	Qualification/Acceptance Criteria	CCS-DRF2	CCS-DRF 4
1	Compressive strength	ASTM C39/C 39M (ASTM 1999)	>3.45 MPa after minimum 28 day curing	8.03 – 16.26 MPa	3.04 – 8.85 MPa
2	Volume Reduction	ASTM C174/174M	<5%	+1.5 – 4.6%	-0.1 to -2.0%
3	Leach Testing	ANSI/ANS 16.1(ANSI 1986)	Leachability Index >6	NO_3 7.5 – 8.5 NO_2 7.5 – 8.6 CrO_4 ~12.4 – 13.3 ^{99}Tc 9.5 – 10.4 ^{129}I >7.9	NO_3 6.1 – 7.5 NO_2 6.0 – 7.5 CrO_4 >10.2
4	Leachability	EPA SW 846 Method 1311 (Toxicity Characteristic Leach Procedure [TCLP]) (EPA 2000)	WAC 173-303-140, 40 CFR 268	Met WAC 173-303-090 Standards and Universal Treatment Standard (UTS) except Cr did not meet UTS at the highest waste loading (24.2%)	Cr did not meet UTS at any level of waste loading
5	Free standing Liquids	ANSI/ANS 55.1 Appendix 2 (ANSI 2000)	<0.5% pH >9	0	0
6	Bleed Water after 1 day	Modified ASTM C-940 (ASTM 1998)	<5%	<1%	1.5%
7	Hydraulic conductivity	ASTM D 6527-00	None	<1.41 x 10^{-10} - <3.57 x 10^{-10} cm/s	Not Applicable
8	Maximum Curing Temperature	ANSI/ANS 16.1 immersion and subsequent compressive strength measured as per modified ASTM C39/39M	Maximum Temperature	60 ºC: 15.28 MPa 70 ºC: 12.68 MPa 75 ºC: 12.45 MPa 80 ºC: 14.53 MPa 85 ºC: 13.11 MPa	Not Applicable
9	Thermal Cycling	Modified ASTM B553	>3.45 MPa after 30 thermal cycles of -40 – 60 ºC	Not Applicable	Not Applicable
10	Thermal Transmission	ASTM C177 (ASTM 1997)	None	0.278 – 0.785 Btu/hr ft °F	Not Applicable
11	Near-adiabatic curing heat evolution	Informal procedure. Calculated heat of hydration	None	Heat of hydration: 10.8 cal/g. Max heat rise in a gallon volume: 30.2 ºC	Not Applicable

Table 2.3. Performance Evaluation of Cast Stone (Lockrem et al. 2005b)

No	Parameter	Test Method	Qualification/Acceptance Criteria	CCS-DRF2	CCS-DRF 4
12	Explosive or toxic gases test	Evaluated from chem. reactions, radiolysis, and container corrosion	None	No toxic or explosive gas generated	--
13	Hydrogen gas generation rate test	Radcalc calculation from 100% gamma absorption	None	Not significant in vented containers	Not Applicable

Tests 1, 3, 5, 8, and 9 are recommended by the NRC (1991); Test 4 (EPA, SW 846) is required for WAC 173-303-140, 40 CFR 268. All other tests were performed as part of waste-form qualification (Lockrem 2005)

2.1.1.2 Saltstone

Saltstone is a cementitious waste form made by mixing a salt solution (that is pumped from SRS F- and H-Area liquid storage tanks) with a dry mix that contains BFS, fly ash, and cement or lime. As illustrated in Table 2.4, the components used to make Saltstone are similar to the materials used in Hanford Cast Stone. The primary soluble salts contained in the salt solution in descending order are sodium nitrate, sodium hydroxide, sodium nitrite, sodium aluminum hydroxide, sodium carbonate, and sodium sulfate. The primary solid oxide components in the dry blend in descending order are silicon dioxide, aluminum oxide, calcium oxide, magnesium oxide, and iron (III) oxide. Once solidified, Saltstone becomes a dense, alkaline, reducing, micro-porous, monolithic, cementitious matrix composed of solids such as calcium aluminosilicate and a salt solution in its pore structure. The pore fluid consists mainly of sodium, nitrate, and nitrite (Phifer et al. 2006).

Table 2.4. Dry Reagent Compositions Used in Saltstone

Ingredient	Saltstone (wt%)	Clean Grout (wt%)
Blast furnace slag (grade 100 or 120)	25	28
Cement (ASTM 150 Type II) or lime	3	6
Fly ash (Class F)	25	28
Salt solution (average 28% by weight salt)	47	Not applicable
Water (maximum)	Not applicable	38

2.1.2 Chemically Bonded Phosphate Ceramics

Ceramicrete is one of a family of chemically bonded phosphate ceramics (CBPC) that form at ambient temperatures using an exothermic acid-base reaction. Although a number of approaches are used to create a variety of CBPCs (Singh and Wagh 1998, Singh et al. 2000, Wagh and Jeong 2002, Wagh and Jeong 2004, Wagh et al. 2003, Wagh et al. 1998, Wagh et al. 2000), the general fabrication process consists of mixing a metal phosphate (such as mono-potassium hydrogen phosphate) with a metal oxide (such as magnesium and iron) in a step-wise process to produce a hard insoluble ceramic (Figure 2.2). Equation (2.1) indicates the reaction that results in a magnesium potassium phosphate ceramic.

$$\mathrm{MgO + KH_2PO_4 + 5H_2O \rightarrow MgKPO_4 \bullet 6H_2O} \qquad (2.1)$$

A combination of ionic and covalent bonds between the mineral phases and ceramic matrix provides a sound structural, essentially nonporous, pH-neutral mineral matrix that can incorporate high concentrations of metals and salts. The specific aspects of the fabrication process change with the various applications of the material for this patented technology (Singh et al. 1997, Wagh 2004). These applications include, but are not limited to, 1) treating mixed and low-level wastes (LLWs) (magnesium potassium phosphate and iron phosphate), 2) macro-encapsulating and containerizing uranium (doped ceramicrete), 3) repairing roads and highways, 4) drilling casing and capping in the oil industry (aluminum phosphate [Berlinite]), and 5) medical/dental industry application (calcium and zinc phosphate). Although all of the applications of CBPCs are important, the treating of mixed and LLW is germane to this discussion, as is, more importantly, the use of CBPCs to immobilize specific contaminants of concern (COCs), such as ^{99}Tc and ^{129}I, from WTP secondary waste streams and to control their release from a sub-surface disposal facility environment such as IDF.

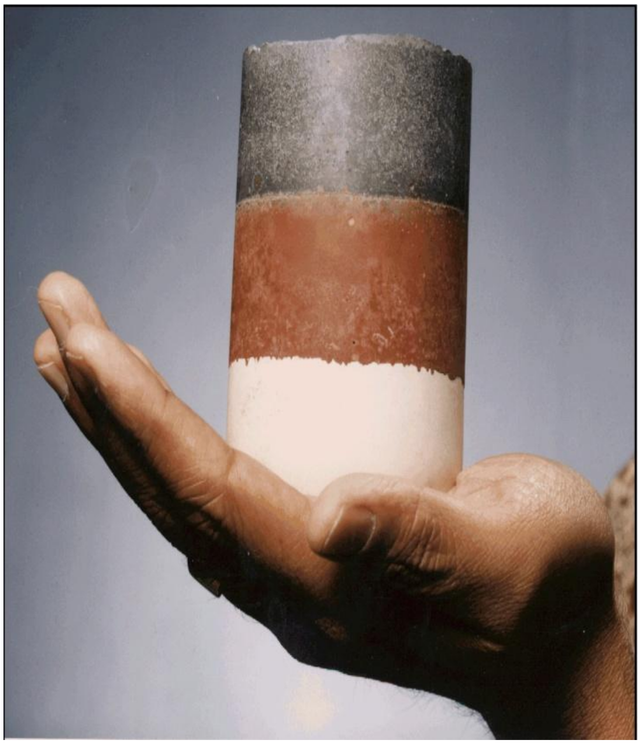

Figure 2.2. Picture of Chemically Bonded Phosphate Ceramics (image taken from www.netl.gov/technologies/oil-gas/petroleum/projects/EP/images/FigAKCeramic_1.jpg)

Recently, Singh et al. (2006) evaluated the use of two CBPC (magnesium potassium phosphate) forms for ^{99}Tc immobilization. The material was fabricated with two processes:

- 1st Process: MgO and KH_2PO_4 (MKP) were mixed under aqueous conditions. A powder binder mixture was added that consisted of 38-wt% fly ash and 2- to 3-wt% tin chloride ($SnCl_2$), and the mixture was cured for 14 days.
- 2nd Process: MKP was mixed with $TcO_2•2H_2O$. The $TcO_2•2H_2O$ was formed by reacting a ^{99}Tc aqueous solution with $SnCl_2$ to change the valence state from Tc(VII) to Tc(IV).

In the first approach, the optimal loading of the MKP waste form was 36 wt%, and the concentration of ^{99}Tc in the waste form ranged from 20 to 150 ppm. In the second approach, ^{99}Tc loading in the waste forms was as high as 900 ppm. A number of characterization techniques were used to evaluate the physical and chemical properties of the waste forms, and a summary of the results is provided in Table 2.5.

In addition to the results discussed above, Russell et al. (2006) tested a CBPC made with Hanford liquid secondary waste stimulant. Their results suggested that CBPC performed well in Toxicity Characteristics Leaching Procedure (TCLP) and compressive strength tests (Table 2.5), but during ANS 16.1 tests, the CBPC specimens exhibited cracking and spalling, indicating problems with formulations).

Although CBPCs illustrated promise as a waste form for Hanford secondary waste, the effectiveness of CBPCs to immobilize relatively mobile radionuclides, such as ^{99}Tc and ^{129}I, and their long-term performance needs to be addressed.

Table 2.5. Summary of Important Chemical and Physical Properties of CBPC

Ingredient	1st Process[a]	2nd Process[a]	Russell et al. (2006)
Density, kg/m^3	0.0018	NM[b]	0.00206
Compressive Strength, MPa	30 ±7	NM	33.6 ±5.2
Porosity	4%	NM	ND[c]
Surface Area, m^2/g	NM	NM	10.9
PCT for ^{99}Tc, g/(m^2 d)[d]		1.0 to 8.5 × 10^{-3} at 23°C 0.7 to 1.1 × 10^{-1} at 90°C	ND
ANS16.1 Leach Index for ^{99}Tc or Re[e]	13.3 to 14.6		12.7

(a) Process discussed in Singh et al. (2006)
(b) NM = Not measured
(c) ND = Not detected
(d) Normalized element release from product consistency test
(e) Re used as a chemical analogue for ^{99}Tc

2.1.3 Geopolymers

Geopolymers, also known as alkali-activated alumino-silicate binders, form through the reaction of aluminosilicate materials, such as clay or fly ash, in a caustic solution. When the reactions proceed at near ambient temperatures, polymerization takes place, forming amorphous to semi-crystalline aluminosilicate networks (Perera et al. 2005). Structural integrity and mechanical strength, as determined by slumping and compressive strength, are usually obtained within minutes to hours, depending on the specifics of the materials and processing. Davidovits (1994a, 1994b, 1994c) is attributed with the early development and formulation of geopolymers, for which he has been awarded several patents. Khalil and Merz (1994) and Perera et al. (2004) have also studied the formulation and application of geopolymers for waste solidification.

Geopolymers are thought to be composed of a three-dimensional matrix of poly sialate (- Si – O – Al – O -), and/or poly sialate-siloxo (- Si – O – Al – O – Si -), and/or sialate-disiloxo (- Si – Al – Si – O – Si – O -). The material is largely amorphous with some minor crystalline structure, again dependent on the source materials. Contaminant distribution studies showed that Cs was concentrated in the amorphous phase, while Sr was present in both the amorphous and crystalline phases (Perera et al. 2004).

A specific geopolymer called “Duralith” was included in a study of low-temperature immobilization technologies for Hanford WTP secondary wastes (Russell et al. 2006). A patent application has been submitted for this low-temperature solidification technology for radioactive and hazardous wastes (Gong et al. 2006). The Duralith geopolymer is composed of three components: an activator, a binder, and an enhancer. The activator is a solution of sodium hydroxide and/or potassium hydroxide with a rapidly dissolving form of silica, such as silica fume or fly ash. The binder is a mixture of metakaolin, ground BFS, fly ash, or other additives. The binder and activator are the two main components that yield the geopolymer material. The enhancers are essentially getter materials, described in Section 2.2 in this report, that are added to further reduce the mobility of hazardous metals and radionuclides within the waste form.

The Duralith geopolymer prepared with the Hanford secondary waste simulant showed compressive strengths above 22 MPa before and after irradiation, easily meeting the greater than 3.45-MPa ASTM specification for 28-day cured specimens. The material also easily passed the TCLP test for Cr, Cd, Ag, Hg, and Pb included in the simulant. The ANSI/ANS 16.1 LI was 8.6 for Na and above 10 for Re, which was used as a surrogate for Tc in the tests. These are better than the targets of 6 and 9 for the LI for Na and Re, respectively. However, several of the test specimens fractured during the immersion testing. The waste-form provider speculated that there may have been some formulation problems and was able to adjust the quantity of one of the batching materials so that subsequent samples did not crack in water. Russel et al. (2006) concluded that there were some formulation problems associated with the Duralith geopolymer that needed to be addressed but that the material shows potential as a waste-form material for the Hanford liquid secondary wastes.

2.1.4 Hydroceramic Cement

A cementitious waste form specifically tailored for Hanford low-activity tank waste has been proposed (Bao et al. 2005, Kyritsis et al. 2009, Siemer 2002). The waste form, designated as a "hydroceramic," seeks to replicate the mineralogy of zeolitized rocks, similar to those that make up the bedrock at Yucca Mountain, Nevada (Siemer 2002). The waste formulation takes advantage of the high sodium, hydroxide, nitrate, and nitrite concentrations in the tank sludge to form "cage" minerals, such as hydroxysodalite ($Na_8(Al_6Si_6O_{24})(Cl,SO_4,OH)_{1-2}$), cancrinite ($(Na,Ca)_{6-8}(Al_6Si_6O_{24})\ (CO_3,SO_4,Cl)_{1.5-2.0}\bullet 1\text{-}5H_2O$), and Zeolite-A ($Na_{12}(Al_{12}Si_{12}O_{48})\bullet 27H_2O$; see Figure 2.3). Adding metakaolinite,(a) vermiculite, sodium/calcium sulfide, and water at hydrothermal conditions (500°C to 600°C) will convert the inorganic components of the sludge into a fairly coarse-grained interconnected multiphase material that has a ceramic-like structure. The molecular frameworks of these solid phases, which are similar in structure to feldspar minerals, possess large vacancies in their structure that can accommodate cations such as Cs^+ or Sr^{2+} in Zeolite-A (Figure 2.3), or anions, such as nitrate (NO_3^-), nitrite (NO_2^-), and pertechnetate (TcO_4^-) in hydroxysodalite. In some formulations, sugar is added to impart a reducing environment in the material (Bao et al. 2005). One advantage afforded by this composition over that of grout is that it avoids generating large amounts of the amorphous C-S-H phase. A further benefit is that the high sodium content present in almost all of the Hanford liquid wastes is taken up in the mineral structure of these phases.

On the other hand, it is not immediately clear where radionuclide-bearing anions would reside in a hydroceramic. Presumably, the reducing conditions would cause Tc(VII) to be reduced to Tc(IV), usually in the form of TcO_2(s). Alternately, the reduced Tc(IV) could form a surface precipitate or may be incorporated into sulfide phases. As discussed above in the section on grout/cement, reduced Tc(IV) can be re-oxidized if it forms an isolated phase. If manifested as a sulfide phase, reduced Tc(IV) may remain in the reduced state if the primary sulfide phase oxidizes and breaks down to form goethite and a sulfate

---

(a) "Metakaolinite refers to the mineral kaolinite ($Al_2Si_2O_5(OH)_4$) that has been "activated" through the process of calcination.

phase. In either case, there are no data that bear on the question of the long-term fate of ^{99}Tc in hydroceramics.

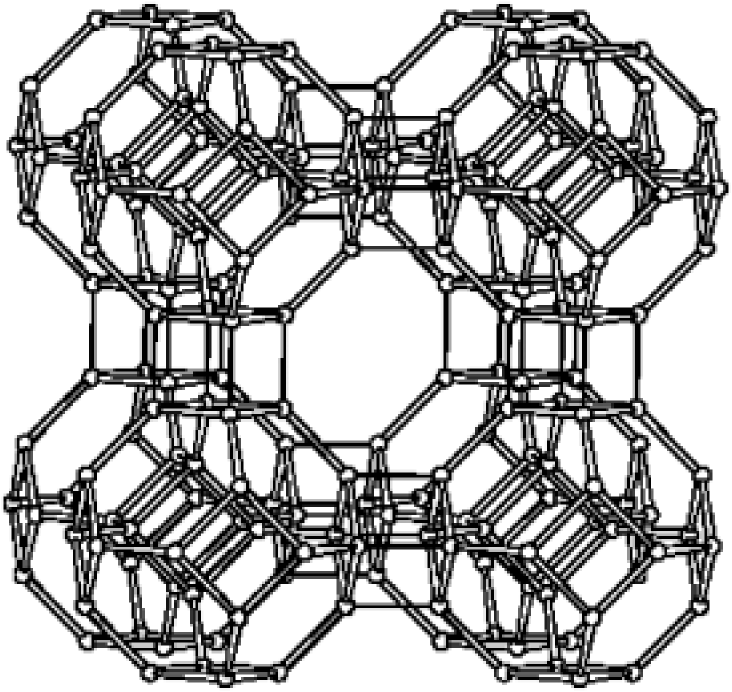

Figure 2.3. Molecular Structure of Zeolite-A, in Which the Eight Corners of the Cube Are Made up of Sodalite Cages. The large void between the cages can accommodate a variety of cations (e.g., Cs^+, Sr^{2+}). (Figure from the International Zeolite Association [IZA]).

There are, however, some chemical durability data on hydroceramics that pertain to major element release. After fabrication, Bao et al. (2005) subjected powdered specimens of the monolithic hydroceramics to static leach tests that ranged from 1 to 7 days in duration at 90°C (a modified ASTM C1285 product consistency test [PCT]). The monoliths had been calcined at temperatures between 375°C and 675°C to improve crystallinity and density. They were then powdered and sieved to the desired size fraction; the powders were not washed before the tests, which may have influenced test results. They found that the higher the temperature of calcination, the smaller the loss of elements (mainly Na, Al, NO_3^-, and SO_4^{2-}) to solution. Overall, they concluded that the greater inherent stability of zeolites and sodalite phases compared to glass or grout in shallow, aerobic terrestrial environments makes hydroceramics a better choice for hosting LAW.

Finally, an additional drawback of hydroceramics is the relatively high temperature of calcination that could impact the incorporation of volatile COCs, such as ^{99}Tc and ^{129}I. Bao et al. (2005) found that the optimal temperature of calcination is 525°C, a temperature at which a fraction of the pertechnetate would volatilize and escape the waste form. Although Bao et al. (2005) suggest that calcination could be effective at a much lower temperature, e.g., 90°C, the lower calcination temperature would result in a lack of transition of amorphous phases to crystalline phases and a higher porosity, thereby making the material more vulnerable to leaching.

Further, compressive strength tests show that hydroceramics (or least those produced at Mississippi State) perform poorly, with compressive strengths on the order of 2 to 4 MPa, compared to values of 40 to 45 MPa for other candidate materials. In the low-temperature immobilization study reported by Russell et al. (2006), attempts were unsuccessful in making a hydroceramic cement at low temperatures with a Hanford secondary waste simulant that could meet the minimum 3.45-MPa (500-psi) compressive strength. The studies used sodium hydroxide, metakaolin, silica, vermiculite, and sodium sulfide as the source materials for the hydroceramic with curing times of up to 49 days at room temperature or 14 days at 90°C. Because a waste form could not be produced that met compressive strength requirements, no further characterization of the low-temperature hydroceramic cement was conducted as part of that study. Russel et al. (2006) concluded that the hydroceramic cement did not appear to be a viable option for low-temperature immobilization of the wastes considered in their study, but that it does not preclude hydroceramic cements as a viable waste form when prepared under hydrothermal conditions.

Due to the vulnerability of the waste form to dissolution, its lack of sufficient compressive strength, and the high temperature required for processing, we suggest that the hydroceramics are not a strong candidate for use as a matrix for immobilizing Tc from WTP secondary waste streams.

2.1.5 Fluidized Bed Steam Reformer

Steam reforming is a process in which pretreated LAW is denitrified and stabilized. The specific treatment technology that has been previously evaluated is the THermal Organic Reduction (THOR) fluidized-bed steam reformation (FBSR) process that operates by introducing tank waste with high sodium nitrate content into a moderate temperature (650°C to 800°C) fluidized bed vessel. The tank waste is reacted with carbon- and iron-based reductants to convert nitrates and nitrites directly to nitrogen gas. Radionuclides, alkali metals, sulfate, chloride, fluoride, and non-volatile heavy metals in the waste stream are reacted with clay (kaolinite) or other inorganic materials to produce a multiphase mineral assemblage of feldspathoid minerals (sodalite, nosean, and nepheline). Several demonstrations have been conducted to evaluate the capability of the FBSR technology to treat simulated Hanford LAW and Idaho National Engineering and Environmental Laboratory (INEEL) sodium-bearing waste (SBW). For additional details on and a discussion of the results from these demonstrations and the FBSR product, see Jantzen (2002, 2006, and 2008), Jantzen et al. (2007), Olson et al. (2004), or Soelberg et al. (2003), or visit the THOR Treatment Technologies LLC website (www.thortt.com). Here we provide a general overview of the results.

In 2002, a single sample of FBSR product (SCT02–98) was analyzed and tested with single-pass flow-through (SPFT) and pressurized unsaturated flow apparatus (PUF) leach-testing methods (McGrail et al. 2003b). The FBSR product was found to consist of two primary mineral phases, nepheline ($(Na,K)AlSiO_4$) and nosean ($Na_8Al_6Si_6O_{24}(SO_4)\bullet H_2O$). Results from the SPFT tests, show little pH dependence on the release rate of Re, a chemical stand-in for ^{99}Tc, and a declining release rate at a pH greater than 8 at 90°C. Dissolution rates for the nepheline phase show conventional pH rate dependence with increasing rate as a function of pH. The SPFT data were used to calculate a bounding release rate for an FBSR waste package, and this was compared with the available data from LAW glasses. The bounding case release rates are about 20 times higher for the FBSR product compared to glass. However, because of uncertainty regarding the true reactive surface area of the FBSR product, actual differences in release rate at 90°C probably range from 2 to 20 times higher than LAW glass. Additional testing was recommended to determine relative bounding rates at actual disposal system conditions (15°C), irrespective of reactive surface-area assumptions. Fractional release rates, again based on Re release, calculated from PUF experiments with the FBSR product, showed essentially identical performance with a reference LAW glass (LAWA44) tested under the same conditions (McGrail et al. 2003b). However, the temperature dependence of the measured rate is not known, so the relative rates at 15°C cannot be estimated at this time. Assuming an activation energy similar to that of glass for the temperature dependence of the dissolution kinetics of the primary silicate phases, the FBSR product performance appears to be approximately equivalent to that of LAW glass. Additional testing was recommended to reach a scientifically defensible conclusion regarding actual FBSR product performance based on rigorous disposal system simulations equivalent to what has been done for LAW glasses.

A second sample of FBSR product, designated FBSR LAW 1123, was tested with the PUF apparatus to simulate long-term repository conditions. The major difference between the two tested FBSR waste forms is an iron content in SCT02–98 that is 20 times higher than that in FBSR LAW 1123. Details about the sample compositions, testing, and results can be found in a report by Pierce (2007). Preliminary results show that after 300 days of testing, the ^{99}Tc release from LAW glass sample LAWAN102 is 11 times greater than the release of Re from the FBSR product. Assuming that Tc and Re are sufficiently chemically similar, this suggests that the FBSR product may be a viable option for immobilizing LAW. As previously stated, the uncertainty in the reactive surface area of the FBSR product complicates direct comparison of this material to glass (see Figure 2.4 and Table 2.6). Testing is continuing to evaluate this product as an alternative waste form.

In addition to the performance testing on the granular FBSR material, recent experiments have focused on converting the granular material into a monolith by using one of several binders (Jantzen 2006, THOR 2009). These experiments focused on determining the physical properties of the monolith, such as compressive strength and density, and the impact, if any, that these binders have on the chemical durability of the FBSR product. The chemical durability was evaluated with the PCT, and the results were compared to previous data obtained for the granular material, correcting for the surface area difference. The binder materials used were ordinary Portland cement (OPC), ceramicrete, and hydroceramics (three compositions).

Five compositions of OPC were fabricated in these experiments with Type II Portland cement. Three of the five compositions were loaded with 84 wt%, 87 wt%, and 80 wt% FBSR without additives, while the remaining two consisted of 80- to 81-wt% FBSR loaded with precipitated silica (representing a chemically pure pozzolanic material such as fly ash). In compressive strength tests, four out of the five monoliths performed well (compressive strength >3.45 MPa [500 psi]) after 7 days of curing. The fifth sample, which contained an approximately 17.5 wt% substitution of SiO_2, had a lower compressive strength.

The ceramicrete monoliths were made with 35.7-wt% FBSR and cured at ambient temperature for 2 weeks. This resulted in a compressive strength of ~27.6 MPa.

Three hydroceramic monolith samples were produced with FBSR loadings of 50 wt%, 60 wt%, and 80 wt% on a dry basis. The initial samples were cured overnight in a humidity chamber at 40°C and then placed in steam at 40°C for an additional 24 hours. The humidity chamber and steam treatment verifies that the NaOH and metakaolin react to form zeolite mineral phases. This process was repeated, and the samples were cured at 70°C, but in each case, the hydroceramic-produced material had insufficient compressive strength. The third set of samples were cured overnight at 90°C and used in the compressive strength and durability tests. The compressive strength for the 90°C cured sample was >10.3 MPa. In each case, the material passed the PCT durability limits set for glass in the performance test.

The most recent evaluation of the FBSR process for treating Hanford LAW and WTP secondary waste was conducted in 2008 as part of the DOE Advanced Remediation Technologies (ART) Program (THOR 2009, Jantzen 2008, Vora et al. 2009). Under this project, an engineering-scale technology demonstration of the FBSR process was conducted at THOR Treatment Technologies LLC with a simulated WTP secondary waste stream. The results of this test demonstrated that scaling up the FBSR process still produced a granular, mineralized solid product that captured >99.99% of the Cs, I, and Re (based on data from manual sampling of the off-gas stream) (THOR 2009). Although additional optimization of the FBSR process may be required, these results indicate that the FBSR product may be a viable waste form for the liquid secondary waste stream. For comparison to other low-level waste forms, data on the performance in the ANS/ANSI 16.1 LI test are needed for the FBSR product encapsulated in a binder material.

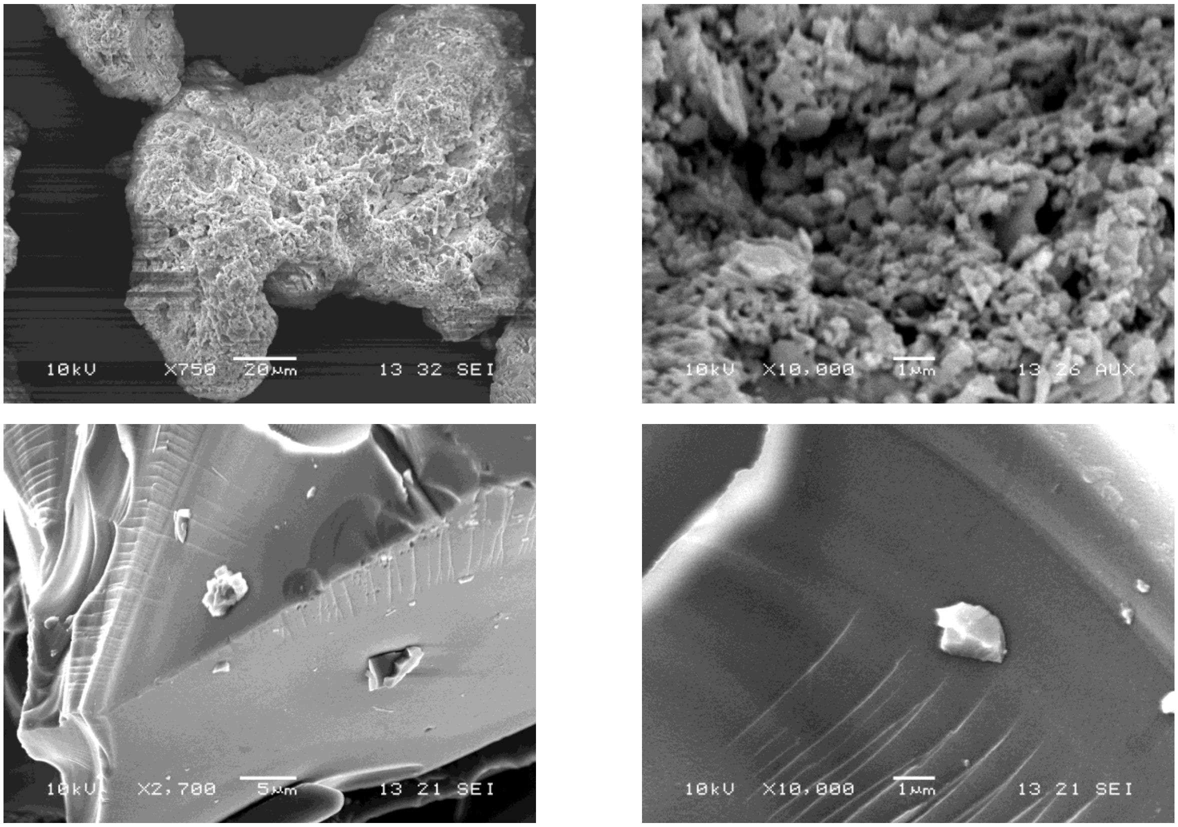

Figure 2.4. Scanning Electron Microscope Image of FBSR 1123 Product (top) and Glass (bottom)

Table 2.6. Comparison Among the Particle Density, BET, Geometric Surface Area, and Surface Roughness Factor of FBSR 1123 and Various Glasses

Sample ID	Particle Density (kg/m^3)	Geo. Surf. Area[a] (m^2/g)	BET Surf. Area[b] (m^2/g)	Surf. Rough.[c]
FBSR LAW 1123[d]	Not available	0.0212	4.427[i]	208.8
FBSR LAW 1123[e]	$2.663 \pm 0.005 \times 10^3$	0.0200	4.148 ± 0.01[i]	216.4
SCT02-98[f]	$2.764 \pm 0.004 \times 10^3$	0.0193	2.37 ± 0.5[i]	122.8
NeB0[g]	$2.491 \pm 0.001 \times 10^3$	0.0214	0.03757 ± 0.0003[j]	1.8
LAWA44[h]	$2.698 \pm 0.008 \times 10^3$	0.0198	0.0324 ± 0.0002[j]	1.6
LAWBP1[h]	2.68×10^3	0.0200	0.0575 ± 0.0002[j]	2.9

(a) Geo. Surf. = Calculated geometric surface area.
(b) BET Surf. = Braunauer-Emmet-Teller surface area.
(c) Surf. Rough. = Surface roughness is the ratio of the BET to the geometric surface area.
(d) Lorier et al. (2005)
(e) This study
(f) McGrail et al. (2003a, 2003b)
(g) Pierce et al. (2009)
(h) McGrail et al. (2000)
(i) N_2-adsorption BET results
(j) Kr-adsorption BET analysis results. Kr was used as an analysis gas because it provides a more accurate estimate for particles with a surface area <1 $m^2\ g^{-1}$.

2.1.6 Goethite

Goethite (α-FeO·OH) is a low-temperature secondary weathering product of primary iron phases. Because goethite is at or very near equilibrium at Earth's surface, there is little impetus for reaction and dissolution. Further, the iron in goethite is in the ferric state [Fe(III)], so there is no tendency to undergo redox reactions in near-surface oxidative environments. Goethite appears to co-precipitate with $Tc(IV)O_2$ or incorporate Tc(IV) within its mineral lattice (Livens et al. 2004, Wharton et al. 2000, Zachara et al. 2007).

A number of experiments that examined the reduction and retention of ^{99}Tc in natural sediments whose oxidation states have been artificially altered (Burke et al. 2006, Burke et al. 2005, Fredrickson et al. 2004, Morris et al. 2008, Zachara et al. 2007) yielded some interesting and useful results for secondary ^{99}Tc sequestration. Reduction of Tc(VII) to Tc(IV) by ferrous iron (Fe(II)) in solution is sluggish (homogeneous kinetics), even though the reaction

$$\mathrm{Tc(VII)O_4^-} + 3\mathrm{Fe}^{2+}(\mathrm{aq}) + (n+7)\mathrm{H_2O} \rightleftarrows \mathrm{Tc(IV)O_2}\bullet n\mathrm{H_2O} + 3\mathrm{Fe}(\mathrm{OH})_3(\mathrm{s}) + 5\mathrm{H}^+ \qquad (2.2)$$

is thermodynamically feasible ($\log K_{298} = -21.8$) (Fredrickson et al. 2004). However, when Fe(II) is adsorbed or surface precipitated on solid phases, especially oxyhydroxides of iron, a surface-mediated catalysis of Tc(VII) reduction is more rapid (Cui and Eriksen 1996a, Cui and Eriksen 1996b, Peretyazhko et al. 2008a, Peretyazhko et al. 2008b, Zachara et al. 2007). Other experiments aimed at assessing the interaction of pertechnetate with iron sulfide minerals, such as mackinawite (FeS), pyrrhotite (Fe_7S_8), and greigite (Fe_3S_4), showed that Tc(IV) has an affinity for the surface of sulfide minerals and, upon oxidation to form goethite and sulfate minerals, the ^{99}Tc is reduced and is associated with goethite (Livens et al. 2004, Watson et al. 2001, Wharton et al. 2000). However, the circumstance and rate of reoxidation of the reduced Tc associated with goethite has not been determined.

Irrespective of the nature of the starting iron phase, reduced Tc(IV) associated with secondary or primary ferric oxyhydroxides, such as ferrihydrite, goethite, or hematite, is effectively immobilized, although the relationship between Tc(IV) and the Fe(III) phase is unclear. On the one hand, substituting Tc(IV) for Fe(III) in goethite, for example, is plausible because the Tc(IV)—O and Fe(III)—O bond lengths are similar (1.99 and 2.026 Å, respectively) (Yang et al. 2006). The atomic radii of Tc(IV) and Fe(III) are also closely related in size (78.5 vs. 69 to 78.5 pm,(a) respectively), and both are octahedral (6-fold) coordinated (Huheey et al. 1993), so a coupled substitution scheme is possible. The atomic structure of goethite, recently determined by Yang et al. (2006), is shown in Figure 2.5. On the other hand, examining the reduced run products with X-ray absorption spectroscopy (XAS) methods (briefly described in Appendix A) has revealed that the ^{99}Tc-bearing phase is a separate, reduced Tc(IV) oxide phase and may not be substituting for Fe(III)-O in the host ferric oxyhydroxide phase (Burke et al. 2006, Fredrickson et al. 2004, Fredrickson et al. 2009, Morris et al. 2008, Peretyazhko et al. 2008a, Watson et al. 2001, Wharton et al. 2000, Zachara et al. 2007). In the most detailed study, Fredrickson and co-workers (Fredrickson et al. 2009) found that Tc(IV)O_2-like compounds could exist in a number of states, including physically separate phases or those that are inter-grown with Fe(III)-O compounds. Technetium in the latter state appears to be much more resistant to re-oxidation and mobilization than Tc(IV) compounds that form physically separate phases. Therefore, the key to producing an oxidation-resistant material may be dependent on how the reduced Tc(IV) product formation can be manipulated. If a reduced Tc(IV) compound can be inter-grown with an iron oxyhydroxide, the latter may impart an oxidation-resistant property to the material.

Recently, based on the information cited above, a study has been initiated to determine the efficacy of iron oxyhydroxides as a matrix or substrate for Tc immobilization. The synthesis methods for producing goethite from aqueous solutions and the method by which pertechnetate can be reduced to Tc(IV) in a simulated high carbonate scrubber solution are briefly described below. The experiments are discussed in more detail in a report by Um et al. (2009 draft).

(a) pm = picometer [10^{-12} m; 1 Ångstrom (Å) = 100 pm]

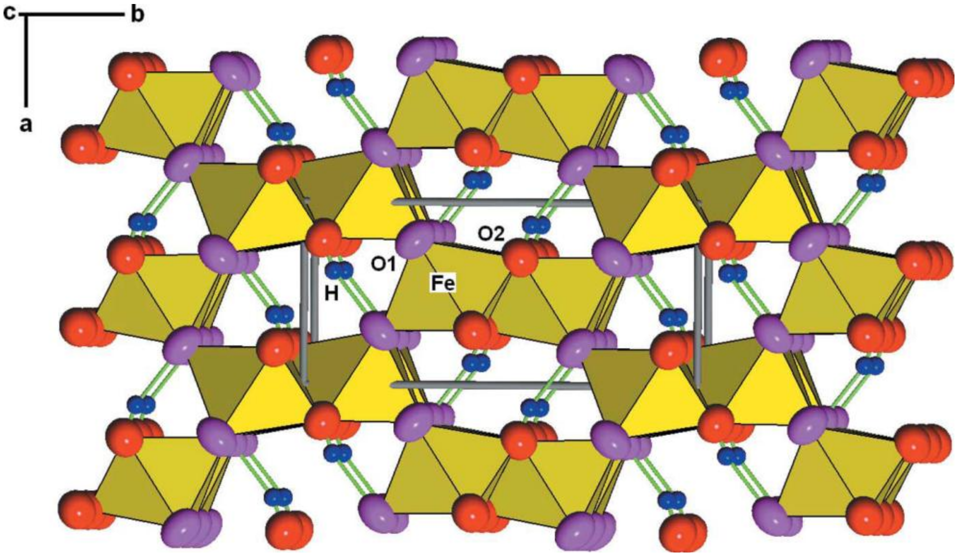

Figure 2.5. Diagram of the Crystal Structure of Goethite, α-FeOOH (after Yang et al. 2006). The gold-colored octahedrals represent FeO_6 octahedra, and the red and purple ellipses denote an O-atom in either corner—or face-sharing configuration—respectively. The octahedrals are also partially linked through H-bonding (green lines).

Iron oxyhydroxides were precipitated from solution by mixing ferric nitrate with sodium hydroxide until a pH of 7 was reached. The resulting solids (likely ferrihydrite) were heated at 70°C to 80°C for 10 days to cause crystal ripening and growth during mineral transformation to a more crystalline goethite phase. The heating caused transformation of the amorphous ferrihydrite to goethite, as confirmed by XRD studies. The XRD data also indicated that there were probably trace quantities of magnetite and hematite. The presence of any crystalline carbonate minerals in the synthesized product could not be detected as they were below the method detection limits (~2 to 5% by mass, depending on the matrix). The solid was kept in contact with a low pH (2.5) solution until a solution spiked with aqueous Fe(II) was added. The Fe(II) solution was made in a controlled atmosphere chamber in which the partial pressure of O_2 was minimized. The Fe(II) solution was added to the goethite-solution mixture and allowed to react with the expectation that the aqueous Fe(II) would sorb onto the goethite substrate, creating an environment conducive for pertechnetate reduction. A potassium pertechnetate solution was then added, and additional iron(III) nitrate and sodium hydroxide were added, with subsequent heating at 80°C. Even though no high concentration of adsorbed Fe(II) was found on the goethite substrate, especially at low pH (<3), additional NaOH introduction could have increased Fe(II) adsorption and/or surface precipitates on the primary goethite surface, which enhanced ^{99}Tc reduction. The purpose of the second addition of ferric nitrate and sodium hydroxide was to precipitate a layer of goethite over the reduced technetium, effectively isolating Tc(IV) compounds from solution. The results showed that >94% of the pertechnetate was removed from solution. After drying the solid material, it was completely dissolved in strong acid, and the resulting solution was assayed for technetium concentration in a final goethite phase. The high concentration of ^{99}Tc in the solid confirmed that >94% of the technetium had been reduced and was associated with goethite. Powdered specimens were placed in Teflon reactors at pH values of 4, 7, and 10 and in synthetic Hanford groundwater to assess the leachability of ^{99}Tc from the solid phase. Although the experiments are ongoing, leachate solutions analyzed to-date contain no detectable ^{99}Tc. This latter result is consistent with the experimental conclusions reached by Zachara and co-workers (Fredrickson et al. 2009, Zachara et al. 2007).

The preliminary evidence indicates that a goethite-based substrate for immobilizing technetium from secondary waste streams shows excellent promise. However, long-term tests, TCLP, ANSI-16.1, and compressive strength testing, have not yet been completed. It is difficult, therefore, to compare the efficacy of this potential waste form with other materials that have a longer history of testing and development.

2.1.7 L-TEM Technology

L-TEM is a patent-pending low-temperature material developed by Llyons technologies, LLC that has been designed to encapsulate liquid and solid hazardous or radioactive waste streams (Figure 2.6). Llyons supplied additional information for this report in response to a request for information by PNNL. The information discussed in this section is a summary of the packet of information provided to PNNL by Llyons.

The L-TEM technology uses a three-phased approach to treating a waste stream. These three phases include a seed phase, a link phase, and a binder phase. The seed phase is a treated, sometimes synthetic, aluminosilicate molecular structure. The size and structure of the ceramic oxide seed used to attract and retain COC is a product of the Llyon Process coupled with specific laboratory tests. The link phase is a series of chemical reactions that result from mixing ceramic oxide(s) with alkaline earth atoms to form a crystalline build-up around the seed core. The binder phase consists of a blend of magnesia (MgO), mono-calcium aluminate ($CaAl_2O_4$), and tricalcium silicates. Mixing the alkali and alkaline earth elements with the complementary chemical compounds forms a solid, low-porosity material matrix when hydrated. L-TEM has been evaluated as a monolithing agent, encapsulation compound, and a selective chemical treatment for LLW and mixed LLW. The majority of the testing to-date conducted with the L-TEM material is under non-disclosure agreements or other legal bindings, but some of the physical and chemical results are provided in Table 2.7. Given the limited test data provided and the lack of short-term test data of the L-TEM material with simulated Hanford secondary waste streams, it is difficult to assess whether the material will demonstrate adequate leachability or physical strength. Therefore, it is difficult to provide any recommendation on whether this material is a viable candidate.

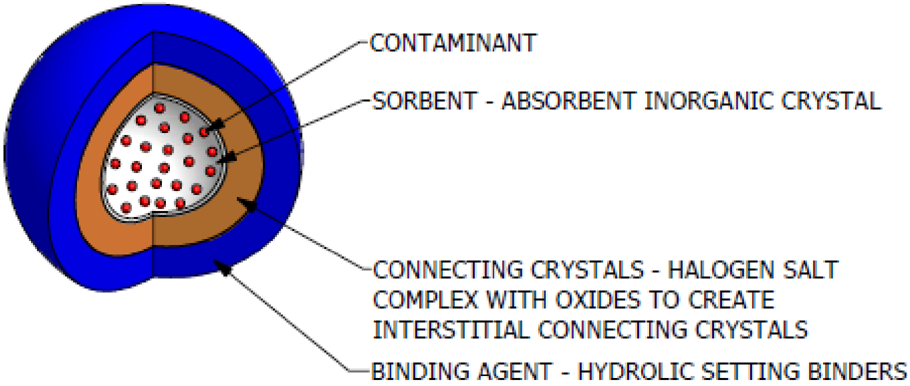

Figure 2.6. Depiction of L-TEM Material Surrounding the Contaminant. Schematic provided by Llyons Technology.

Table 2.7. Physical and Chemical Data on the L-TEM Product provided by Llyons Technologies

Sample ID	Units	Initial	Cured > 28 days	Notes
Density	Kg/M^3		2150 – 2250	Typical
Rheology		Flowable	Solid	Hygroscopic
Electrical Conductivity	mS	2000/g/L H_2O		
pH		10.5–12.5	10.4 – 11.5	Typical
Cation Exchange Capacity	Meq	70–80	80	nominal
Crystal			Multicrystalline	
Thermal Conductivity	W/(m C)		1.82	
Color		Light gray		
Heat Capacity	J/(kg C)		~980	
Mix ratios		5:95–20:80	"	L-TEM: Waste
Compressive Strength	MPa		3.45 – 13.86	ASTM C39
Modulus of Rupture	MPa		0.37 – 1.38	ASTM C78
Hydrogen evolution	%	<1	Not expected	Maintains pH
Leachate reduction	ppm			Per requirement
Modulus of Elasticity	MPa		1.55 – 2.24	ASTM C469-87a

2.1.8 Sodalite

Sodalite group minerals and other framework aluminosilicates, such as cancrinite, with the general formula $Na_8[AlSiO_4]_6X_2 \cdot nH_2O$, X = $B(OH)_4^-$, Br^-, Cl^-, CO_3^{2-}, I^-, NO_3^-, NO_2^-, OH^-, ReO_4^-, SCN^-, SO_4^{2-}, etc., n = 0 to 4, have been synthesized in a large variety of compositions (Brenchley and Weller 1994, Buhl et al. 2001, Fechtelkord 2000, Johnson et al. 2000, Mattigod et al. 2006, Srdanov et al. 1994). The cage-like structure of these minerals can trap and immobilize up to 9 mol% oxyanions. In the case of sodalite group minerals, the structure is derived from corner-sharing TO_4 tetrahedra (T = Si^{4+} and Al^{3+}) in four- and six-member rings that give rise to the cage structure. The negative charge of the cage is balanced by four cations linked to form a tetrahedron that is close to a six-member ring with an enclathrated guest anion in the center (Figure 2.7). This framework can collapse by tilting and deformation of the TO_4 tetrahedra to accommodate ions of various sizes. Previously, Mattigod et al. (2006), using XRD, Raman spectroscopy, and magic-angle spinning nuclear magnetic resonance (MAS NMR) of ^{29}Si and ^{27}Al, demonstrated that perrhenate ion (as an analog of pertechnetate) can be trapped in the β-cages of the sodalite structure. Such structural trapping of pertechnetate is advantageous in that no reduction step is necessary for sequestration to occur. The resulting perrhenate-sodalite (Figure 2.7) had the structural formula of $Na_8(AlSiO_4)_6(ReO_4)_2$.

Although the redox chemistry for Re and ^{99}Tc has been demonstrated to be significantly different (Maset et al. 2006, McKeown et al. 2007) because of the similarities in atomic radii of 1.373 Å for Re and 1.358 Å for ^{99}Tc as well as ionic radii for Re(VII) and Tc(VII) oxyanions at 0.56 Å, the perrhenate anion is commonly considered to be a chemical analogue for the pertechnetate anion (Darab and Smith 1996). Therefore, based on perrhenate-sodalite prepared by Mattigod et al. (2006), a pertechnetate-containing sodalite should have a similar structure. Figure 2.8 illustrates the results of SEM and background-corrected spectra of the elemental composition of a cluster of perrhenate-sodalite. The perrhenate-sodalite was synthesized with the method described by Mattigod et al. (2006) from a 3.0-M solution of ReO_4^-.

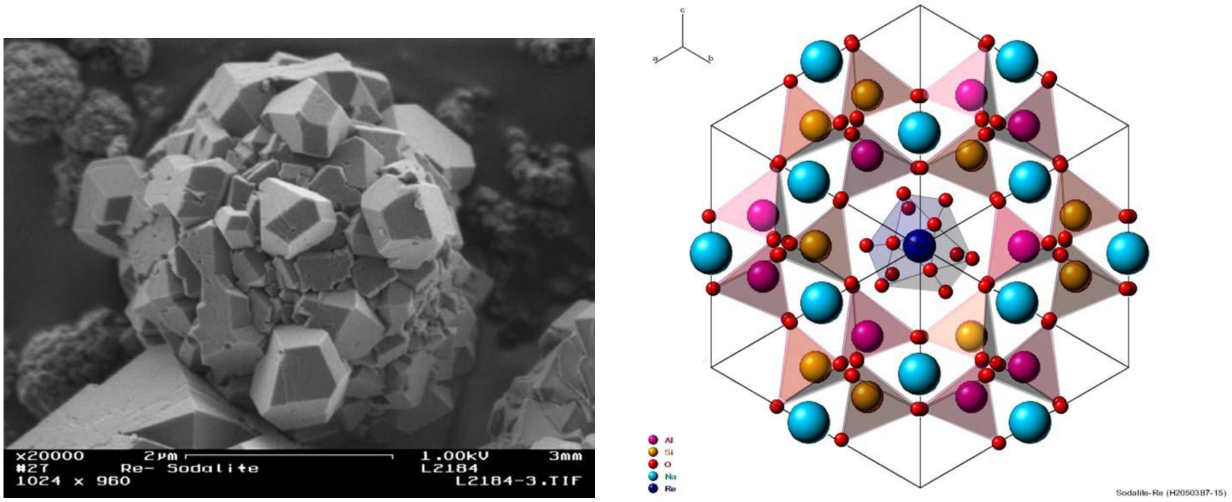

Figure 2.7. Cluster of Doubly Terminated Trapezohedral Crystals of Synthetic Perrhenate-Sodalite (left). The crystal structure of perrhenate-sodalite viewed along the [101] plane.

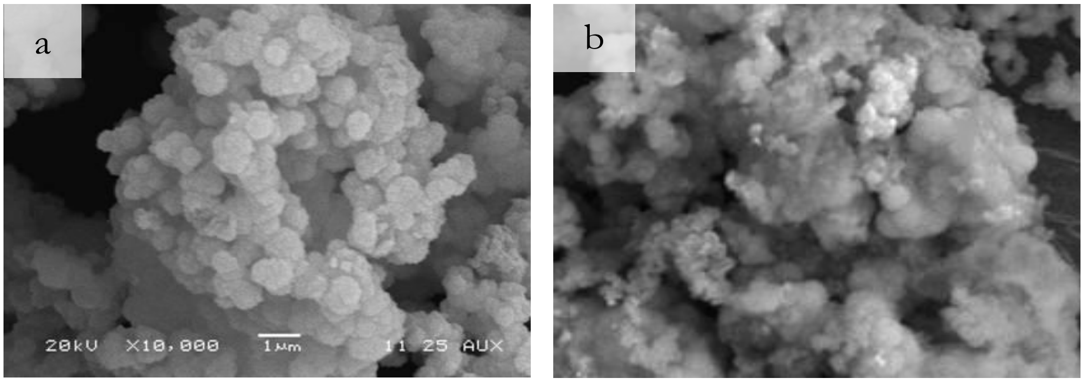

Figure 2.8. SEM Images of a Cluster of Perrhenate-Sodalite. The image on the left (b) was taken at a higher magnification.

The synthesis of perrhenate-sodalite suggested that pertechnetate-sodalite can also be successfully synthesized because the pertechnetate ion radius is only 1% smaller than the ionic radius of the perrhenate ion. Also, McGrail et al. (2003) reported data that suggested the presence of perrhenate/sulfate sodalite in steam reformer waste forms. Recently, a pertechnetate-containing feldspathoid phase was synthesized with a procedure similar to that described by Mattigod et al.(2006), and the resulting material was characterized with SEM-EDS (energy dispersive spectroscopy) and XRD analyses as well as inductively coupled mass spectroscopy (ICP-MS) analyses of an acid-digested subsample of the material to determine the ^{99}Tc content. The results of the SEM-EDS and elemental analysis are shown in Figure 2.9. These results suggest that Al, Na, and Si are well distributed throughout the particles. The relatively homogenous distribution is similar to the perrhenate-sodalite shown in Figure 2.8. Because the concentration of ^{99}Tc (5.0×10^{-8} M) used to synthesize ^{99}Tc-bearing feldspathoid was significantly lower than the Re sodalite, the ^{99}Tc distribution is not readily distinguishable from the background (Figure 2.9).

Therefore, the subsample of the solid phase was chemically digested and analyzed for ^{99}Tc. Results from the chemical digestion of the material suggest that approximately 0.1-wt% ^{99}Tc is present in this sample. Although these results provided evidence that ^{99}Tc can be incorporated into a feldspathoid phase, long-term tests, TCLP, ANSI-16.1, and compressive strength testing have not yet been completed. Therefore, it is difficult to compare the efficacy of this potential waste form with other materials that have a longer history of testing and development.

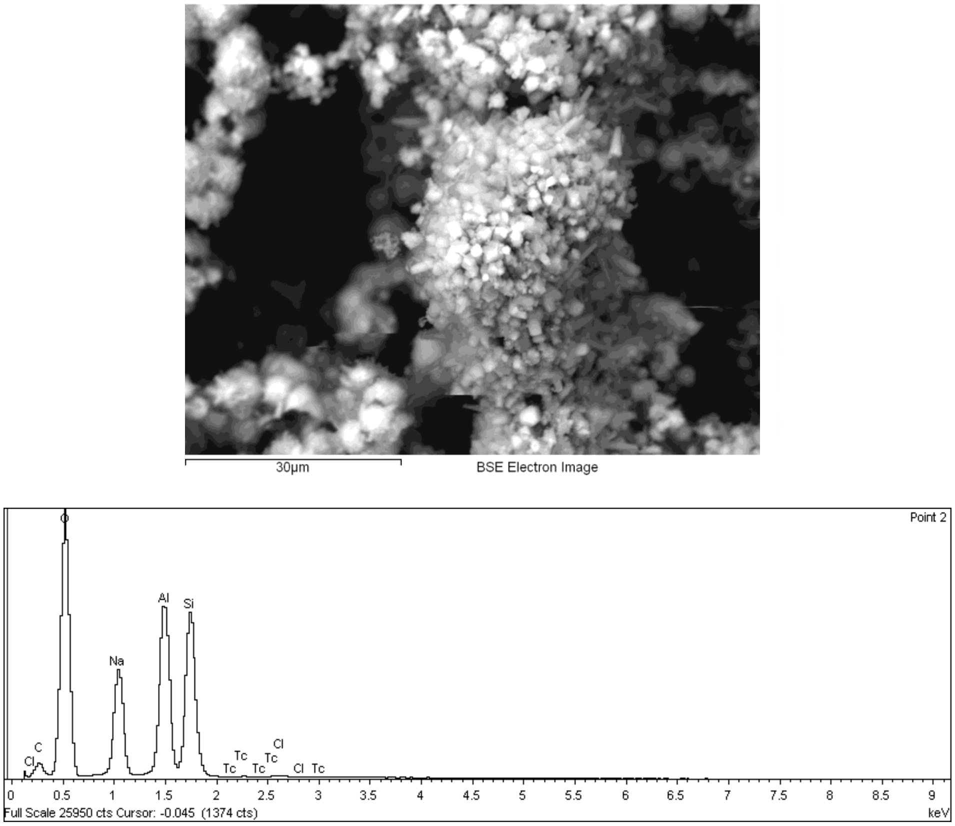

Figure 2.9. SEM Image and Energy Dispersive Spectroscopy Spot Analysis of ^{99}Tc-Bearing Feldspathoid Crystals. The amount of ^{99}Tc used to synthesize this material was approximately 5.0×10^{-8} M $^{99}TcO_4^-$ in comparison to the 3 M ReO_4^- used to synthesize the perrhenate-sodalite shown in Figure 2.8.

2.2 Getters

Getters are most commonly inorganic materials that selectively adsorb radionuclide and metallic contaminants. Typically, these materials have been deployed in two different modes to immobilize and retard contaminant release. The first mode is to reduce the release of radionuclides from monolithic waste forms, for which there are two basic methods. The first is to use getters to selectively scavenge the radionuclide of interest from a liquid waste stream and subsequently incorporate the loaded getters in a cementitious or another monolithic waste form. The second method consists of mixing getters and liquid waste together during formulation of monolithic waste forms. Another mode of getter use consists of deploying the materials in near-field barriers of repositories to adsorb and attenuate any long-lived radionuclides that may be released from the physically degrading and chemically weathering waste packages.

Considerable research effort has been expended during the last several decades to identify suitable getter materials that can immobilize or delay the transport of anionic radionuclides (^{129}I and $^{99}TcO_4$) that would be released from degrading waste packages. Metallic copper and its oxides (Haq et al. 1980), soils and soil minerals (Rancon 1988), cementitious forms (Atkins and Glasser 1990), various types of minerals (Couture and Seitz 1983, Fetter et al. 1996, Gradev 1987, Kang et al. 1999, Krumhansl 2003, Taylor 1990), organophilic clays (Bors et al. 1994a), modified montmorillonites (Sazarashi et al. 1995), and novel adsorbents (Kaplan et al. 2000, Mattigod et al. 2000) have been tested and evaluated for their getter properties for radioiodine. A similar effort was conducted to identify suitable getters for ^{99}Tc (Balsley et al. 1985, Balsley et al. 1996, Balsley et al. 1997, Bock et al. 1988, Byegard et al. 1992, Cui and Eriksen 1996b, Ito and Kanno 1988, Kang et al. 1999, Kang et al. 1996, Krumhansl 2003, Kunze et al. 1996, Liang et al. 1996, Lieser and Bauscher, 1988, Mattigod et al. 2000, Moore 2003, Palmer and Meyer 1981, Strickert et al. 1980, Viani 1999, Wellman et al. 2006, Winkler et al. 1988, Zhuang et al. 1988).

Depending on the intended application, getters can be grouped into two categories: getters used as monolithic waste-form additives and getters used as repository backfills. The typical characteristics of each category of getters are tabulated in Table 2.8.

Table 2.8. Characteristics of Getters

Characteristic	Waste-Form Getter	Backfill Getter
Adsorptive Capacity	Moderate to high (K_d 1000–5 × 10^4 mL/g)	Low (K_d 10–1000 mL/g)
Contaminant Selectivity	High	Low
Contaminant Desorption	Very low	Low to high
Long-term Stability: Chemical physical, and radiation	High	Low to medium
Waste-Form Compatibility	Medium to high	Not applicable
Cost	Moderate to high	Low

The aforementioned investigations indicate that deploying suitable getter materials can be an important aspect of effective long-term containment of contaminants in monolithic waste forms. The main focus of Section 2.2 is to 1) conduct a literature search for data on ^{129}I and ^{99}Tc getters, 2) evaluate the efficacy of these materials to specifically minimize the release radionuclides of concern, and 3) suggest a scheme for selecting appropriate getters for WTP secondary wastes incorporated into waste monoliths.

2.2.1 Getter Properties

Adsorbent materials need to possess certain critical properties to be designated as a getter material. Several investigators have identified a number of important performance characteristics that getter materials should possess for effective deployment (Coons et al. 1980, Klingsberg and Duguid 1980, Moak

1981, Nowak 1980, Viani 1999). Viani (1999) provided a more comprehensive list of criteria (described below) that can be used to assess the properties of potential getter materials.

2.2.1.1 Adsorption Potential

The getter material should specifically adsorb the radionuclide of interest and should exhibit very high selectivity toward radionuclides of concern in concentrations that are likely to be several orders of magnitude less than the concentrations of competing anions and cations. The adsorption capacity of the getter materials should be sufficiently high so that practical amounts of material are needed. Based on laboratory experiments, it should be feasible to reliably predict the long-term adsorption and retention behavior of the getter material.

2.2.1.2 Physical Stability

The getter material should possess sufficient physical and chemical stability that its radionuclide retention performance will not degrade significantly during the designed lifespan of the waste form. It should be physically robust so that its particles will not disintegrate when subjected to moisture, temperature, and the expected radiation regime. The getter media should also be chemically stable under the range of redox conditions (Eh), pH, and solution conditions that are predicted to exist without noticeable degradation in its functionality. The getter material should not adversely affect the chemical and physical integrity of waste forms. It should be possible to predict the physical and chemical stability of the getter material from a combination of laboratory-scale, field-scale, and natural analog studies.

2.2.1.3 Deployment

The getter material deployment should be technically feasible. If the getter material is difficult to deploy and needs special handling, the cost of deployment may preclude its use.

2.2.1.4 Material Cost

The cost of a getter material should be commensurate with its performance. The getter material cost/performance ratio is critical for the deployment decision.

For a getter material to be selected, it should substantially meet all of the above criteria. In the following review, we will examine the published data and suggest a scheme for evaluating and selecting suitable getter materials.

2.2.2 Iodine Getters

Several types of natural and modified minerals have been tested for their suitability as getters for radioiodine. These getters include minerals and synthetic adsorbent materials such as oxides, hydroxides, natural and modified aluminosilicates, synthetic magnesium silicates, sulfides, and coal (see Table 2.9 for references). Recently, novel getter materials designed specifically to remove radioiodine have been synthesized and tested for their getter properties (Mattigod et al. 2000, Krumhansl et al. 2006). Published data on iodine getters from various sources are listed in Table 2.9. It is important to note these data when comparing the K_d values because changes to the geochemical conditions may result in much different K_d

values. Therefore, those K_d values shown in Table 2.9 should be considered more of a guide as to whether a particular getter is effective at immobilizing iodine and should not be used to evaluate the magnitude of effectiveness. To evaluate the magnitude of effectiveness, one must conduct this analysis under the geochemical conditions of interest.

2.2.2.1 Oxide and Hydroxide Minerals

Oxides, hydroxides, and oxyhydroxide minerals typically exhibit low affinity for iodide anions. The distribution coefficient values for these minerals tested in distilled water matrices range from 0 to 6 mL/g (Rancon 1988, Zhuang et al. 1988). In one study involving copper oxides, a K_d value as high as 40 mL/g was reported (Haq et al. 1980). When these minerals were tested in either groundwater or alkali chloride media, lower K_d values (0 to 3 mL/g) were observed (Allard et al. 1981, Hakem et al. 1996).

Recently, various layered double hydroxide (LDH) compounds (commonly known as hydrotalcites) with higher anion-exchange capacities than the natural minerals have been synthesized and tested for their capability to adsorb iodide (Balsley et al. 1996, 1997; Kang et al. 1999, Krumhansl 2003). Kang et al. (1999) reported iodide K_d values that ranged from 38 to 31,000 mL/g for an Mg-Al hydrotalcite compound tested in competing anion-free solutions. However, when various hydrotalcites were tested (Krumhansl 2003) in dilute sodium salt (nitrate, nitrite, aluminate, hydroxide) solutions, the measured K_d values were 5 to 3390 mL/g or about an order of magnitude lower than the values obtained in tests without any competing anions (Kang et al. 1999). Tests conducted by Krumhansl et al. (2006) on hydrotalcites in Yucca Mountain groundwater simulant yielded K_d values of 8 to 36 mL/g and 83 to 263 mL/g for iodide and iodate, respectively. Similarly, low K_d values that ranged from 25 to 290 mL/g were reported for iodide adsorption when samples of Zn-bearing hydrotalcites were tested in 0.01-M sodium chloride solutions (Balsley et al. 1996, 1997). Recently, various mixed metal oxides (Cu-delafossites) have been synthesized and tested as getters for iodine species (Krumhansl et al. 2006). These materials exhibited distribution coefficients that ranged from 3.5 to 31.6 mL/g for iodide and from 0 to 43.7 mL/g for iodates.

The adsorption sites on these minerals are surface hydroxyls that ionize from either protonation or deprotonation; consequently, they exhibit adsorption capacities that vary as a function of pH. Typically, there is a critical pH point of zero change (PZC) at which each of these minerals has an equal number of protonatated and deprotonated adsorption sites. Therefore, the anion adsorption capacities of these minerals increase with decreasing pH, whereas the adsorption capacity decreases as pH values increase above the pH PZC. Also, because the anion adsorption sites are not very selective, the adsorbed anions can be easily desorbed by other anions that are present in higher concentrations in the contacting solution. When encased in high pH matrices, such as cementitious monoliths, radioiodine retained on oxide and hydroxide minerals would be mobilized with the concomitant loss in getter efficacy.

Due to their poor capacity and selectivity for radioiodine and their potential lack of chemical stability, oxide and hydroxide minerals would not meet two important criteria to be reliable getter materials. Although synthetic LDH compounds exhibit better iodide adsorption characteristics than oxide/hydroxide minerals, their desorptive properties have not been tested. Additional testing is needed to adequately evaluate the potential of the LDH compounds as iodine getters.

2.2.2.2 Silicate Minerals

Aluminum and magnesium silicate minerals, such as allophane, montmorillonite, kaolinite, attapulgite, sepiolite, illite, halloysite, vermiculite, and clinoptilolite, have been tested as potential iodine getters. These minerals typically have distribution coefficients that range from 0 to 10 mL/g (Allard et al. 1981, Rancon 1988, Sazarashi et al. 1994). In one case, a K_d value as high as 28 mL/g was reported for illite (Kaplan et al. 2000). These data show that the silicate minerals are no better in their selectivity for radioiodine than oxide and hydroxide minerals. This is not surprising, considering that the major anion adsorption mechanism of silicates is similar to that of oxide-hydroxide minerals. In the case of illite, though, it is hypothesized that a minor fraction of radioiodine may substitute for structural hydroxides in the illite structure.

Several attempts have been made to improve the capacity and selectivity of the silicate minerals by treating them with organic compounds (Bors 1990, 1992; Bors et al. 1998, 1994b, 1996; Sazarashi et al. 1995). Treated silicate minerals, such as montmorillonite and vermiculite, yielded K_d values as high as 5000 mL/g. An improved adsorption performance of these organic-modified minerals has been demonstrated in synthetic groundwater and seawater matrices in which the competing anion (such as chloride) was present in concentrations up to nine orders of magnitude higher than radioiodine in solution (Bors 1992; Bors et al. 1998). However, the desorption characteristics of these organic-modified silicates are unknown. Additionally, the desorptive properties, the long-term chemical stability of these materials in monolithic waste forms, and the cost of deploying these materials are not known.

2.2.2.3 Sulfide Minerals

A number of sulfide minerals have been tested as potential iodide getters. These include copper sulfides, a variety of Cu-Fe-bearing sulfides, and sulfides of Fe, Pb, Ag, and Hg. For Cu-sulfide minerals (covellite and chalcocite), Balsley et al. (1996, 1997) reported K_d values ranging from approximately 60 to 1400 mL/g. Tests on Pb sulfide indicate K_d values that range from 30 to 140 mL/g (Rancon 1988, Strickert et al. 1980; Zhuang et al. 1988). A number of Cu-Fe-bearing sulfides were tested in a de-ionized (DI) water matrix by Strickert et al. (1980) for their iodide adsorption affinities. They reported K_d values for these minerals that ranged from 4 to 3000 mL/g. The Cu-Fe sulfide minerals on average exhibit higher iodide K_d values than both oxide-hydroxide and unmodified silicate minerals. Among the sulfide minerals, the data indicate that Hg-sulfide (cinnabar) and Ag-sulfide (argentite) show high iodide selectivity. Tests conducted in different media, such as groundwater, surface water, waste glass leachate, and concrete leachate, showed that K_d values can be as high as ~3000 mL/g for Hg-sulfide and ~80,000 mL/g for Ag-sulfide (Kaplan et al. 2000, Mattigod et al. 2000).

One of the principal reasons for the better performance of sulfide minerals in general can be ascribed to the nature of cationic species in the sulfide minerals. The cations that form sulfides typically have larger ionic radii, low electro-negativity, and high polarizability. Such characteristics are categorized as soft acid behavior. According to the hard and soft acid and base (HSAB) principle (Sposito 1982), soft cations tend to bind strongly with soft bases (low electro-negativity, high polarizability, prone to oxidation), such as iodide and sulfide. Therefore, relatively softer cations, such as Hg and Ag, have better iodide getter properties compared to less soft cations, such as Cu (I, II), Fe(II), and Pb.

Although sulfides show the best getter characteristics among all minerals, their long-term chemical stability as getters has not been established. It is well known that sulfides oxidize and form highly soluble sulfate minerals. Such a reaction would result in the mobilization of not only radioiodine but also toxic constituents, such as Hg and Ag, from these oxidized getters, and well established acidic conditions (acid mine drainage). Currently, there is a dearth of data on the rate of oxidation and concomitant release of radioiodine and other toxic components from these sulfide-based getters.

2.2.2.4 Other Materials

Materials such as bituminous and lignitic coals have been tested for their capacity to adsorb radioiodide (Balsley et al. 1997). In these tests, coals exhibited higher K_d values at low pH values (~500 to 800 mL/g at pH 3.3 to 3.9). At higher pH values (9.9), these materials showed a significantly reduced K_d value (0 to 25 mL/g), indicating that coals behave very much like oxides and hydroxides in that their anion adsorption capacity declines drastically at pH values above PZC. Therefore, coals as iodine getters have the same limitations (low adsorption affinity under typical closure conditions in IDF) as oxide and hydroxide minerals. Additionally, coal surfaces have an inherent tendency to oxidize very slowly and release adsorbed constituents. Thus, the long-term stability of coal-like solids is practically unknown.

Tests conducted on a synthetic material (calcium monosulfate aluminate) in dilute sodium chloride solutions indicated that the radioiodine affinity (K_d) of this material varied from 25 to 290 mL/g (Balsley et al. 1997). Other materials, such as a Pb-carbonate mineral (cerrussite) and metallic copper, have also been tested as iodine getters (Haq et al. 1980, Rancon 1988). Due to the limited test data on these miscellaneous materials, their potential as getters for iodine cannot be fully evaluated.

2.2.2.5 Novel Synthetic Materials

During the last 10 years, a new class of getter materials has been developed. It consists of mesoporous ceramic substrates with specifically tailored pore sizes (from 20 to 100 Å) and very high surface areas (~1000 m^2/g). These high-surface-area substrates are functionalized with monolayers of well-ordered functional groups that have a high affinity and specificity for specific types of free or complex cations or anions. These self-assembled monolayers on mesoporous silica (SAMMS) materials with high adsorption properties have been successfully tested on a series of cations (Hg, Cu, Cd, and Pb), oxyanions (As, Cr, Mo, and Se), anions (I), and actinides (Pu, U, and Np). Detailed descriptions of the synthesis, fabrication, and adsorptive properties of these novel materials have been published (Fryxell et al. 1999a, Fryxell et al. 1999b, Kemner et al. 1999, Liu et al. 1998, Liu et al. 2000, Mattigod et al. 1997, Mattigod et al. 1998).

Recently, some of the metal-capped thiol-SAMMS materials specifically designed to adsorb soft-base anions like iodide have been tested for their getter properties. The tests included iodide adsorption from aqueous matrices that are expected to prevail in post-closure environments, such as groundwater, surface water, glass leachate, and concrete leachate. The data showed that the metal-capped SAMMS materials had iodide K_d values as high as 10^5 to 10^6 mL/g (Kaplan et al. 2000, Mattigod et al. 2000). These high values indicate the remarkable selectivity of these novel materials in adsorbing iodide, especially since the test solutions contained competing halide ions, such as Cl, Br, and F, at concentrations 8 to 10 orders of magnitude greater than the concentrations of radioiodine.

Another recently developed set of novel materials is layered bismuth hydroxides (LBHs) (Krumhansl et al. 2006). These materials were shown to be capable of incorporating both iodide (K_d: 6.3×10^2 to

2.5×10^4 mL/g) and iodate ions (K_d: 50 to 4.0×10^4 mL/g) in the structure. Presently, the long-term performance of these getters as part of monolithic waste forms is unknown; therefore, the viability of these novel getter materials cannot be assessed.

Table 2.9. Iodide Distribution Coefficient Data for Natural and Synthetic Getter Materials

Getter Material	Kd (mL/g)	Matrix Solution	Eq. pH	Molar Conc Ratio (Cl, Br, F)/I	Reference
Cu delafossites	3.5 – 31.6 (I^-) 0 – 43.7 (IO_3^-)	Yucca Mtn groundwater simulant (J13)	7	--	Krumhansl et al. 2006
Hydrotalcites	7.8 – 36.3 (I^-) 83.2 – 263.0 (IO_3^-)				
Layered Bi hydroxides	631 – 25,119 (I^-) 50 – 39,811 (IO_3^-)				
Hydrotalcites (Al, Bi, Cu^{2+}, Cu^+, La, Sn^{2+}, Sn^{4+}, Zn)	5 – 3,390	Dilute $NaNO_3$-$NaNO_2$, NaOH-$NaAlO_2$ Solution	--	--	Krumhansl 2003
Hg-thiol SAMMS	100,000	Groundwater	6.32 – 7.24	Cl/I: 3×10^{10} – 9×10^{10}	Mattigod et al. 2000
	420,000	Glass Leachate	3.46 – 8.34	Br/I: 2×10^8	
Ag-thiol SAMMS	99,000	Groundwater	6.79 – 7.37	F/I: 1×10^9	
	100,000	Glass Leachate	4.41 – 8.35		
Cinnabar	2600	Glass Leachate	7.97 – 8.03		
Argentite	18,000	Glass Leachate	2.66 – 8.33		
Chalcocite	50 – 200	Glass Leachate	8.32 – 8.47		
Chalcopyrite	10 – 50	Glass Leachate	8.18 – 8.27		
Hg-thiol SAMMS	2,000 – 2,000,000	Surface water	3.00	Cl/I: 1×10^{10}	Kaplan et al. 2000b
	8,000 – 600,000	Conc Leachate	9.55	Br/I: 2×10^7- 1×10^8	
Ag-thiol SAMMS	20,000 – 300,000	Surface water	3.72	F/I: 4×10^8 - 1×10^9	
	9,000 – 600,000	Conc Leachate	11.94		
Cinnabar	700 – 3,000	Surface water	8.15		
	0 – 100	Conc Leachate	12.17		
Argentite	0 – 80,000	Surface water	5.98		
	20,000 – 700,000	Conc Leachate	11.94		
Ag-carbon	1,000 – 5,000	Surface water	7.56		
	2 0 – 4,000	Conc Leachate	11.18		
Illite	15 – 28	0.01 M $CaCl_2$		Cl/I: 3×10^{12}	Kaplan et al. 2000a
Hydrotalcite (Al)	38 – 31,000	4.6×10^{-6} M ^{125}I in 1.8×10^{-5} – 5.3×10^{-2} M NaI and HI solution	10.62 -11.5		Kang et al. 1999
Titanium Oxide	0.25 – 3	0.001 M NaCl	9.5 - 3.5	--	Hakem et al. 1996
Titanium oxide	0.05 – 0.11	0.1 M NaCl	9.5 - 3.5		
Cinnabar	70 – 3,400	0.01 M NaCl	10.0 – 4.0	Cl/I: 100	Balsley et al. 1996, 1997
Covellite	145 – 1,380	0.01 M NaCl	8.3 – 4.0		
Chalcocite	60 – 1,290	0.01 M NaCl	10.0 – 4.0		
CMSA 1	34 –110	0.01 M NaCl	10.0 – 4.0		
CMSA 2	30 – 100	0.01 M NaCl	10.9 – 5.6		
Zn hydrotalcite-Cl	25 – 290	0.01 M NaCl	10.0 – 4.1		
Zn hydrotalcite-SO_4	50 – 290	0.01 M NaCl	10.0 – 4.1		
Zn hydrotalcite-CO_3	40 –80	0.01 M NaCl	10.5 – .8		
Lignite Coal	0 –520	0.01 M NaCl	9.9 –3.9		
Subbituminous Coal	25 – 840	0.01 M NaCl	9.9 – 3.3		
Ag-thiourea mont	61 – 4,900	NaI and NaCl	~7.0	Cl/I: ~0 - 19	Sazarashi et al. 1994
Allophane	2.1 – 3.6	0.01 M KI	5.6 –6.0		1995
Attapulgite	0.2 – 0.9	0.01 M KI	8.0		
Montmorillonite	0	0.01 M KI	7.7 – 8.1		
Chalcopyrite	14.1 – 15.1	0.01 M KI	6.3 – 6.6		
Cinnabar	4,000 – 20,000	0.01 M KI	6.9 – 7.0		
Cinnabar	0 – 50	NaI and NaCl	9.4	Cl/I: 1	Ikeda et al. 1994
Org-treated bentonite	2 – 1,500	DI water	10.0 – 8.7	--	Bors 1990

Table 2.9. Iodide Distribution Coefficient Data for Natural and Synthetic Getter Materials

Getter Material	Kd (mL/g)	Matrix Solution	Eq. pH	Molar Conc Ratio (Cl, Br, F)/I	Reference
Org-treated vermiculite	1 – 26,000	DI water	10.0 –9.4		
Org-treated Cretaceous clay	4 – 30,000	DI water	9.6 –8.4		
HDPY-vermiculite	10 – 5,500	DI water	--	--	Bors 1992
HDPY-vermiculite	10 – 4,500	syn groundwater	--	Cl/I: ~2 × 10^{10}	
HDPY cretaceous Clay	10 – 5,500	DI water	--		
HDPY-cretaceous Clay	10 – 800	syn groundwater	--	Cl/I: ~2 × 10^{10}	
HDPY-vermiculite	2 – 10,000	KI soln	--	--	Bors et al. 1994
HDPY-cretaceous Clay	1 – 10,000	KI soln	--		
HDPY-vermiculite	25 – 3,390	DI water	--	--	Bors et al. 1996
HDPY-MX80 bentonite	3 – 5,000	DI water	--	Cl/I: ~3 × 10^{9}	Bors et al. 1998
HDPY-MX80 bentonite	2 – 1,000	syn groundwater	--	Cl/I: ~4 × 10^{6},	
HDPY-MX80 bentonite	10 – 450	natural water	--	F/I:~1 × 10^{8}	
HDPY-MX80 bentonite	0 – 350	1/2 strength seawater	--	Cl/I: ~5 × 10^{6}	
Chalcopyrite	700	NaI solution	7.2	--	Rancon 1988
Chrysocolla	40	NaI solution	7.2		
Cerussite	8	NaI solution	7.0		
Galena	80	NaI solution	8.6		
Bauxite, goethite, hematite, laterite, limonite, siderite	0 – 6	NaI solution	6.5 – 7.6		
Quartz, attapulgite, bentonite, illite, clinoptilolite, kaolinite, sepiolite, vermiculite, zeolite	0 - 4	NaI solution	6.0 – 8.4		
Chalcopyrite	42 –97	DI water	7.73 – 8.24	--	Zhuang et al. 1988
Galena	62 – 137	DI water	3.53 – 6.14		
Pyrite	3 – 6	DI water	7.05 – 8.10		
Stibnite	2 – 3	DI water	4.52 – 5.66		
Molybdenite	1 – 3	DI water	7.62 – 7.89		
Rare-earth hematite	1 - 2	DI water	7.91 – 8.34		
Cinnabar	10 – 100	Groundwater,	9.0 – 3.0	Cl/I: ~3 × 10^{8} - 4 × 10^{6}	Allard et al. 1981
Chalcopyrite, Galena	0.1 –10	4M NaCl	9.0 – 3.0		
Fe, Al, Pb hydroxides	0.1 – 100	Groundwater,	9.0 – 3.0		
Olivine, attapulgite, sepiolite, halloysite, montmorillonite, quartz	0.1 – 10	4M NaCl Groundwater, 4M NaCl	9.0 – 3.0		
Metallic Cu	0.4 – 190	NaI soln	7.2	--	Haq et al. 1980
Cuprite	4 – 40	NaI soln	7.2		
Tenorite	0.5 – 23	NaI soln	7.2		
Bournonite	200 – 1,000	DI water	--	--	Strickert et al. 1980
Pyrite	300 – 3,000	DI water	--		
Tetrahedrite	4 – 1,500	DI water	--		
Bornite	30 – 970	DI water	--		
Tennantite	100 – 350	DI water	--		
Enargite	150	DI water	--		
Chalcopyrite	190	DI water	--		
Galena	26	DI water			

2.2.3 Technetium Getters

The same types of minerals that have been tested as getters for radioiodine have also been tested for their technetium getter properties. A number of studies have been conducted to evaluate the getter properties of various oxides, hydroxides, silicates, sulfides, and activated carbon. Published data on technetium getters are listed in Table 2.10. It is important to note these data when comparing the K_d values because changes to the geochemical conditions may result in much different K_d values. Therefore, these K_d values shown in Table 2.9 should be considered more of a guide as to whether a particular getter is effective at immobilizing iodine and should not be used to evaluate the magnitude of effectiveness. To evaluate the magnitude of effectiveness, one must conduct this analysis under the geochemical conditions of interest.

2.2.3.1 Oxide and Hydroxide Minerals

Adsorption tests showed that iron oxides and hydroxides have a relatively low affinity (K_d: 0.2 to 5 mL/g) for the pertechnetate ion (Palmer and Meyer 1981). Their data also indicated that these minerals exhibited anion adsorption behavior that is typical for minerals with variable surface charges (i.e., these minerals exhibited decreasing affinity for the pertechnetate ion with increasing pH of the contacting solution). Studies conducted on hematite by Zhuang et al. (1988) and Bostick et al. (1990) resulted in K_d values that were similar in magnitude (1 to 5 mL/g) to that noted by Palmer and Meyer (1981). Another study involving extensive tests of various types of iron oxides in granitic groundwater indicated K_d values of 0 to 5 mL/g under oxic conditions and relatively higher K_d values of 0 to 190 mL/g under anoxic conditions (Vandergraff et al. 1984). The increases in K_d values were attributed to the potential reduction of Tc(VII) to the less-soluble Tc(IV) form. Recently, it was shown that precipitating Fe(II) hydroxide in a Tc(VII) spiked raffinate simulant resulted in K_d values ranging from 1.3×10^3 to 2.8×10^3 mL/g (Aloy et al. 2007). These values, no doubt, reflect the reduction of ^{99}Tc and the co-precipitation of Tc(IV) with iron hydroxide. This was confirmed by the fact that after exposure to air for 11 days, about 30% of the co-precipitated ^{99}Tc was released into solution.

Also, other experiments conducted to investigate the effects of various matrix solutions on ^{99}Tc immobilization by magnetite yielded K_d values ranging from 4 to 490 mL/g (Vandergraff et al. 1984). However, lower K_d values (4 to 57 mL/g) were observed in matrix solutions containing Tc(IV) complexing ligands, such as chlorides and phosphates. In another study, Bird and Lopata (1980), in which solutions containing only trace concentrations were used, noted no measurable pertechnetate adsorption by magnetite. Studies by Lieser and Bauscher (1988), in which groundwater was used, and Bostick et al. (1990), in which simulant raffinate was used, also showed negligible adsorption of ^{99}Tc (K_d: <0.1 to 3 mL/g). These observations were confirmed by Byegard et al. (1992), who observed that magnetite, when tested in synthetic and natural groundwater matrices (containing relatively high concentrations of SO_4) under both oxic and anoxic conditions, showed relatively poor affinity for ^{99}Tc (K_d: 0.3 to 1.3 mL/g). However, in tests conducted in groundwaters containing relatively low concentrations of SO_4 and fortified with 6 mg/L of ferrous iron, Byegard et al. (1992) observed enhanced attenuation of ^{99}Tc (K_d: 1 to 343 mL/g), which was attributed to the oxidation of Fe (II) coupled with the reduction of Tc(VII) to more insoluble Tc(IV) species.

Detailed studies of the reductive immobilization mechanisms for ^{99}Tc by Fe(II)-bearing minerals were conducted by Cui and Eriksen (1996a, 1996b). They found that the specific surface area, the Fe(II) content, and the mode of bonding of Fe (II) in the mineral were the principal factors that influenced the rate of ^{99}Tc reduction. They found that among Fe(II)-bearing minerals, magnetite was the most efficient reductant for Tc(VII) because of its low band gap between valence and conduction bands.

A number of studies have been conducted to examine the effectiveness of metallic iron for promoting the immobilization of ^{99}Tc through a reduction reaction (Del Cul et al. 1993, Ding et al. 2001, Duncan et al. 2008, Kunze et al. 1996, Vandergraff et al. 1984). Studies conducted by Vandergraff et al. (1984)

with metallic iron substrate in granitic groundwater yielded relatively high K_d values of 190 to 4990 mL/g. The effectiveness of metallic iron for reductive immobilization of ^{99}Tc (in heavy metal sludge filtrates and simulated raffinate solutions) was also confirmed by studies conducted by Del Cul et al. (1993) and Bostick et al. (1990), who observed K_d values as high as 18 900 to 33 233 mL/g. Metallic iron was also observed (Kunze et al. 1996) to successfully immobilize ^{99}Tc in 6- to 12-M magnesium chloride brine (K_d ~121 700 mL/g). Testing of metallic iron by Ding et al. (2001) using 0.1-M NaCl, $NaNO_3$, and $NaClO_4$ solutions yielded K_d values in the range of 1800 → 200 000 mL/g). In another test conducted with a concentrated brine (~28% W/V) as the medium, metallic iron showed very low K_d values (0 to 14 mL/g) (Duncan et al. 2008). These low values could be, no doubt, attributed to the interference effect of ions in the high ionic strength solution.

Results from adsorption tests conducted by Bird and Lopata (1980) indicated that Cu and Pb oxides (CuO, Cu_2O, and PbO) did not adsorb any pertechnetate. In contrast, recent results from Balsley et al. (1997) indicated that when tested in a DI water matrix, Cu oxides did adsorb (K_d: 43 to 55 mL/g) TcO_4^- ions. However, they did not test the affinity of these oxides for technetium in the presence of competing tetrahedral anions such as sulfate. In another study, Zhang et al. (2000) demonstrated that boehmite (Al oxyhydroxide mineral) can adsorb perrhenate. Their data also showed significantly less adsorption with increasing pH, with no adsorption at pH values greater than ~8. They noted decreasing perrhenate adsorption in the presence of concentrations of a competing oxyanion in solution, such as NO_3, ranging from 0.005 to 0.1 M. Palmer and Meyer (1981) also observed that when tested in a sodium chloride brine medium, a number of oxide/hydroxide minerals exhibited relatively low adsorption affinity (K_d: 0 to 26 mL/g) for ^{99}Tc. Tests conducted by El-Wear et al. (1992) on Ti oxide and Li-based mixed hydroxides also showed very low K_d values (1 to 31 mL/g). Recent testing of bismuth hydroxides in Tc(VII)-spiked Yucca Mountain groundwater simulant yielded K_d values that ranged from 23 to 340 mL/g (Krumhansl et al. 2006).

Synthetic LDH compounds (hydrotalcites) have been tested for their capability to adsorb pertechnetate (Balsley et al. 1997, Kang et al. 1996, Krumhansl 2003). Kang et al. (1996) reported K_d values that ranged from 265 to 6160 mL/g for an Mg-Al hydrotalcite compound tested in competing anion-free solutions. Also, various hydrotalcites tested by Krumhansl (2003) adsorbed pertechnetate (K_d: 137 to 4890 mL/g) from dilute sodium salt (nitrate, nitrite, aluminate, hydroxide) solutions. Significantly lower K_d values (1 to 84 mL/g) for pertechnetate adsorption were obtained for a sample of Zn-bearing hydrotalcite (Balsley et al. 1997).

These studies indicate that relatively poor capacity and selectivity and a potential lack of chemical stability preclude the use of many of the oxide and hydroxide minerals as effective getter materials for technetium. Synthetic LDH compounds appeared to exhibit better getter properties than natural materials. Similarly, magnetite and metallic iron under certain limited conditions appear to be effective getters for ^{99}Tc. However, the chemical stability and the tendency for ^{99}Tc mobilization from radiolysis effects and the potential influx of oxic groundwaters and/or leachates (reflecting site-specific conditions) need to be evaluated for LDH, magnetite, and metallic iron materials.

2.2.3.2 Sulfide Minerals

Studies conducted in DI water matrices (Lieser and Bauscher 1988, Strickert et al. 1980), in 0.1 to 4-M sodium chloride solutions (Palmer and Meyer 1981), and in 0.1-M ammonium hydroxide solution

(Zhuang et al. 1988) indicated that sulfide minerals, such as chalcopyrite, chalcocite, enargite, bornite, galena, molybdenite, pyrite, tennantite, and Ag-tetrahedrite, had a relatively low affinity for pertechnetate ion (K_d: <0.1 - ≤ 3 mL/g). Greenockite (cadmium sulfide, CdS), tested without any ionic strength controlling electrolyte, showed K_d values in the range of 2 to 13 mL/g (El-Wear et al. 1992). However, using finely ground (<63 µm) material in a DI water matrix, Bock et al. (1988) noted that galena and pyrite exhibited higher K_d values of 50 to 1000 and 70 to 100 mL/g, respectively. These investigators also observed that other sulfide minerals, such as pyrrhotite and stibnite, had a very high affinity (~50 000 mL/g) for the pertechnetate ion. In studies using a <10-µm particle-size pyrrhotite in a groundwater matrix, Lieser and Bauscher (1988) showed that this mineral had only moderate affinity to attenuate Tc(VII). Similar attenuation affinity for Tc(VII) was measured (K_d: ~143 to 1980 mL/g) for sand-sized (125- to 250-µm) stibnite. Another sulfide mineral, greigite, was also found to effectively remove technetium from raffinate simulant (K_d: ~1170 mL/g) and from heavy metal sludge filtrate (K_d: ~110 to 6100 mL/g) (Bostick et al. 1990, Del Cul et al. 1993). Recently, Liu et al. (2008), upon testing an amorphous form of iron sulfide in 0.1-M NaCl solution, found that it exhibited K_d in excess of 6×10^3 mL/g.

Published data indicate that the ^{99}Tc attenuation performance of sulfide minerals is highly variable and appears to depend on a number of factors, such as the type of mineral, particle size, type of contacting solution, pH, ionic strength, and Eh (Balsley et al. 1997, Bock et al. 1988, Fried et al. 1978; Lee and Bondietti 1983, Lieser and Bauscher 1988, Palmer and Meyer 1981, Strickert et al. 1980; Zhuang et al. 1988, Zhuang et al. 1995). It is generally recognized that the principal mechanisms of ^{99}Tc attenuation by sulfide minerals are through either reduction of Tc(VII) to low-solubility Tc(IV) phases such as $TcO_2 \cdot x\ H_2O$ (Bock et al. 1988) or by direct precipitation of Tc(VII) as the sparingly soluble sulfide mineral Tc_2S_7 (Bidoglio and Plano 1985, Lee and Bondietti 1983, Lieser and Bauscher 1988). However, spectroscopic work (extended X-ray absorption fine structure [EXAFS] and XANES) on reducing grouts indicated that Tc(IV) may exist as Tc_3S_{10} (Lukens et al. 2005). Although some sulfide minerals show better ^{99}Tc attenuation characteristics, their long-term stability for deployment as ^{99}Tc getters has not been established. It is also necessary to establish the rate of oxidation and the concomitant rate of release of Tc(VII) from various sulfide getters.

2.2.3.3 Blast Furnace Slag and Other Minerals

When used as a part of cementitious waste form, BFS is known to reduce Tc(VII) release through reduction (Aloy et al. 2007, Gilliam et al. 1990, Gilliam et al. 1988, Kaplan et al. 2008, Langton 1988a, Langton 1988b, NRC 2001, Spence and Shi 2005). Blast furnace slag is also used as part of a base mix in Cast Stone monolithic waste forms that are being developed for treating Tc(VII)-bearing secondary waste streams at Hanford (Cooke et al. 2009, Lockrem 2005b). Depending on the source, BFS has reductive capacities that range from 0.82 to 4.79 meq/g (Aloy et al. 2007, Kaplan et al. 2008, Lukens et al. 2005). Test data indicate that unless protected from oxygen intrusion, the BFS getter-based waste forms tend to release ^{99}Tc by oxidation of Tc_3S_{10} (Aloy et al. 2007, Lukens et al. 2005).

Materials such as activated carbon (charcoal) have been tested for their capacity to adsorb pertechnetate (Ito and Akiba 1991, Nowak 1980). Tests with activated carbon conducted by Nowak (1980) in 5-M sodium chloride solution showed a moderate affinity (K_d: 310 to 380 mL/g) for Tc(VII). However, tests conducted by Ito and Akiba (1991) showed that although activated carbon showed very high affinity for Tc(VII) in a DI water matrix (K_d: 8000 to 10 000 mL/g), the affinity decreased in 1-M sodium chloride solution (K_d: 300 to 5000 mL/g) and in $NaClO_4$ solution (K_d: 10 to 300 mL/g).

Minerals such as gypsum, dolomite, apatite, and monazite have a relatively low affinity (K_d: 0.3 to 6 mL/g) for Tc(VII) (Palmer and Meyer 1981). Zirconium phosphate and Sb silicophosphate also showed low affinities (K_d <0.1 to 11 mL/g) for Tc(VII) (El-wear et al. 1993). Materials such as bone black, fishbone, and Fe(III) phosphate also showed very low selectivity (K_d: 0 to 5 mL/g). The same materials when treated with a reductant such as Fe(II) sulfate showed higher selectivities (1800 to 6400 mL/g). These data showed that Fe(II) reduced Tc(VII) and precipitated it as a low solubility Tc(IV) compound.

Tests conducted on a synthetic compound (calcium monosulfate aluminate) in dilute sodium chloride solutions indicated that Tc(VII) adsorption (K_d) was ~134 mL/g (Balsley et al. 1997). Tests conducted by Zhao et al. (2002) with Sn(II)- and Fe(II)-treated synthetic and bovine apatites in 0.1-M KNO_3 solution showed very high K_d values (7110 to 357 100 mL/g). Later tests by Moore (2003) confirmed that Sn(II)-treated apatite was a very effective getter for pertechnetate (K_d: 475 000 to 3 202 100 mL/g in a groundwater matrix, 5140 to 4890 mL/g in concentrated sodium salt solutions consisting of $NaNO_3$-$NaNO_2$, and NaOH-$NaAlO_2$).

2.2.3.4 Novel Synthetic Getters

A self-assembled monolayer functionality (Cu-ethylenediamine complex) with high specificity for tetrahedral oxyanions has been synthesized (Fryxell et al. 1999a, Fryxell et al. 1999b, Kemner et al. 1999, Liu et al. 1998, Liu et al. 2000). Substrates consisting of mesoporous silica and resin have been monolayered with Cu-ethylene di-amine (EDA) functionality and tested for their Tc(VII) affinity in matrix solutions that are expected to prevail in post-closure environments, such as groundwater and glass leachate. The data indicate that Cu-EDA SAMMS material could specifically adsorb ^{99}Tc from both groundwater (K_d: 50 to 790 mL/g) and simulated glass leachate (K_d: 340 to 720 mL/g). Comparatively, the same functionality (Cu-EDA) on a resin substrate exhibited very high specificity in a groundwater matrix (K_d: 3,400 to 37,500 mL/g), but poor specificity in a simulated glass leachate (K_d: 1 to 30 mL/g). These differences indicate that the adsorption performance of the Cu-EDA functional monolayer is dependent on the type of substrate to which it is attached.

Scoping tests conducted on Sn(II)-bearing nanoporous phosphates in dilute $NaHCO_3$ solution indicated K_d values exceeding 90 000 mL/g (Wellman et al. 2006). However, more extensive tests are needed to fully evaluate the ^{99}Tc getter potential of these novel synthetic materials.

In Section 2.1.8, sodalite is highlighted as a waste form, but it can be an effective getter for ^{99}Tc also. Several studies have shown that the cage-like structure of sodalite can trap and immobilize up to 9 mol% of oxyanions (Brenchley and Weller 1994, Buhl et al. 2001, Buhl and Lons 1996, Hund 1984, Johnson et al. 2000, Srdanov et al. 1994). However, further study is needed to demonstrate the effectiveness of sodalite as a stable getter for long-term sequestration of Tc(VII).

Table 2.10. Technetium Distribution Coefficient Data for Natural and Synthetic Getter Materials

Getter Material	K_d (mL/g)	Matrix Solution	Eq. pH	SO_4/TcO_4 Molar Conc Ratio	Reference
Iron Sulfide (Am)	>6000	0.1 M NaCl	6.1 – 9.0	--	Liu et al. (2008)
Bone Black	4.7	TcO_4 solution (28% W/V)	5 to 6	--	Duncan et al. (2008)
	30.8		12		
	3.5		12		
Fishbone	0		5 to 6		
	41.7*		12		
	11.3		12		
Metallic Iron	0		5 to 6		
	97.7*		12		
	0		12		
Fe(III) Phosphate	14.7		5 to 6		
	0*		12		
	90 to 1029		12		
Tin apatite	531 to 2045		5 to 6 12		
Fe Hydroxide	1280 - 2770	Savannah River site alkaline raffinate simulant	12.37 – 12.60	--	Aloy et al. (2007)
Nanoporous tin phosphates	>90,000	0.002M $NaHCO_3$	8	--	Wellman et al. (2006)
Bismuth hydroxides (with and without Li)	23 - 340	J-13 simulant (Yucca Mount., groundwater	7	--	Krumhansl et al. (2006)
Sn(II) treated Apatite	475,000 – 3,202,100	9.11×10^{-6} – 1.15×10^{-5} M Tc in groundwater	6 – 10	--	Moore (2003)
	5,140 – 6,510	9.11×10^{-6} – 9.11×10^{-5} M Tc in conc. $NaNO_3$-$NaNO_2$, NaOH-$NaAlO_2$ solution	13		
Hydrotalcites (Al, Bi, Cu(II), Cu(I), La, Sn(II), Sn (IV), Zn)	137 – 4,890	Dilute $NaNO_3$-$NaNO_2$, NaOH-$NaAlO_2$ Solution	--	--	Krumhansl (2003)
Sn(II) and Fe(II) treated Synthetic & Bovine Apatites	7,110 – 357,100	0.1M KNO_3	8	--	Zhao et al. (2002)
Fe Metal	1,800 - >200,000	0.1M NaCl, $NaClO_4$, $NaNO_3$	6.4 – 7.0	--	Ding et al. 2001
Cu-EDA SAMMS	50 – 440	Groundwater	5.83 – 7.44	6 x 10^3	Mattigod et al. 2000
	66 –- 790	Groundwater		7 x 10^2	
	340 -720	Sim glass leachate		1 x 10^2	
Cu-EDA Resin	3,400 – 7,300	Groundwater	7.76 – 8.04		
	8,400 – 37,500	Groundwater			
	1 – 30	Sim glass leachate			
Boehmite, Al hydroxide	0 – 110	0.001 M ReO_4 in 0.001 M $NaNO_3$	5.2 – 9.7	--	Zhang et al. 2000
Cu Oxides	43 – 55	TcO_4 solution	6.8 – 7.1	--	Balsley et al. 1997
Chalcocite	31		8.6		
Covellite	67		5.4		
Zn hydrotalcites	1 – 84		5.3 – 7.7		
CMSA	134		11.7		
Imogolite	23		6.4		
Hydrotalcite	265 – 6,160	0.3 M NH_4TcO_4, 0.1	10.59 – 12.51		Kang et al. 1996

Table 2.10. Technetium Distribution Coefficient Data for Natural and Synthetic Getter Materials

Getter Material	K_d (mL/g)	Matrix Solution	Eq. pH	SO_4/TcO_4 Molar Conc Ratio	Reference
		M NH_4OH, 0.1 M $HTcO_4$ solution			
Fe metal	~121,700	1 × 10^{-5} M TcO_4 in ~6 – 12 M $MgCl_2$ brine	--	60 – 1.8 × 10^4	Kunze et al. 1996
Ti Oxide	1 – 31	TcO_4 solution	1.3, 6.5, 12.7	--	El-Wear et al. (1992)
Greeknockite (CdS)	2 – 13				
Zr Phosphate	1-11				
Sb silicophosphate	<0.1 – 9				
Li-Mn-Al hydroxide	2 – 10				
Li-Ti-Cr hydroxide	2 – 11				
Fe Metal	1,490 – 18,700	13 mg/L TcO_4 in heavy metal sludge filtrate	8.5	SO_4/TcO_4	Del Cul et al. 1993
Greigite	110 – 6,100				
Magnetite	0.3 – 1.3	5 × 10^{-9} M TcO_4 in oxic and anoxic syn and natural groundwater	7.4 – 8.8	6 x 10^3 – 6.6 x 10^5	Byegard et al. 1992
Magnetite	1 – 343	6 × 10^{-6} M $TcO_4$$^{+6}$ mg/ L Fe^{2+} in oxic and anoxic syn and natural groundwater	7.4 – 8.8	5.2 – 550	
Activated carbon	8,000 – 10,000	TcO_4 solution	10 – 2	--	Ito and Akiba 1991
	300 – 5,000	1 M NaCl	10 – 2		
	90 –300	0.001 M $NaClO_4$	10 – 2		
	10 – 90	0.1 M $NaClO_4$	10 – 2		
Fe Metal	33233	0.2. mg/L TcO_4 in surrogate raffinate solution	7 – 9	1.3 x 10^4	Bostick et al. 1990
Greigite	1166		8.1 – 8.3		
Hematite	5		3.9 – 6.9		
Magnetite	3		3.9 – 8.9		
Pyrrhotite	~50000	TcO_4 solution in 0.007 M bicarbonate groundwater	~5.2 – 7.2	--	Bock et al. 1988
Stibnite	~2000 – 50,000		~7.2 – 7.5	--	
Galena	~50 – 1,000		~6.8 – 7.2	--	
Pyrite	~70 – 100		~2.5 – 7.2	--	
Loellingite	~0.4 – 400		~6.8 – 7.2	--	
Chalcocite	~0.4 – 5		~5.2 – 7.2	--	
Sphalerite	~0.1 – 0.3		~7.2 – 9.8	--	
Stibnite	~200	TcO_4 (2 × 10^7 Bq/mL) in 0.1 M NH_4OH	--	--	Zhuang et al. 1995
Stibnite	143 – 1,980	TcO_4 (2 × 10^7 Bq/ml) in 0.1 M NH_4OH	3.84 – 6.22	--	Zhuang et al. 1988
Molybdenite	0.6 – 2.7		--		
REE hematite	1.0- 5.1		8.02 - 8.04		
Silicate minerals (oxic conditions)	0.2 – 5	TcO_4 in 0.16 M $NaNO_3$ solution		--	Ito and Kanno 1988
Silicate minerals (anoxic conditions)	13 -71				
Pyrrhotite	443 – 667	10^{-6} M TcO_4 in groundwater	3.5 – 5.4	--	Lieser and Bauscher 1988
Pyrite	<0.1		5.2 – 5.9		
Magnetite	<0.1		6.6 – 7.6		
Hematite, limonite, Goethite, ilmenite,	0 - 5	3 × 10^{-12} M TcO_4 in oxic granite groundwater	~6.5	2 × 10^7	Vandergraff et al. 1984
Fe metal	4990				
Hematite, limonite, Goethite, ilmenite	0 – 190	3 × 10^{-12} M TcO_4 in anoxic granite groundwater		2 × 10^7	
Fe metal	~190				
Magnetite	4 – 490		~6.5 – 8.2	2 × 10^7 –	

Table 2.10. Technetium Distribution Coefficient Data for Natural and Synthetic Getter Materials

Getter Material	K_d (mL/g)	Matrix Solution	Eq. pH	SO_4/TcO_4 Molar Conc Ratio	Reference
		$3 \times 10^{-12} – 1 \times 10^{-4}$ M TcO_4 in DI water, granite groundwater, WN-1 saline, Can. Shield saline, Na_2HPO_4 solution, humic acid.		2×10^9	
Na bentonite	132 – 2,269	4.187×10^{-14} M TcO_4 in DI water	5.68 – 10.1	--	Shade et al. 1984
Fe- silicate	0				
Silicates, oxides, hydroxides	0 – 26	TcO_4 in 0.01 – 4 M NaCl solutions		--	Palmer and Meyer 1981
Sulfides (Chalcocite, Chalcopyrite,	1.6 – 3.2			--	
Galena,	1.8			--	
Molybdenite,	0.3			--	
Pyrite)	0.8 – 6.3				
Gypsum					
Dolomite					
Phosphates (Apatite, monazite)					
Chrysocolla	10 – 20	5×10^5 dpm TcO_4 solution	--	--	Strickert et al. 1980
Chalcopyrite,	≤3		--	--	Fried et al. 1978
Enargite, bornite,			--	--	
pyrite, tennantite,			--	--	
Ag- tetrahedrite	1 – 10		--	--	
Galena	2 – 2,000		--	--	
Tetrahedrite	200 – 2,000		--	--	
Bournonite					
Activated Charcoal	310 -380	6- 6×10^{-5} M TcO_4 in ~5 M NaCl brine	--	--	Nowak 1980b
Bentonite, hectorite	0 - 1		--	--	
Augite	23	1×10^{-4} M TcO_4 solution	--	--	Bird and Lopata 1980
Biotite	1				
Galena, sphalerite	0				
Smithsonite	0				
CuO, Cu_2O, PbO,	0				
Magnetite, graphite	0				

*Oxidation-Reduction Potential adjusted

2.2.4 Process for Getter Selection and Evaluation

Good adsorption performance (capacity, kinetics, and selectivity for contaminants of interest) is an essential characteristic that potential getter materials must exhibit. However, additional criteria should be met by any potential getter material before it can be effectively deployed in a waste form. Additional proposed evaluation steps taken to verify that the criteria are met are shown in the flow chart in Figure 2.10. The proposed tiered approach for the getter selection and evaluation scheme is based on the critical performance factors listed below:

- adequate selectivity and capacity for radionuclide of concern
- low desorption characteristics
- chemically and physically stable

- compatibility with waste form
- cost effectiveness.

If getters are needed to improve the performance of a waste form, a preliminary screening of currently available mineral and synthetic getters needs to be conducted. The getters would be initially evaluated with first tier testing that consists of measuring their adsorption capacity, weathering kinetics, and the contaminant specificity. For reductive getters, it may be appropriate to measure reductive capacity. These tests are typically conducted using the actual waste stream or a simulant. After these tests, desorption tests can be conducted on contaminant-loaded getters. It is appropriate to conduct desorption tests with a simulant of the pore water of selected monolithic waste forms to provide a better understanding of potential contaminant release and partitioning that may occur between getters and the waste-form matrix. Getters meeting the previously established performance specifications can then be subjected to the next tier of tests.

For screening purposes, the waste-form compatibility tests at this level may consist of leach tests, such as ANSI/ANS 16.1, and EPA's recently developed test methods (see Section 4.2.1). Although TCLP testing is also conducted as part of Waste Acceptance Criteria, the typical suite of waste-form testing is not needed in this testing tier. If the results of the leach tests (EPA Draft Methods and ANSI/ANS 16.1) of the getter-containing waste forms show lowered leachability of the contaminant of interest than leachability in the waste form with no getter, it would be appropriate to consider the use of getters.

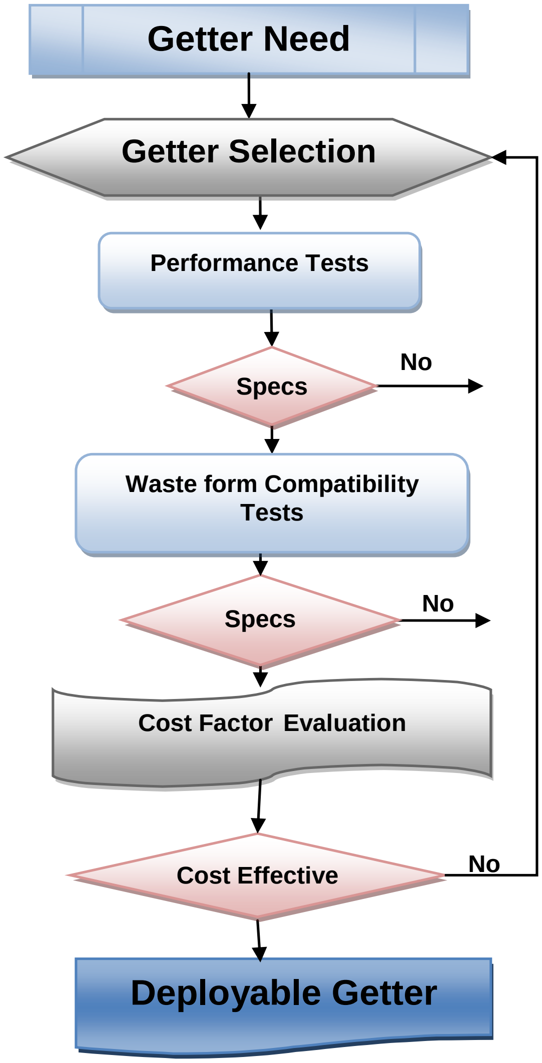

Figure 2.10. Flow Chart for Getter Selection and Evaluation

Finally, the cost effectiveness of getter deployment needs to be assessed, including factors such as the cost per mass of contaminant sequestered, any reduction in waste-form loading of contaminants caused by the need to add getters, and the cost savings realized from disposal of waste forms with lowered leachability of contaminants.

The literature review generated comprehensive lists of iodide and technetium getters (Table 2.9 and Table 2.10). Based on existing test data, the most promising getters that need additional evaluation include LBH, argentite, and silver-impregnated carbon and Ag-zeolites as I getters and nanoporous tin phosphates, Sn(II)-treated apatite, nano zero-valent iron (nano ZVI), and ground BFS as ^{99}Tc getters. BFS is part of the base mix for both SRS Saltstone and Hanford Cast Stone cementitious formulations. Because BFS is reductive in nature, it inherently possesses ^{99}Tc “gettering” properties. Therefore, testing BFS-based waste forms with added ^{99}Tc getters may result in significant improvement in long-term waste-form performance.

2.2.5 Getter-Waste-Form Interactions

Typically, when incorporated into monolithic waste forms, getters interact both physically and chemically with the encapsulating matrix. Ideally, while performing the targeted task of sequestration and attenuation of radionuclides, getters should not adversely affect the physical and leaching performance of the monolithic waste forms. Although the getters and waste forms have been studied extensively, the published literature includes a limited number of studies that have thoroughly characterized these interactions. Recent studies by Lockrem et al. (2005) and Cooke et al. (2009) demonstrated that including BFS as a getter in the Cast Stone formulation did not degrade the performance of this monolithic waste form. However, the compatibility of various effective getter materials with selected monolithic waste forms needs to be studied and better understood before the composite waste form can be deployed. Therefore, such a compatibility evaluation has been suggested as part of getter selection criteria (Figure 2.10).

2.3 Summary of Liquid Stabilization Options

In summary, it is our recommendation, based upon the available literature, that Cast Stone, chemically bonded phosphate ceramics (Ceramicrete), and alkali-aluminosilicate geopolymers (Duralith) should be considered for further testing and evaluation for the baseline addition of an STU at the ETF evaporator. Low-temperature alkali-aluminosilicate hydroceramics do not appear to be a viable waste form for the liquid secondary wastes. The challenge for hydroceramics is associated with obtaining the needed physical strength for a disposal system without having to process the material at high temperatures. The process of forming the hydroceramic material under hydrothermal conditions could volatilize ^{99}Tc or ^{129}I, thereby reducing the concentration of these contaminants in the waste form and creating yet another waste stream for treatment. The FBSR product in an encapsulation matrix is another viable waste form that warrants further testing and evaluation. Recent results on the performance of the FBSR process with simulated secondary waste indicates that the higher processing temperature does not impact the capability of the FBSR product to incorporate Cs, Re (or ^{99}Tc), and ^{129}I in the matrix. For geothite and sodalite, it is our recommendation that these activities continue being evaluated, either as a waste form or getter, with separate applied research funding from the DOE EM Office of Engineering and Technology in FY10. For proprietary materials, such as L-TEM, it is our recommendation that a process be developed to solicit additional information from industry through a Request for Information process.

Based on existing test data, it is our recommendation that the most promising getters that have been identified and that merit additional evaluation include layered bismuth hydroxides, argentite, and silver-impregnated carbon and Ag-zeolites as iodide/iodate getters and goethite, sodalite, nanoporous tin phosphates, Sn(II) treated apatite, nano zero-valent iron, and BFS as ^{99}Tc getters. In closing, the selection of a getter must include an evaluation of the getter for the intended use that accounts for any physical and/or chemical interactions between the getter and waste form that may impact the performance of both materials.

In addition to this literature review, WRPS issued a call for expressions of interest for secondary waste immobilization technologies. They received responses regarding 1) a glass waste form produced with the Geomelt Vitrification Technology, 2) a tailored waste form technology based on synroc ceramic titanate minerals by the Austrailian Nuclear Science and Technology Organization (ANSTO), and Nochar polymers including AcidBond which is a blend of acrylics and acrylamide co-polymers for extremely high and low pH liquids. These materials are mentioned here for completeness.

3.0 Solid Waste Stabilization Options

In addition to the secondary liquid waste stream, solid wastes from the waste-treatment facilities may include failed equipment, decontamination wastes, high-efficiency particulate air filters, carbon absorption beds, ion exchange resin, and silver mordenite iodine sorbent beds. This literature review looked specifically at sulfur-impregnated activated carbon used for controlling mercury emissions, ^{137}Cs-laden spent ion exchange resin (resorcinol-formaldehyde resin), and reduced-silver mordenite (Ag^0Z) to control ^{129}I emissions from the WTP. Some discussion on these potentially problematic solid wastes is provided with emphasis on the potential disposal pathways for each material. Additional discussion on solidification techniques for spent ion-exchange resins and the problems that have steered disposers away from this technique are also provided.

3.1 Carbon Beds

In the WTP, sulfur-impregnated activated carbon is to be used for controlling mercury emissions. Various strategies have been used to manage mercury-bearing activated carbon or charcoal wastes and other mercury-bearing wastes arising from industrial operations, including coal power plants. These strategies include direct land disposal or stabilization and solidification (S/S) before disposal (Graydon et al. 2009, Liu et al. 1999). The S/S methods that have been used or evaluated for activated carbon include immobilization in Portland cement (Zhang and Bishop 2002) and chemically bonded phosphate ceramics (Wagh et al. 2000, Randall and Chattopadhyay 2004).

Liu and coworkers (2000) found that both virgin and sulfur-impregnated activated carbon containing 65 to 1500 µg Hg/g and 550 to 2500 µg Hg/g, respectively, released less than the RCRA release limit of 0.2 mg Hg/L TCLP extract for the waste to be considered a toxic characteristic hazardous waste (40 CFR 261). They found that with time, the mercury-loaded sulfur-free carbon lost mercury over 310 days of storage, and they concluded that only the sulfur-treated activated carbon was acceptable for use and disposal. They attributed the difference in performance to simple physisorption on the untreated carbon and formation of HgS in the sulfur-treated carbon. Luo et al. (2006) found that elemental and $HgCl_2$-loaded activated charcoal (0.63 and 0.22µg Hg/g, respectively) released less than 0.01 µg/L in TCLP testing consistent with Liu and co-workers' results. Liu et al.'s studies indicate that direct land disposal of mercury-loaded sulfur-impregnated activated carbon will be acceptable while the spent untreated activated carbon may not. The authors concluded that even though elemental mercury-containing untreated carbon will satisfy RCRA disposal requirements, it would have to be managed as a hazardous waste because during long-term storage the elemental mercury could reenter the gas phase.

Graydon and coworkers (2009) found that untreated, gaseous elemental sulfur-treated, and sulfur dioxide-treated carbons loaded to 224 µg Hg/g released less than the 0.2 mg Hg/L TCLP extract toxic hazardous waste criterion. They found that nearly 60% of the elemental mercury loaded onto the elemental sulfur-treated carbon as HgS. In the untreated and SO_2-treated carbon, 75% of the Hg was bound in non-labile organic and elemental forms. Most of the Hg in the SO_2-treated carbon was chemisorbed to the thiophene and physisorbed, and 8 to 13% was present as the sulfide. Graydon et al.'s work indicates that treatment would not be required for land disposal of spent activated carbons used to control gaseous mercury emissions.

Although Portland cement can be an effective S/S agent for hazardous metals, it is minimally effective for mercury because of the solubility of mercuric hydroxide and oxide (Glasser 1997, Randall and Chattopadhyay 2004). Zhang and Bishop (2002), found that $Hg(NO_3)_2$-containing surrogate soil wastes (1000 µg Hg/g) stabilized with of CS_2-treated reactivated carbon loaded and solidified with Type I ordinary Portland cement (1 g surrogate waste:1 g cement), released less than the RCRA limit of 0.025 mg Hg/L TCLP extract (40 CFR 268). The acceptable performance of grouted sulfide-treated activated carbon may be due to the formation of mercuric sulfide with its solubility product (k_{sp}) of 2.0×10^{-49} (4.5×10^{-25} $\underline{M}$ Hg at Hg:S = 1:1). Zhang and Bishop conclude that mercury-containing wastes can be acceptably stabilized with sulfide-treated activated carbons and solidified by grouting with Type I ordinary Portland cement.

Chemically bonded phosphate ceramic is another potential media for S/S. Wagh et al. (Wagh et al. 2000; Randall and Chattopadhyay 2004) found that K_2S-doped chemically bonded phosphate ceramic containing 40 wt% of a 0.5 wt% Hg-containing waste released 0.00085 mg Hg/L TCLP extract which is well below the regulatory land disposal requirement of less than 0.025 mg Hg/L TCLP extract. The waste was 5 wt% activated carbon, 20 wt% vermiculite, 40 wt% Class F fly ash, and 33 wt% coal bottom ash with 0.5 wt% Hg added as $HgCl_2$. The chemically bonded phosphate ceramic was prepared by mixing water with a dry mixture of 0.5 wt% K_2S, magnesium oxide and dihydrogen phosphate to form magnesium potassium phosphate hexahydrate ($MgKPO_4 \bullet 6H_2O$). Higher levels of sulfide reduce the Hg^{2+} leading to higher Hg releases. Efficient formation of the stabilization form HgS is highly pH dependent and must be controlled to between 4 and 8 to prevent loss of H_2S at low pH and formation of $HgSO_4$ at high pH. Mercuric phosphate has a solubility product of 7.9×10^{-46} (1.1×10^{-9} $\underline{M}$ Hg at Hg:PO_4 = 3:2) compared to mercuric sulfide's k_{sp} of 2.0×10^{-49}. Although the encapsulated waste was only a small fraction of activated charcoal, chemically bonded phosphate ceramics appear to be a potential disposal form for the WTP's mercury-containing activated carbon waste. Further development would be required to qualify chemically bonded phosphate ceramics as an acceptable waste form for Hg-loaded sulfur-treated activated charcoal.

Several options appear to be suitable for disposal of WTP's mercury-containing activated carbon waste. These options are direct disposal without treatment, S/S in Portland cement, and encapsulation in chemically bonded phosphate ceramic. No other information on these waste and disposal forms other than TCLP leaching is available.

3.2 Ion-Exchange Resins (resorcinol-formaldehyde resins)

As part of the pre-treatment of liquid wastes in the WTP LAW processing flowsheet, most of the ^{137}Cs will be removed with resorcinol-formaldehyde ion exchange resins (Fiskum et al. 2006a). The ^{137}Cs-laden ion-exchange resins will be eluted with numerous bed volumes of 0.5-M nitric acid to remove the ^{137}Cs in a more concentrated form that is then sent to the high-activity glass waste stream so that most of the ^{137}Cs ends up in the high-activity glass product.

Once the resorcinol-formaldehyde resins are determined to be "spent," they will need to be disposed of as one of the secondary solid waste streams. Fiskum et al. (2006b) studied the loading of two actual tank waste streams onto small resorcinol-formaldehyde ion-exchange columns that were placed in a dual train series. After loading (i.e., upon significant breakthrough of ^{137}Cs through the first column and some minor breakthrough out of the second column in the series), the ^{137}Cs was eluted using ~30 bed volumes of 0.5-M nitric acid. The mass of ^{137}Cs loaded on the columns was calculated from knowledge of the initial ^{137}Cs concentration in the actual tank waste streams and the volume of waste liquid percolated through the columns and the measured breakthrough of cesium into the effluent. Then during the nitric acid elution, the ^{137}Cs content was monitored in each bed volume of acid eluant. It was then possible to calculate the residual ^{137}Cs still on the spent resins. There is a limit for the amount of ^{137}Cs (total mass includes stable and radioactive cesium of 4.2 µg Cs/g of dry spent resin). After three loading cycles and a total of 475 bed volumes of waste, ~10 bed volumes of acid were required to get the "spent" resins down to the design criteria.

Fiskum et al. (2006b) also investigated the residual RCRA metal and transuranic (TRU) content of the acid-stripped spent resins. The RCRA metal contents of the acid-stripped spent resins were low except for chromium, and the TRU content was ~2 nCi/g of the resin. Based on the low RCRA metal content, Fiskum et al. (2006b) suggest that the spent resin would meet TCLP leach testing requirements for disposal. The TRU contents of the spent resorcinol-formaldehyde resins were well below the 100 nCi/g limits that would cause them to be designated as TRU.

Nash and Fowley (2007) created spent resorcinol-formaldehyde spent resins with simulated tank waste for Tank AN-107, which had been spiked with two differing levels of RCRA-regulated metals. The high RCRA metal-loaded simulant contained tens to thousands of mg/L concentrations, and the low RCRA metal-loaded simulant contained 0.1 to a few hundred mg/L RCRA metals, depending on the metal. These lower concentrations were selected based on those present after the Sr/TRU precipitation pre-treatment step that is to be used in the WTP flowsheet.

The RCRA metal-laden spiked simulant was run through three loading cycles on each ion-exchange column. A cycle consisted of first percolating ~500 bed volumes of simulant through the resin columns for cycle 1 and ~160 bed volumes for cycles 2 and 3. After each simulant run, the columns were rinsed with ~3 bed volumes of 0.1-M sodium hydroxide to remove excess simulant, followed by 3 bed volumes of deionized water rinse, 15 bed volumes of the 0.5-M nitric acid eluant, and 3 bed volumes of deionized water rinse. Between cycles 1 and 2, the ion-exchange resins were re-constituted into the sodium form with 0.5-M sodium hydroxide. At the end of the third nitric acid elution, the "spent" resins were rinsed with 3 bed volumes of deionized water and de-watered by passing argon gas through the columns. Portions of the dewatered resins were then used in TCLP testing (EPA 2000, Method 1311), and portions were used to determine the total composition of the spent resins. The results of the TCLP testing showed that both resins passed with RCRA metals being leached at less than regulatory limits (including chromium, which both Fiskum et al. [2006a] and Nash and Fowley [2007] found at rather high concentrations [several 1000 ppm] in the spent resin). All metals except chromium were below the laboratory quantification limit or detection limit in the TCLP leachates.

Chromium was the only metal found at levels high enough to quantify, but these values were below characteristic hazardous levels. The spent resin samples retained the chromium in a very recalcitrant form that does not leach in the dilute acetic acid TCLP extractant or the 0.5-M nitric acid eluant to be used to strip ^{137}Cs out of the spent resins.

3.2.1 Review of Disposal Options for Spent Resins

A review of the current practices for ultimate disposal of spent organic-based spent resins yielded several observations. Although cement solidification of spent ion-exchange resins is still being considered or actively practiced in countries such as China, Serbia, and Turkey, currently spent resins at U.S. commercial LLW burial grounds are disposed of (after dewatering) in either steel containers for Class A wastes or in high-density polyethylene high-integrity containers (HICs) for Class C wastes. The following synopsis was obtained in telephone conversations with an environmental health physicist at one of the few commercial LLW burial grounds in operation within the United States.(a) The Class C dewatered spent resins within HICs are placed within concrete boxes to provide structural support after burial. Most states that regulate commercial LLW burial grounds do not allow any credit for the integrity of the steel containers once they are buried in the subsurface sediments. Hence, only Class A designated dewatered spent resin wastes can be transported and disposed of in the steel containers. State regulators give the concrete boxes a lifetime of at least 1000 years and also assume that the high-density polyethylene HICs provide additional containment. The concern with the HICs is that they cannot take the overburden pressures of the sediment that is used to backfill the trenches. Thus, the HICs are overpacked with the concrete boxes to provide the rigidity needed to keep the overburden compressive forces from crushing the HICs. Herbst (2002) also concluded that the best option for disposing of spent ion-exchange resins generated as a secondary waste stream from vitrification of sodium-bearing waste from the Idaho Nuclear Technology and Engineering Center was dewatering, placement in HIC containers, and disposal in shallow-land burial facilities. A current draft report that collates the types and quantities of secondary wastes that are to be produced at the WTP suggests that the spent resorcinol-formaldehyde resins are to be placed in HICs and, because of the high dose rates, need to be remotely handled during transit and burial in IDF (Gehner et al. 2009). There is no mention whether the HICs are to be high-density polyethylene or some other material. If high-density polyethylene HICs are used, placing the HICs in concrete overpacks as is done for Class C commercial waste would be advised.

3.2.2 Review of Cement Solidification of Spent Resins

In the past, spent resins often were solidified into cement waste forms, but several problems have caused this solidification process to be mostly abandoned, at least in the United States. The benefits for solidification of spent ion-exchange resins in cement include the use of simple equipment and ease of scale-up. Low temperatures are adequate for solidification, the final products are relatively resistant to physical deformation from overburden pressures after burial or during transport to the burial ground, and the costs are relatively low. A major drawback to solidification of spent resins into cement is the loading limitations, which are in the range of 20% wet resins, to the dry blend of solidification agents. For example, an optimum recipe used in China in the 1990s (Pan et al. 2001) to solidify spent resins was BFS 24 wt%, fly ash 24 wt%, OPC 8 wt%, 24 wt% of spent resin, and 20 wt% water. These limitations are necessary to prevent swelling and cracking of the product after or during short-term curing (see Li and Wang 2006).

Compared to many liquid and solid radionuclide-bearing wastes, spent ion-exchange resins are more difficult to solidify. Ion-exchange beads that are not already saturated with water swell when contacted with water, generating internal pressures that can reach 50 MPa. Even when water-saturated resins are used, if the ratio of resin to other ingredients rises much above 25%, swelling and cracking is generally observed. The most likely cause is that the resins and hydrating cement phases compete with each other for free water. Neilson and Columbo (1982) found that cement solidification of ion-exchange resins,

---

(a) This information was obtained during two phone conversations with Bob Haight, Environmental Health Physicist with U.S. Ecology Washington, Inc., Richland, Washington, in August 2009.

especially large cement right-cylinder monoliths, deteriorated after several weeks when monoliths were leached in water. Hairline cracks developed and then widened with time. The authors hypothesized that heat generated during cement hydration built up internally and drove water out of the resins, which caused swelling pressures in the larger specimens. Sperazini and Buckley (1981) recommended that spent organic exchange resins first be incinerated to form ash before solidification into cement to avoid swelling and cracking. They found that incineration of resins to ash improved ^{137}Cs leach resistance of the final cement product by over a factor of 10.

In China, a new type of cement, ASC, with higher aluminum and sulfur oxide content, less silicon and calcium oxides (see Table 3.1), and a mixture of zeolites has been found to be superior for encapsulating spent ion-exchange resins (Li et al. 2005). Li et al. (2005) recommend a recipe of 35-wt% ASC cement, 7-wt% zeolite, 42-wt% spent resins (that have a gravimetric moisture content of 50%, i.e., close to saturated), and 16-wt% water. The zeolite helps in sequestering radionuclides (e.g., ^{137}Cs and ^{60}Co) that desorb from the spent resins during the cement hydration reactions that generate high-ionic-strength pore waters.

Table 3.1. Oxide Composition of ASC Specialty and Ordinary Portland Cements

	ASC	OPC
Oxide	(wt%)	
SiO_2	9.21	24.19
$A1_2O_3$	31.36	4.87
CaO	40.9	58.23
MgO	3.79	2.64
Fe_2O_3	3.28	5.19
SO_3	9.45	1.96
TiO_2	1.21	0.26
Na_2O	ND	0.44
K_2O	ND	0.65
Ign. Loss	0.55	1.31
Total	99.75	99.74

ND = No data

The spent ion-exchange resins do not interact with the crystalline and amorphous gel minerals that form upon cement hydration; rather, they are simply physically encapsulated within the cement or grout solids as shown in Figure 3.1 (taken from Li and Wang 2006). The diffusion of constituents from a cement or grout that solely physically encapsulates waste can be reduced by decreasing the pore sizes, pore throat sizes, and pore connectivity (i.e., increased tortuosity) in the cement matrix. The porosity can be altered by varying the types of solid oxides and minerals and their amounts used in the dry blend. However, lowering the porosity of the hardened product by changing the dry blend generally leads to lowered compressive strength of the hardened cement.

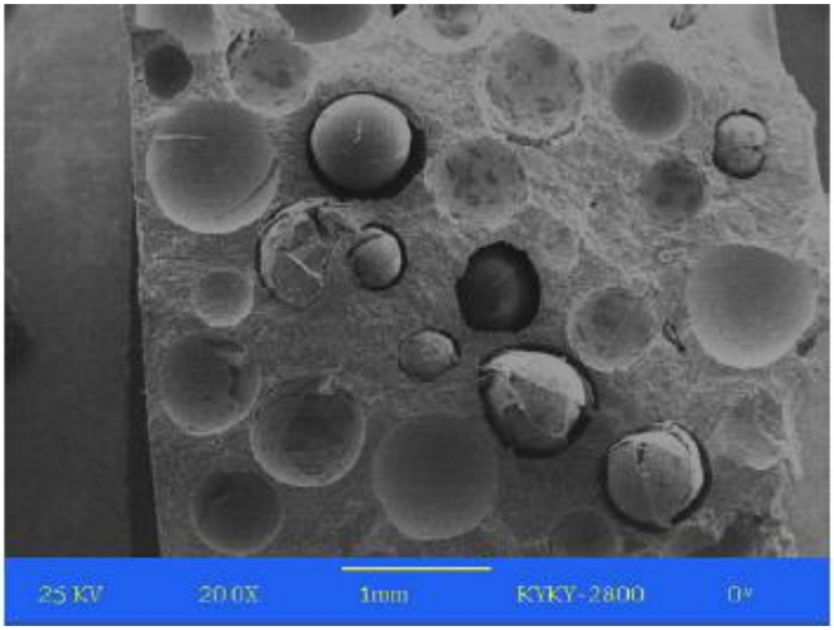

Figure 3.1. Ion-Exchange Resin Beads Physically Encapsulated in an Ordinary Portland Cement

Another concern is the release of ^{137}Cs from cemented spent resins that is typically larger than the release from the spent resins themselves. This occurs because the cement pore water has high concentrations of calcium liberated during hydration reactions as well as readily soluble sodium and potassium ions that compete with the Cs ions sorbed on the resin. Leach rates of ^{137}Cs solidified in OPC and grouts are relatively high compared to most other metals. Much research (see, for example, Bagnosi and Csetenyi 1999, Plecas et al. 2009, 2004, 1992) has been performed on the addition of clays (e.g., kaolinite, bentonite) and zeolites (e.g., clinoptilolite) to the dry blend that strongly adsorbs cesium, generating tailored cement/grouts that can encapsulate spent resins containing ^{137}Cs so that acceptable leach performance is obtained. The high concentrations of cations that dissolve as the cement dry blend is wetted compete for adsorption sites on the spent resins, causing the release of adsorbed cesium from the wet cement-solidified resins both before and after curing. A large proportion of the original cesium that was originally bound with ion exchange resin ends up in the pore waters in the hardened cement. The cesium present in the cement pore water is more prone to leaching from the hardened product than cesium adsorbed to spent resins placed in HICs or other containers that come into contact with the relatively low ionic strength waters that infiltrate through subsurface burial grounds. In fact, Arora and Dayal (1984) showed that much of the ^{137}Cs bound to ion-exchange resin beads is released into cement pore water before the hardening of the cement waste forms, in contrast to ^{90}Sr, which is incorporated into the calcium cement gels that are formed during cement set.

Bagnosi and Csetenyi (1999) found that after more than 3 years of leaching, the cemented resin containing no zeolite lost 70.4% of its originally bonded Cs content. Only 25% of the Cs was leached from cements with the natural zeolite, clinoptilolite, over the same time. Plecas et al. (1992, 2003, 2004) studied the leachability of ^{60}Co and ^{137}Cs from spent ion-exchange resins (both cation and mixed cation-anion types) in cement with and without bentonite clay at concentrations from 2 to 5 wt%. The presence of bentonite lowered the leach rates of both radionuclides, but the overall magnitude of the reduction was greater for ^{137}Cs than ^{60}Co. Similar studies by Osmanlioglu (2007), where bentonite and fly ash mixtures with cement were used to solidify spent ion-exchange resins, yielded similar results in that bentonite lowered the leach rates of these two radionuclides over cement-fly-ash-only waste forms. The optimum leach rates were obtained when bentonite was present from 5 to 7 wt%, and the resin loading was between a ratio of 0.36 and 0.67 of the cement-fly ash-bentonite dry-blend proportions.

Other studies on the leaching of radionuclides sorbed to spent ion-exchange resins that have been solidified into cementitious waste forms include one by Aalto and Ipatti (1992), who solidified boric acid-laden resins containing ^{134}Cs, ^{137}Cs, and ^{85}Sr in a mixture of BFS-cement waste form and conducted leach tests for over 4 years with cement-equilibrated groundwater. As expected, the leachability of Cs was larger than for Sr, and the leach rates did not follow simple diffusion theory where the cumulative fraction leached would be linear with the square root of time. This discrepancy suggests that chemical reactions besides simple diffusion are controlling the radionuclide leach rates. Moriyama et al. (1977) found similar results for spent resins solidified in cement.

3.3 Silver Mordenite

The WTP design contractor has chosen reduced-silver mordenite (Ag^0Z) to control radioiodine emissions (^{129}I, $t_{1/2} = 1.7 \times 10^7$ a) (Lide 2009, Scheele et al. 2002). Because the spent Ag^0Z contains silver, an EPA “hazardous” (40 CFR 261) and Washington State “dangerous” (WAC 2000a) material, the challenge for disposing of the used Ag^0Z will be two-fold because it will contain both ^{129}I and silver. To date, limited studies have been performed to develop a disposal form for the various loaded silver sorbents proposed for radioiodine control. Of particular interest to the development of a disposal form are the disposal form’s compressive strength and its performance in the TCLP and ANS 16.1 leach test.

The land disposal of silver is regulated by RCRA (40 CFR 268) and Washington State Regulations (WAC 2000b). Regulations regarding land-disposal sites governed by NRC limit the concentration of ^{129}I to 0.08 Ci/m^3, but waste that contains 0.008 and 0.08 Ci/m^3 must be stabilized (10 CFR 61.55; 10 CFR 61.56). EPA requires a waste form to have a likelihood of less than 1 chance in 10 of releasing 100 Ci ^{129}I/MTHM in 10 000 years. According to Mark Ellefson of PNNL’s Waste Management Group,(a) DOE’s limits are based on site-specific performance assessments, and for the Hanford burial grounds, the limit is 1.8 Ci/m^3. However, waste streams containing over 1.0 µCi/m^3 must be evaluated for their contribution to the overall landfill inventory.

In the WTP, the Ag^0Z will be exposed to a complex and variable mixture of water, oxides of nitrogen, sulfur compounds, and halogens. Using Burger and Scheele’s (2004) predictions for the once proposed Hanford Waste Vitrification Plant, the WTP’s melter off-gas could have maximum concentrations of 4×10^{-8} mol F/m^3, 6×10^{-9} mol Cl/m^3, and 6×10^{-14} mol I/m^3. The fluorine is likely present as hydrogen fluoride (HF), the chlorine as elemental chlorine (Cl_2), and the iodine as the mixed halogen iodine chloride (ICl). The spent Ag^0Z will likely differ from the spent silver sorbents derived from nuclear fuel reprocessing in the amount of other halogens present in the off-gases.

The actual halogen reaction(s) with either ionic or metallic silver mordenite is largely uncharacterized and unknown even though extensive trapping studies have been performed for elemental iodine (I_2) and methyl iodide (CH_3I) sorption. The evidence indicates is that elemental iodine will react with the silver in silver mordenites to produce silver iodide (AgI). Vance and Agrawal (1982) found AgI in iodine-loaded

---

(a) Personal Communication.

silver mordenite but also found that some elemental iodine was chemisorbed on its surface. Matsuoka et al. (1984) in their study of iodine-loaded silver faujasite concluded that the iodine is present as AgI, chemisorbed iodine [e.g. $(AgI)^{+}$--X^{-}], and physisorbed iodine depending on the silver site within the zeolite. Burger and Scheele (1981) used thermogravimetric analysis, differential scanning calorimetry, X-ray photoelectron spectroscopy and Auger spectroscotpy to characterize iodine-loaded silver sorbents. Iodine-loaded Ag^0Z strongly exhibits and iodine-loaded ionic-silver mordenite weakly exhibits AgI's characteristic 421 K (148°C) crystal transition and 831K (558°C) melting point (Barin 1989) and, at low iodine loadings, AgI's light yellow color. However, as more iodine is sorbed, the ionic silver mordenite takes on the characteristic purple color of elemental iodine, and additional mass losses and enthalpic events occur. Very limited x-ray photoelectron spectroscopy and Auger spectoscopic analyses found that the sorbed iodine in both the metallic- and ionic-silver mordenites differed from that of AgI. This behavior illustrates the complexity of the interactions between silver in or on an alumino-silicate framework. Further complicating the iodine sorption and retention chemistry is the presence of nitrogen oxides, Cl_2, and ICl. Nitrogen oxides are strong oxidants that can also react with the metallic silver in the Ag^0Z to produce silver oxide (Ag_2O) or silver nitrate ($AgNO_3$). The Cl_2 will react similarly to I_2 to produce silver chloride (AgCl) and will compete with iodine for the silver. Iodine chloride should react similarly to form AgCl and AgI athough no ICl sorption studies have been performed.

Based on thermodynamic calculations with Barin's reported free energies (Barin 1989) and the predicted chlorine-to-iodine ratio, silver chloride should be the predominant silver compound in spent Ag^0Z, assuming there is no reaction of the sulfur compounds with silver. Chlorine is 10^5 times more abundant than iodine (Cl:I molar ratio = 10^5) and has a more favorable free energy of reaction at 298 K with elemental silver (ΔG_{rx} = -110 kJ/mol Ag) than either elemental iodine (ΔG_{rx} = -76 kJ/mol Ag) or HF (ΔG_{rx} = +88 kJ/mol Ag) at 298 K. Strachan's discovery that only chlorine and no iodine remained on silver nitrate-coated beryl saddles used at Hanford's Plutonium-Uranium Extraction (PUREX) Plant to control radioiodine emissions (Strachan 1978) supports the preferential retention of chlorine over iodine; i.e. the chromatographic displacement of iodine by chlorine. Exchange of the more abundant fluorine for sorbed chlorine is unlikely because of the unfavorable endothermic (ΔG_{rx} = +103 kJ/mol Ag at 298 K) free energy for the reaction of HF with AgCl. This free energy is equivalent to an equilibrium constant of 1×10^{-12}, which makes the exchange extremely unlikely even at a F:Cl ratio of 10. Thus, the spent Ag^0Z should be predominantly chlorine-loaded with traces of iodine.

Disposal forms that have been considered or proposed for silver sorbents used to control radioiodine emissions from spent nuclear fuel reprocessing plants include direct disposal, immobilization of low solubility iodides and iodates in cement (Atkins and Glasser 1992, Burger and Scheele 1981, Morgan et al. 1978, Scheele et al. 1984), immobilization in CaI_2-modified cement (Scheele et al. 2002), immobilization by hydrothermal reaction with a metal hydroxide (Yamasaki 1987), sintered metal (Fukumoto and Kanzaki 1998), a silver phosphate glass (Fujihara et al. 1998), and vanado-apatite (Uno et al. 2004; Uno et al. 2001). The disposal challenges for silver sorbents used in a reprocessing plant should be similar to those for Ag^0Z or unreduced silver mordenite (AgZ) used at the WTP.

Cement or modified cement is promising as a treatment option for manageing the silver component of the silver-containing WTP waste. Unmodified cement has a high pH (~12.5) (Batchelor 2006), and Yousuf et al. (1998) report that silver forms the low-solubility compounds silver carbonate Ag_2CO_3, Ag_2O through decomposition of silver hydroxide AgOH, and AgCl from chloride impurity in the cement. Atkins et al. (1990) report that silver solubility in cement is controlled by the formation of a silver calcium silicate hydro-gel rather than silver oxide. However, Scheele et al. (2002) found that the native Portland III cement chemistry was ineffective for controlling silver releases from a 25-wt% silver mordenite waste grout to regulatory standards. Silver precipitation agents can be added to the cement to improve silver retention (Batchelor 2006). Candidate cement modifiers for silver precipitation include sulfide from BFS (Batchelor 2006) or calcium iodide or calcium chloride which leverage the low solubilities of silver sulfide (Ag_2S), silver iodide (AgI), and AgCl. Although silver sulfide has a very low solubility in water, its interactions with silver will be complicated due to silver sulfide complexes and sulfide reduction of ionic silver to silver metal (Atkins et al. 1990). The disadvantage of using a silver precipitation agent that is more stable than AgI is that it will free the radioiodine as indicated by Atkins et al. (1990) studies which found iodide concentrations for AgI-containing cements modified with BFS to be 250 times those of unmodified cements. A secondary advantage of adding iodide is the isotopic dilution of the long-lived radioiodine, which helps to mitigate radioiodine release consequences (Burger 1980, Morgan et al. 1978).

From the iodine management perspective, Atkins and coworkers considered using silver as a getter for iodine in a Portland cement waste form (Atkins et al. 1990). They concluded that even though AgI is stable in Portland cement in the near term, after disposal in a repository, the oxidation/reduction conditions will cause the AgI to release I^- and render the Ag^+ inert as Ag^0. From their evaluation of Portland cement and Portland cement containing 85% BFS as S/S agents for iodine, they conclude that even within 300 years, added silver will have no benefit with respect to iodine release.

Morgan et al. (1978) at Oak Ridge National Laboratory considered the use of concrete for disposal of iodine trapped by the Iodox and Mercurex processes, which use hyperazeotropic nitric acid and mercuric nitrate-nitric acid, respectively. The recovered iodine is converted to barium iodate and mixed with cement to produce a 0.18 g I/g concrete. Researchers performed leach tests using a variety of waters where the leachate was removed daily except on weekends and holidays. These studies did not consider conversion of the trapped iodine on a silver sorbent into an iodate.

Burger et al. (1981) investigated 1) ASTM Portland Type III cement S/S of iodine-loaded silver mordenite and various low-solubility iodides and iodates and 2) iodine-containing sodalite. They used static and dynamic leach testing to compare the various tested cement-immobilized iodine compounds in a variety of water types. Of the materials tested, silver iodide in cement proved to be the most leach resistant. The other iodides performed significantly worse, likely because of hydrolysis of the metal. Iodates in cement were not as resistant to leaching as silver iodide. Iodine-loaded AgZ in cement had an intermediate leach resistance between silver iodide and the iodates in the dynamic leach test, but had equivalent leach resistance in the static tests.

Atkins and Glasser (1992) investigated cements as disposal forms for radioiodine. In their studies, they found that iodide is incorporated into the cement solid phases either by sorption and/or incorporation, and the amount in the solid phases increases with aging. After 60 days with the iodide added as 10^{-7} M KI, >99% of the iodide was in the solid phases of OPC. After 100 days, 96% of the iodide added as 0.01- and 0.001-M KI was in the solid cement. In their studies of C-S-H and iodide and iodate interactions, they concluded that the iodide is simply sorbed on the C-S-H and is not co-precipitated. They also found that C-S-H has a stronger affinity for iodate than for iodide.

Building on the 1981 work by Burger et al. (1981), Scheele et al. (2002) developed a RCRA-compliant calcium iodide-modified ASTM Portland Type III cement S/S disposal waste form appropriate for either spent silver or reduced-silver mordenite derived from WTP; the latter study focused solely on compliance with regulations governing land disposal of silver. The study investigated a variety of silver mordenites whose silver chemistries were expected to bound the behavior of any spent Ag^0Z from the WTP. As illustrated in Figure 3.2, only grouted iodine-loaded Ag^0Z (Ag^0ZI) and 10-wt% CaI_2-modified grouted AgZ had acceptable silver releases in the TCLP test. The added iodide prevented silver release by reducing the amount of soluble silver using the low-solubility product of AgI. As a result of this study, the WTP design contractor selected the CaI_2-modified Portland Type III cement as the disposal form.

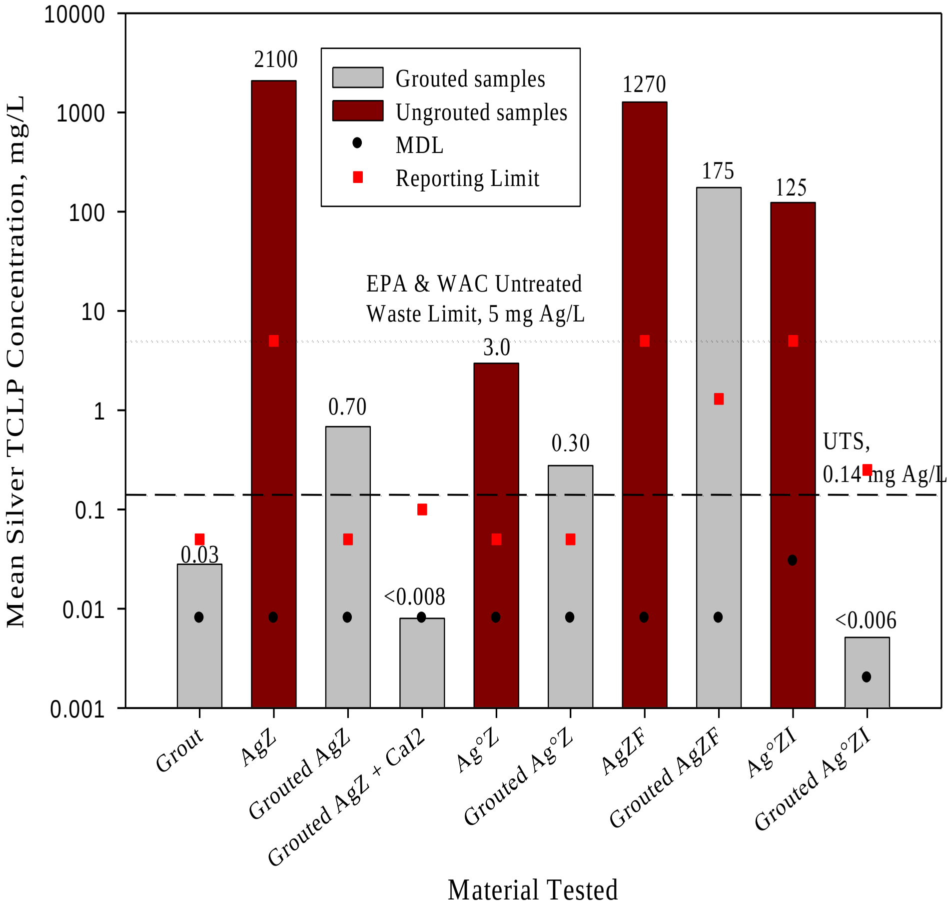

Figure 3.2. Measured Silver Releases from Evaluated Silver Mordenites (Scheele et al. 2002) for Development of a RCRA-Compliant Disposal Form for Spent WTP-Reduced Silver Mordenite. AgZ is as-received silver mordenite, Ag^0Z is hydrogen-reduced AgZ, AgZF is HF-treated/loaded AgZ, and Ag^0ZI is elemental iodine-loaded Ag^0Z. UTS is the universal treatment standard, and MDL is the minimum detection limit (Scheele et al. 2002).

Even though the grouted iodine-loaded reduced-silver mordenite had an acceptable TCLP release, it is unknown whether direct land disposal of grouted spent Ag^0Z would be acceptable because of the potential variability in its chemical composition. Even though the silver in the spent Ag^0Z will be predominately associated with chlorine, likely as AgCl, which has a solubility product a factor of 10^6 greater than AgI, the performance of the chlorine-treated Ag^0Z is unknown.

To make sure that the disposal form for spent reduced-silver mordenite is acceptable for land disposal, the use of the CaI_2-modified grout is indicated. No information other than leaching performance is known about grouted silver mordenites.

Another potential waste form for silver mordenite is encapsulation in a sintered metal. Fukumoto et al. (1998) patented a sintered metal waste form for radioiodine-loaded silver sorbents. In their process, an iodine-containing silver sorbent is solidified and stabilized by hot isostatic pressing with metal at a temperature less than the melting point of the metal to produce a sintered metal waste form. Metals recommended include copper, other precious metals, stainless steel, nickel, and titanium. The waste form produced by hot isostatic pressing of silver faujasite, another silver zeolite, into a copper matrix at 860°C under 195 MPa Ar had the zeolite, which contained iodine distributed through the matrix. This method should be directly applicable to spent Ag^0Z from the WTP with some development.

Another hydrothermal approach for immobilizing an iodine-loaded silver sorbent is proposed by Yamasaki et al. (1987). In this method, a mixture of water, sodium, potassium, or barium hydroxide and iodine sorbent is subjected to hydrothermal reaction at a pressure of $\geq$ 700 kPa and >150°C. The hydroxide converts any elemental iodine to silver iodide and iodate to fix the iodine and encapsulate the iodide and iodate within a three-dimensional aluminosilicate network. This method should also be directly applicable to spent Ag^0Z from WTP. Significant development would be required.

Another mineral-based candidate is iodide sodalite (Badad and Strachan 1979). Winters (1980) did some preliminary development and testing of iodide-sodalite and later prepared material for testing by Burger et al. (1981). The iodide-sodalite is prepared by mixing sodium iodide, alumina, and silica and pressing at 34.5 to 48.3 MPa at 1060°C. Iodide-sodalite showed promise as a disposal agent for radioiodine. In Burger et al.'s static leach tests, sodalite was equivalent to AgI in cement. For its use, the iodine would need to be removed from the spent Ag^0ZI as an iodide, and the alumino-silicate would be prepared.

Fujihara et al. (1998) and Sakuragi et al. (2008) investigated the vitrification of AgI as $AgI\text{-}Ag_2O\text{-}P_2O_5$. Fujihara et al. (1998) described the process for separating trapped iodine as AgI from silver sorbents by vacuum distillation at 800°C. They prepared their glass by blending AgI with silver metaphosphate, silver pyrophosphate, or silver orthophosphate and melting it in an alumina crucible at 623 K (350°C) for 6 hours. For the glass that performed best, the iodine fraction lost during vitrification was estimated to be $<1.5 \times 10^{-5}$ based on the lack of collected iodine during differential thermal analysis of the vitrification mixture. Building on Fujihara et al.'s (1998) work, Sakuragi et al. (2008) prepared their glass by mixing AgI and $Ag_4P_2O_7$ and melting it at 773 K (500°C) for 3 hours. In both studies, investigators studied the behavior of the vitrified AgI in leaching tests or exposure to water. Sakuragi et al. (2008) estimated a leaching period of 1.3×10^6 years for this waste form as a 48-cm-diameter cylinder. Fujihara et al. (1998) measured a melting temperature of <573 K (300°C), a glass transition temperature of 327 K (54°C), a compressive strength of 9000 kPa, and a thermal expansion coefficient of $2 \times 10^{-5}\ K^{-1}$. This approach would need to be combined with a method for removing the iodine before converting it to a waste form for radioiodine in spent Ag^0Z from the WTP. Disposal of the remaining Ag^0Z would be impacted by the amount of residual I and silver.

Uno and coworkers (2001, 2004) investigated silver/lead-, silver/barium-, and lead-vanado-iodoapatites as candidates for radioiodine immobilization. To prepare these materials, stoichiometric amounts of the starting materials $Ba_3(VO_4)_2$ and AgI for making $AgBa_9(VO_4)_6I$, $Pb_3(VO_4)_2$; AgI for

$AgPb_9(VO_4)_6I$, PbO, and PbI_2; and V_2O_5 for $Pb_{10}(VO_4)_6I_2$ were mixed and pressed into pellets. The pressed pellets were sealed into a quartz ampoule in a vacuum and heat treated for 5 hours at 973 K (700°C). The $Pb_{10}(VO_4)_6I_2$ had a Young's modulus of 26 GPa and an iodine Soxhlet leach rate of 3.98×10^{-5} g $cm^{-2}d^{-1}$. The $AgBa_9(VO_4)_6I$ and $AgPb_9(VO_4)_6I$ had a Young's modulus of 13 and 18 GPa, respectively, and a Vickers hardness of 0.67 and 0.63 GPa, respectively. To use the iodo-vanadate apatite as a waste form for spent Ag^0Z from the WTP, the iodine will first have to be removed before being converted into the iodo-vanadate apatite. The Ag^0Z remaining after iodine removal might need to be disposed of.

In summary, the disposal of spent Ag^0Z from the WTP must be managed to be compliant with existing regulations. Material containing silver must comply with RCRA regulations because silver has been designated a hazardous material. The requirements for disposal of ^{129}I are less clear. The WTP design contractor chose CaI_2-modified cement to grout its spent Ag^0ZI to comply with existing RCRA regulations. A sintered metal and a ceramic have been developed to directly incorporate spent silver mordenites, but their application requires elevated temperatures and pressures and would need further development and demonstration. Two glasses and two iodo-apatites also have been studied, but their application would require that a method be developed for separating the iodine from the spent silver mordenite.

3.4 Summary of Solid Waste Stabilization Options

In summary, the WTP secondary solid wastes will include sulfur-impregnated activated carbon used for controlling mercury emissions, ^{137}Cs laden spent ion exchange resin (resorcinol-formaldehyde resin), and reduced-silver mordenite (Ag^0Z) to control ^{129}I emissions. Several options appear suitable for disposal of WTP's mercury-containing activated carbon waste. These options are direct disposal without treatment, solidification/stabilization in Portland cement, and encapsulation in chemically bonded phosphate ceramic. For spent ion exchange resins, direct disposal in either steel canisters or HICs that are placed within concrete boxes is a suitable disposal path. Disposal of silver mordenite (Ag^0Z) is extremely challenging because of the mixture of both silver and ^{129}I. Three methods for stabilizing the material have been discussed in the literature: 1) a sintered metal and ceramic, 2) a glass, and 3) iodo-apatites. Currently, it is unclear which of these three options identified is the most suitable for disposal.

4.0 Stabilization Technology Regulatory and Screening Tests

4.1 Regulatory Testing

This section discusses a series of regulatory test methods that must be performed to provide some of the data needed to screen potential secondary waste stabilization technologies. The methods discussed below include the ANSI/ANS 16.1, compressive strength, and TCLP tests.

4.1.1 Durability with ANSI/ANS 16.1 Leachability Index Test

The ANSI/ANS 16.1 (ANSI 2003) protocol is used to evaluate the diffusivity and surface release of constituents from a monolith and to characterize contaminant release from monolithic waste forms. The ANSI/ANS 16.1 test provides an LI. The LI is calculated from the data obtained by immersion of the waste form in a leachant (generally DI water, but for subsurface disposal evaluations, a site-specific groundwater or vadose zone pore water is more appropriate). The leaching protocol uses 10 sequential and time-varying intervals, with 2 hours being shortest and 43 days being longest, for a total cumulative time of 90 days. The procedure also allows for an abbreviated test protocol using a 5-day test duration. The LI and effective diffusivity are calculated with Equations (4.1) and (4.2), respectively.

$$LI_n = -\log\left(\frac{D_n}{cm^2 s}\right) \tag{4.1}$$

$$D_n = \pi \left[\frac{a_n / A_o}{(\Delta t)_n}\right]^2 \left(\frac{V}{S}\right)^2 T \tag{4.2}$$

where LI = leach index
D_n = effective diffusivity for elements of interest (cm^2/s) during the leach interval n
V = volume of the specimen (cm^3)
S = geometric surface area of the specimen (cm^2)
T = leaching time representing the “mean time” of the n^{th} leach interval (s)
a_n quantity of a given element released from the specimen during the leach interval n
A_o total quantity of a given element in the specimen before testing
t_n duration of the n^{th} leaching interval.

4.1.2 Compressive Strength Testing

The ASTM C-39/C-39M-99 (ASTM 1999) procedure is used to determine the compressive strength of a cylindrical monolithic waste-form sample. Samples are loaded into a testing apparatus (i.e., servo-hydraulic test machine) so that the axis of the specimen is aligned with the thrust center of the spherically seated block of the apparatus. The load is applied at a rate of movement (platen to crosshead measurement) that corresponds to a stress rate on the sample of 0.25 ± 0.05 MPa/s (35 ± 7 psi/s) continuously and without shock until the load indicator shows that the load is decreasing steadily, and the sample displays a well-defined fracture pattern. For each test, a constant displacement rate must be used for each waste-form specimen for consistency. The compressive strength is calculated by dividing the maximum load carried by the sample during the test by the average cross-sectional area determined for the sample before testing. Compressive strength tests may also be conducted after thermal cycling, exposure to radiation, and immersion in water to assess the impact of each.

4.1.3 Toxic Characteristic Leaching Procedure Testing

The TCLP is the current test procedure used to verify that the waste received at a storage site will meet the restrictions associated with several regulated hazardous metals and selected regulated organic compounds in waste destined for land disposal facilities (40 CFR 268). The current TCLP test is EPA Method 1311 (40 CFR 268), and test details taken from the procedure are summarized below.

For wastes containing greater than or equal to 0.5% solids, the liquid, if any, is separated from the solid phase and stored for later analysis; the particle size of the solid phase is reduced, if necessary. The solid phase is extracted with an amount of extraction fluid equal to 20 times the weight of the solid phase. The extraction fluid used is a function of the alkalinity of the solid phase of the waste. Particle-size reduction is required, unless the solid has a surface area per gram of material equal to or greater than 3.1 cm^2, or is smaller than 1 cm in its narrowest dimension (i.e., is capable of passing through a 9.5-mm [0.375–in.] standard sieve). If the surface area is smaller or the particle size larger than described above, the solid portion of the waste is prepared for extraction by crushing, cutting, or grinding the waste to a specific surface area or particle size. The extraction vessel containing the solid/solution mixture is then rotated at 30 ±2 rpm for 18 ±2 hours at 23 ±2°C. Following the extraction, the material in the extractor vessel is separated into its component liquid and solid phases by filtering it through a new glass fiber filter. After collecting the TCLP extract, the pH of the extract is recorded. An aliquot of the extract is taken for analysis. Metals aliquots must be acidified with nitric acid to pH <2. If precipitation is observed after adding nitric acid to a small aliquot of the extract, then the remaining portion of the extract for metals analyses is not acidified, and the extract is analyzed as soon as possible. All other aliquots must be stored under refrigeration (4°C) until analyzed.

4.2 Alternate Screening Testing

Many scientists and regulators are aware that the commonly used leach tests, ANSI/ANS 16.1 and the TCLP tests, have technical deficiencies for use as predictors of the long-term performance of buried wastes in subsurface environments. Thus, there are ongoing efforts to develop more applicable test methods that are more germane to predicting the long-term performance of solid waste forms destined for subsurface burial. The specific test methods to screen candidate liquid stabilization options need to provide a framework to 1) rapidly assess material performance, 2) provide some indication of the dominant release mechanism for specific COCs, 3) evaluate the strengths and weaknesses of a variety of materials (placing each material on a level playing field), and 4) gain regulatory acceptance by being a standard set of test methods approved by the regulatory community. Although these aforementioned criteria focus on the use of standard methods, these analyses need to be augmented with specialized characterization techniques to examine key processes affecting the release of each COC from the waste form that correlates with changes in the measured leachate solution chemistry (increase in concentration of key COCs). This type of integrated approach is expected to provide the defense-in-depth needed to effectively evaluate each of the candidate liquid stabilization options selected for further testing.

To address the above criteria, three draft test methods being developed for EPA can be used to screen each of the "down-selected" stabilization technologies. These test methods examine different aspects of material performance. These methods are currently undergoing EPA approval and are expected to be used in place of the TCLP method for disposal of specific materials, such as waste forms. Each test method to be used—Draft Methods 1313, 1314, 1315, and 1316—are discussed next.

4.2.1 EPA Draft Methods 1313, 1314, 1315, and 1316

The test methods, EPA Draft Methods 1313 (EPA 2009a), 1316 (EPA 2009d), 1314 (EPA 2009b), and 1315 (EPA 2009c), are a combination of static, column, and semi-dynamic leach experiments that can be used to provide more detailed mechanistic information on material performance in comparison to the current standard leach methods, such as ANSI 16.1 and TCLP. The EPA Draft Method 1313 is a static-leach test method where nine parallel extraction experiments are conducted in dilute acid or base with DI water at a fixed pH and liquid-to-solid ratio. The recommend acid is dilute HNO_3 produced by mixing deionized water with ultra pure HNO_3, and the dilute base is potassium hydroxide (KOH) (or equivalent) produced by mixing DI water with analytical-grade KOH. Before starting the experiments, a series of pre-test titration curves need to be derived to determine the required equivalents per gram of acid or base that need to be added to each extraction vessel experiment to yield effluent solutions that span the range of specified pH values between 2 and 13. The time required to conduct these experiments is anywhere from 24 to 72 hours and depends on the disaggregated waste-form particle size used.

Draft Method 1316 uses DI water as the leachant instead of a dilute acid or base at a fixed liquid-to-solid ratio. The EPA Draft Method 1316 (EPA 2009d) is very similar to PCT-A (ASTM C-1285 [ASTM 2002]), which is used for glass waste forms, except that the contact time for glass is typically 7 days for PCT-A, and in this experiment, the longest experimental time is 72 hours. Unlike EPA Draft Methods 1313 (EPA 2009a) and 1316 (EPA 2009d), Draft Method 1314 is a flow-through leach test that uses a packed column containing disaggregated waste-form material. The results from this flow-through column test should provide some indication of the cumulative release of each measured species from the material as well as some details of the kinetics of contaminant release. The target solution residence time for these experiments is approximately 1 day. The EPA Draft Method 1315 is a 60-day semi-dynamic leach experiment that consists of submerging a monolithic sample (with a fixed geometry) in water at a fixed liquid-to-solid ratio for a fixed period of time. At each of the nine pre-determined leaching intervals, the sample mass is recorded, and the leachant is changed. This method is similar to ANSI/ANS 16.1, but the intervals are different. The test specimen preparation accounts for mass transfer from compacted granular samples. The process of mass transfer can be interpreted by more complex release models that account for physical retention of the porous medium and chemical retention at the pore wall through geochemical speciation modeling.

The leachate solutions collected from each of the proposed test methods are analyzed to determine the 1) pH, 2) electrical conductivity, 3) concentration of specific dissolved components, and 4) redox conditions. Finally, the results from the aforementioned EPA test methods are expected to provide detailed information on the amount and release behavior of key contaminants under specific conditions and to gain insight into the processes and mechanisms controlling element release. These results need to be coupled with geochemical modeling and with a select number of chemical and solid-phase characterization techniques to evaluate pre- and post-test solid phases.

5.0 Performance Testing and Chemical Characterization

5.1 Performance Testing

Quantifying the rate and extent of element or contaminant release from minerals, glasses, or other waste forms has been at the heart of predictive geochemistry studies for decades. The majority of the geochemistry studies have focused on understanding the weathering of primary minerals and basaltic glasses contained in the earth’s crust for the purpose of predicting element cycles. The concepts and theories related to mineral and glass weathering developed within the geochemical community have been carried forward and used to predict the release of contaminants from waste forms and other engineered materials. The weathering of these materials is impacted by a series of sequential or simultaneous competing chemical and physical reactions or processes that may control the mass transfer of contaminants from the waste form into solution. These reactions and processes include, but are not limited to, the following:

- diffusion/advection
- dissolution/precipitation
- adsorption/absorption/desorption
- oxidation/reduction
- paragenetic sequence of mineral transformation.

The overall impact of individual or coupled reactions and processes on the long-term performance of a waste form depends on a number of variables, such as the waste-form composition, materials resistance to physical and chemical degradation, dominant mechanism controlling release, and disposal system environment. For example, some of the most common physical degradation mechanisms for cements are associated with shrinkage, thermal cracking, and freezing and thawing (Pabalan et al. 2009). Degradation from chemical reactions involves chloride ingress, carbonation, decalcification, sulfate attack, and alkali silica reactions (Glasser et al. 2008, Pabalan et al. 2009). These are time- and temperature-dependent reactions and processes, as is clearly demonstrated in a recent study, where solid-phase composition and transformation of the pore solution chemistry of hydrated Portland cements are investigated as a function of time and temperature (Lothenbach et al. 2008).

The following physical and chemical variables are the most important ones that may influence or control the extent and time scales of contaminant release from secondary waste materials:

- ***Physical variables***: sample size (reactive surface area), temperature (changes in temperature may cause cracking; in addition, diffusion is a function of temperature), porosity or permeability, or moisture content (water saturation, which may cause cracking and affect concentration gradients).
- ***Chemical variables***: pH and concentrations of different constituents, such as chloride, sulfate, carbonate, calcium, and other elements or chemical species that might affect the contaminant release.

Predicting contaminant release requires the use of tests that are conducted at different time and length scales in comparison to the disposal environment. As a result of these differences, a sound mechanistic understanding of the dominant processes affecting release is needed to provide the defense-in-depth required to successfully assess the long-term performance of a waste form. To overcome the existing differences in scale, models must be developed to capture the key processes controlling the release of contaminants as well as the uncertainty associated with these processes.

Therefore, performance testing must focus on the use of experiments that provide model parameters that explain the key processes and, in some cases, accelerate the weathering process to obtain the data needed to predict performance in a realistic time frame. The results produced from these bench-scale and field-scale experiments must have the capability to provide the parameters needed to predict performance and contaminant release over ~10 000 years, which is the expected period of performance for the engineered system.

Performance testing must address the following issues:

- Identify the key reactions or processes affecting waste-form durability and contaminant release.
- Quantify the extent and rate of these reactions or processes.
- Obtain the model parameters needed to describe these reactions or processes and predict the behavior of the system.
- Validate the derived model parameters.

In summary, performance testing is a strategic process that uses laboratory experimentation to quantify the needed parameters used in numerical or analytical models to calculate the key reactions or processes affecting release over long time frames.

5.2 Chemical Characterization

This section describes the characterization techniques that can be used for leachate solution and solid sample analyses of the secondary waste forms. Many of the characterization techniques explicitly yield the needed values for the parameters used in the predictive models, while other characterization techniques give backup information to support the choice of controlling waste-form weathering or contaminant-release mechanisms. The characterization types are divided into two categories, depending on the purpose and goal of the characterization: solution analysis and solid analysis. Each useful characterization instrument and its application for waste forms and leachates are summarized in Table 5.1 (expanded details are in Appendix A). Solution analysis instruments are used for analyzing solution samples (leachates) from the waste forms to identify and measure the concentrations of each constituent. The composition of solid wasteforms can also be determined by these methods after complete dissolution of the samples. Solid analysis instruments can be used for identifying elements, minerals, solid-phase morphology, chemical composition of the bulk and solid surfaces, chemical bonding or interaction, and the oxidation state of selected elements within the solid.

Table 5.1. Characterization Instruments and Applications for Analysis of Secondary Waste Stabilization Options

Types	Instruments	Applications
Solution	ICP-OES	Major cations concentrations
	ICP-MS	Minor cations as well as ^{129}I, ^{99}Tc, ^{238}U and other long-lived radionuclide concentrations.
	IC	Major anions concentrations
Solid	XRD	Mineral identification, semi-quantitative bulk composition
	XRF	Elemental composition
	ICP-OES, -MS	Elemental Composition after solid solubilization
	SEM/EDS	Surface morphology along with elemental analysis of small regions of the solid
	TEM/EDS	Morphology, mineral identification, elemental analysis of very small regions of the solid (higher resolution than SEM)
	FTIR/Raman	Chemical bonding, molecular structure, compounds identification
	XPS	Oxidation state of element in solid surface, depth profiles of element composition to correlate with dissolution data, and elemental composition of solid surfaces as a function of depth from the surface
	XAS(XANES/ EXAFS	Oxidation state of element, element identity, and bonding information (coordination numbers and bonding distance between the central and the nearest neighboring elements).
	Gas Adsorption	Surface area (BET), pore size distribution
	VSI	Dissolution rate
	XMT	Identification of composite and microstructure, pore structure characterization
	NMR	Coordination information between elements in the solid, bonding structure, and diffusion coefficient
	Mössbauer	Fe^{2+}/Fe^{3+} ratio in phase transformation of Fe oxides

6.0 References

10 CFR 61.55. 2009. "Waste Classification." *Code of Federal Regulations*, U.S. Nuclear Regulatory Commission, Washington, D.C.

10 CFR 61.56. 2009. "Waste Characteristics." *Code of Federal Regulations*, U.S. Nuclear Regulatory Commission, Washington, D.C.

40 CFR 261. 2002. "Identification and Listing of Hazardous Waste." *Code of Federal Regulations*, U.S. Environmental Protection Agency, Washington, D.C.

40 CFR 268. 2002. "Land Disposal Restrictions." *Code of Federal Regulations*, U.S. Environmental Protection Agency, Washington, D.C.

Aalto H and A Ipatti. 1992. "Leach Test of Spent Ion-Exchange Resins Solidified in Concrete." *Cement and Concrete Research* 22:375-380.

Allard G, K Torstenfelt, K Andersson, and J Rydberg. 1981. "Possible Retention of Iodine in the Ground." In: Material Research Society Symposium Proceedings 176:673-680.

Aloy A, EN Kovarskaya, JR Harbour, CA Langton, and EW Holtzscheiter. 2007. "Pretreatment of Tc-Containing Waste and its Effect on Tc-99 Leaching from Grouts." In: Material Research Society Symposium Proceedings 985.

ANSI—American National Standards Institute. 1986 (revised in 2003). "Measurement of the Leachability of Solidified Low Level Radioactive Waste by a Short-Term Test Procedure." In: Institute, A. N. S. (Ed.). American Nuclear Society, La Grange Park, Illinois.

ANSI—American National Standards Institute. 2000. "Solid Radioactive Waste Processing System for Light-Water Reactor Plants, Appendix B, Testing for Free Liquids in Solidified Matrices." In: Institute, A. N. S. (Ed.). American Nuclear Society, La Grange Park, Illinois.

ANSI—American National Standards Institute. 2003. "Measurement of the Leachability of Solidified Low Level Radioactive Waste by a Short-Term Test Procedure." In: Institute, A. N. S. (Ed.). American Nuclear Society, La Grange Park, Illinois.

ASTM—American Society for Testing and Materials. 1997. *Test Method for Steady-State Heat Flux Measurement and Thermal Transmission Properties by Means of the Guarded-hot-plate Apparatus*. ASTM, Easton, Maryland.

ASTM—American Society for Testing and Materials. 1998. *Standard Test Method for Expansion and Bleeding o Freshly Mixed Grouts for Preplaced-Aggregate Concrete in the Laboratory*. ASTM, Easton, Maryland.

ASTM—American Society for Testing and Materials. 1999. *Standard Test Method for Compressive Strength of Cylindrical Concrete Specimens.* ASTM, Easton, Maryland.

ASTM—American Society for Testing and Materials. 2002. *Standard Test Methods for Determining Chemical Durability of Nuclear, Hazardous, and Mixed Waste Glasses: The Product Consistency Test (PCT)*. ASTM C-1285, Easton, Maryland.

Arora H and R Dayal. 1984. *Solidification and Leaching of Boric Acid and Resin LWR Wastes*. NUREG/DR-3909, U.S. Nuclear Regulatory Commission, Washington, D.C.

Atkins M and FP Glasser. 1990. "Encapsulation of Radioiodine in Cementitious Waste Forms." In: Material Research Society Symposium Proceedings 176:15-22.

Atkins, M, et al. 1990b. "The Use of Silver as a Selective Precipitant for ^{129}I in Radioactive Waste Management." Waste Management 10:303-08.

Atkins M and FP Glasser. 1992. "Application of Portland Cement-Based Materials to Radioactive Waste Immobilization." *Waste Management* 12:105-131.

Babad H and DM Strachan. 1979, American Ceramic Society Bulletin 58, 327.

Balsley SD, A Avogadro, and AD Plano. 1985. "Influence of Redox Environments on the Geo-chemical Behavior of Radionuclides." In: *Scientific Basis for Nuclear Waste Management IX* 50:709-716.

Balsley SD, PV Brady, JM Krumhansl, and HL Anderson. 1996. "Iodide Retention by Metal Sulfide Surfaces: Cinnabar and Chalcocite." Environmental Science and Technology 30:3025-3027.

Balsley SD, PV Brady, JM Krumhansl, and HL Anderson. 1997. *129I and 99TcO$_4$ Scavengers for Low Level Radioactive Waste Backfills*. SAND95-2978, Sandia National Laboratories, Albuquerque, New Mexico.

Bao Y, S Kwan, DD Siemer, and MW Grutzeck. 2004. "Binders for Radioactive Wasteforms Made From pretreated Calcined Sodium-bearing Waste" *Journal of Material Science* 39:481-488.

Bao Y, MW Grutzeck, and CM Jantzen. 2005. "Preparation and Properties of Hydroceramic Waste Forms Made with Simulated Hanford Low-Activity Waste." *Journal of American Ceramic Society* 88:3287-3302.

Barin I. 1989. *Thermochemical Data of Pure Substances*. VCH, New York.

Batchelor B. 2006. "Overview of Waste Stabilization with Cement." *Waste Management* 26:689-698.

Bidoglio G, A Avogadro, and A De Plano. 1985. "Influence of Redox Environments on the Geochemical Behavior of Radionuclides." In: *Scientific Basis for Nuclear Waste Management IX, Material Research Society Symposium Proceedings*, Vol 50, ed LO Werme, pp. 709-716. September 9-11, 1985, Stockholm, Sweden. North-Holland, New York.

Bird GW and VJ Lopata. 1980. "Solution Interaction of Nuclear Waste Anions with Selected Geological Materials." In: *Scientific Basis for Nuclear Waste Management, International Symposium on the Scientific Basis for Nuclear Waste Management*, Vol 2, ed CJM Northrup, pp. 419-426. 1979, Boston, Massachusetts. Plenum Press, New York.

Bock WD, H Bruhl, C Trapp, and A Winkler. 1988. “Sorption Properties of Natural Sulfides with Respect to Technetium.” In: *Scientific Basis for Nuclear Waste Management XII, Materials Research Society Symposium Proceedings*, Vol 127, eds W Lutze and RC Ewing, pp. 973-977. October 10-13, 1988. Berlin, Federal Republic of Germany. North-Holland, New York.

Bors J. 1990. “Sorption of Radioiodine in Organo-Clays and Soils.” *Radiochimica Acta* 51:139-143.

Bors J. 1992. “Sorption and Desorption of Radioiodine on Organo-Clays.” *Radiochimica Acta* 58-59:235-238.

Bors J, A Gorny, and S Dultz. 1994a. “Some Factors Affecting the Interactions of Organophilic Clay-Minerals with Radioiodine.” *Radiochimica Acta* 66-7:309-313.

Bors J, A Gorny, and S Dultz. 1994b. “Studies on the Interaction of Radionuclides with Organo-Philic Clays.” *Radiochimica Acta* 66/67: 309-313.

Bors J, A Gorny, and S Dultz. 1996. “Studies on the Interaction of Radionuclides with Organophilic Clays.” *Radiochimica Acta* 74:231-234.

Bors J, S Dultz, and A Gorny. 1998. “Sorption of Iodide, Cesium and Strontium on Organophilic Bentonite.” *Radiochimica Acta* 82:269-274.

Bostick WD, JL Shoemaker, PE Osborne, and B Evans-Brown. 1990. *Treatment and Disposal Options for a Heavy Metals Containing Soluble Technetium-99 Emerging Technologies in Hazardous Waste Management*. American Chemical Society, Washington, D.C.

Brenchley ME and MT Weller. 1994. “Synthesis and Structure of M8[AlSiO4]6•(XO4)2, M=Na, Li, K; X=Cl, Mn Sodalites.” *Zeolites* 14:682-686.

Buhl JC and J Lons. 1996. “Synthesis and Crystal Structure of Nitrate Enclathrated Sodalite Na8[AlSiO4]6(NO3)2.” *Journal of Alloys and Compounds* 235:41-47.

Buhl JC, TM Gesing, and C Gurris. 2001. “Synthesis and Crystal Structure of Rhodanide-Enclathrated Sodalite Na8[AlSiO4]6(SCN)2.” *Microporous and Mesoporous Materials* 50:25-32.

Burger LL. 1980. *Determining Criteria for the Disposal of Iodine-129*. Technical Report PNL-3496, Pacific Northwest National Laboratory, Richland, Washington.

Burger LL and RD Scheele. 1981. Iodine-Fixation Studies at the Pacific Northwest Laboratory. [Silver mordenite] In: Conference: Specialists' Meeting on Radioiodine Management, September 25, Brussels, Belgium. Other Information: Portions are illegible in microfiche products.

Burger LL and RD Scheele. 2004. *HWVP Iodine Trap Evaluation*. PNNL-14860, Pacific Northwest National Laboratory, Richland, Washington.

Burger LL, RD Scheele, and KD Wiemers. 1981. *Selection of a Form for Fixation of Iodine 129*. PNL-4045, Pacific Northwest Laboratory, Richland, Washington.

Burke IT, C Boothman, KR Lloyd, RJG Mortimer, FR Livens, and K Morris. 2005. "Effects of Progressive Anoxia on the Solubility of Technetium in Sediments." *Environmental Science and Technology* 39:4109-4116.

Burke IT, C Boothman, JR Lloyd, F R Livens, JM Charnock, JM McBeth, RJG Mortimer, and K Morris. 2006. "Reoxidation Behavior of Technetium, Iron and Sulfur in Estuarine Sediments." *Environmental Science and Technology* 40:3529-3535.

Byegard J, G Albinsson, G Skanemark, and M Skalberg. 1992. "Field and Laboratory Studies on the Reduction and Sorption of Technetium (VII)." *Radiochimica Acta* 58/59:239-244.

Clark BA, DG Atteridge, M Avila, VR Baca, KM Bishop, GA Cooke, LL Lockrem, RJ Lee, and MR Silsbee. 2005. "Development of a Cast Stone Formulation for Hanford Tank Wastes." Presented at the RemTech 2005 Symposium, Banff, Alberta, October 19-21, 2005. CH2M Hill, Richland, Washington. Available at: RPP-RPT-27297-FP (Full Paper).

Clark BA, LL Lockrem, GA Cooke, M Avila, R Westberg, MR Silsbee, and RJ Lee. 2006. "Hanford Site Cement-Based Waste Stream Solidification Studies." Presented at the *Cementitious Materials for Waste Treatment, Disposal, Remediation and Decommissioning Workshop*, December 12-14, 2006, Savannah River National Laboratory, Aiken, SC, CH2M Hill, Richland, Washington. Available at: RPP-31811-VA.

Cooke GA and LL Lockrem. 2005. *ETF Waste Stream Stabilization Testing*. RPP-RPT-26851 Rev. 0, CH2MHill, Richland, Washington.

Cooke GA, KM Bishop, and LL Lockrem. 2003. *Containerized Cast Stone Facility, Task 1 – Process Testing and Development Final Test Report*. Fluor Federal Services (entered into RMIS as: LL Lockrem, RPP-RPT-26742, 07-13-2005, *Hanford Containerized Cast Stone Facility Task - 1 Process Testing And Development Final Test Report*. Text thru Appendix E, and Appendix F thru Appendix J, CH2M Hill, Richland, Washington.

Cooke GA, LL Lockrem, M Avila, and RA Westberg. 2006a. *Effluent Treatment Facility Waste Stream Monolith Testing, Phase II*. RPP-RPT-31077, CH2M Hill, Richland, Washington.

Cooke GA, LL Lockrem, MD Guthrie, KJ Lueck, and M Avila. 2006b. Development and Testing of a Cement-Based Solid Waste Form Using Synthetic UP-1 Groundwater, CH2M Hill, Richland, Washington. Available at: RPP-RPT-31740.

Cooke G, LL Lockrem, M Avila, R Westberg, MR Silsbee, B Clark, MD Guthrie, GL Koci, and KJ Lueck. 2006c. "Cement Solidification of Ammonium Sulfate Rich Basin 42 Waste Water from the Hanford Effluent Treatment Facility." Presented at the *Cementitious Materials for Waste Treatment, Disposal, Remediation and Decommissioning Workshop*, December 12-14, 2006, RPP-31803-VA, Savannah River National Laboratory, Aiken, SC, CH2M Hill, Richland, Washington.

Cooke G, LL Lockrem, M Avila, R Westberg, MR Silsbee, GL Koci, MD Guthrie, and KJ Lueck. 2006d. "Radionuclide & Heavy Metal Waste Stream Stabilization Testing at The Hanford Site" (Abstract). RPP-31816-A, for presentation at the *WM'07 33rd Waste Management Conference*, Tucson, Arizona, February 25-March 01, 2007, CH2M Hill, Richland, Washington.

Cooke GA, JB Duncan, LMD Guthrie, and LL Lockrem. 2009. "Assessment of Pertechnetate Getters, Reductants and Stabilization." Presented at the *DOE Technical Exchange*, Denver, Colorado, Washington River Protection Solutions, LLC, Richland, Washington. Available at: RPP-41231-VA.

Coons WE, EL Moore, MJ Smith, and JD Kaser. 1980. *The Functions of an Engineered Barrier System for a Nuclear Waste Repository in Basalt. RHO-BWI-LD-23*, Rockwell International, Richland, Washington.

Couture RA and MG Seitz. 1983. "Sorption of Anions of Iodine by Iron Oxides and Kaolinite." *Nuclear Chemistry Waste Management* 4:301-306.

Cui D and TE Eriksen. 1996a. "Reduction of Pertechnetate by Ferrous Iron in Solution: Influence of Sorbed and Precipitated Fe(II)." *Environmental Science and Technology* 30:2259-2262.

Cui D and TE Eriksen. 1996b. "Reduction of Pertechnetate in Solution by Heterogeneous Electron Transfer from Fe(II)-Containing Geological Material." *Environmental Science and Technology* 30:2263-2269.

Darab JG and PA Smith. 1996. "Chemistry of Technetium and Rhenium Species during Low-Level Radioactive Waste Vitrification." *Chemistry of Materials* 8:1004-1021.

Davidovits J. 1994a. *Method for Obtaining a Geopolymeric Binder Allowing to Stabilize, Solidify, and Consolidate Toxic Waste Materials*. U.S. Patent No. 5,349,118. Abstract accessed October 27, 2009, at http://www.freepatentsonline.com/5349118.html.

Davidovits J. 1994b. *Process for Obtaining a Geopolymeric Alumino-silicate and Products Thus Obtained*. U.S. Patent No. 5,342,596. Abstract accessed October 27, 2009, at http://www.freepatentsonline.com/5342595.html.

Davidovits J. 1994c. *Method for Obtaining a Geopolymeric Binder Allowing to Stabilize, Solidify, and Consolidate Toxic Waste Materials*. U.S. Patent No. 5,349,118.

Del Cul GD, WD Bostick, DR Trotter, and PE Osborne. 1993. "Technetium-99 Removal from Process Solutions and Contaminated Groundwater." *Separation Science and Technology* 28:551-564.

Diamond S and KO Kjellsen. 2006. "Resolution of Fine Fibrous C-S-H in Backscatter SEM Examination." *Cement & Concrete Composites* 28:130-132.

Ding M, NC Schroeder, and PW Reimus. 2001. "Zero-Valent Iron Immobilizes Technetium." American Chemical Society. Extended Abstracts of the Division of Environmental Chemistry, 222nd ACS National Meeting, August 26-30, Chicago, Illinois 41(2):118-120.

Duncan JB and SP Burke. 2008. *Results of IONSIV® IE-95 Studies for the Removal of Radioactive Cesium from KE Basin Spent Nuclear Fuel Pool During Decommissioning Activities*. CH2M Hill, Richland, Washington. Available at: RPP-RPT-37055, Rev. 0.

Duncan JB, GA Cooke, LL Lockrem, and MD Guthrie. 2008. *Assessment of Technetium Leachability in Cement-Stabilized Basin 43 Groundwater Brine.* RPP-RPT-39195. CH2M Hill Hanford Group, Inc., Richland, Washington.

Duncan JB, GA Cooke, and LL Lockrem. 2009. *Assessment of Technetium Leachability in Cement-Stabilized Basin 43 Groundwater Brine*. Washington River Protection Solutions, LLC, Richland, Washington. Available at: RPP-RPT-39195, Rev. 1).

Ecology, EPA, and DOE. 1989. *Hanford Facility Agreement and Consent Order, As Amended*. Washington State Department of Ecology, U.S. Environmental Protection Agency, and U.S. Department of Energy, Olympia, Washington.

El-Wear SK, KE German, and VE Peretrukhin. 1992. "Sorption of Technetium on Inorganic Sorbents and Natural Minerals." *Journal of Radioanalytical and Nuclear Chemistry* 157:3-14.

EPA—U.S. Environmental Protection Agency. 2000. Toxicity Characteristics Leaching Procedure. SW846 Method 1311 for VOCs, SVOCs, Chlorinated Pesticides, Herbicides, Metals, and Mercury. Cincinnati, Ohio.

EPA—U.S. Environmental Protection Agency. 2009a. Leaching Test (Liquid-Solid Partitioning as a Function of Extract pH) of Constituents in Solid Materials Using a Parallel Batch Extraction Test, Draft Method 1313. .

EPA—U.S. Environmental Protection Agency. 2009b. Leaching Test (Liquid-Solid Partitioning as a Function of Liquid-Solid Ratio) of Constituents in Solid Materials Using an Up-Flow Percolation Column, Draft Method 1314.

EPA—U.S. Environmental Protection Agency. 2009c. Mass Transfer Rates of Constituents in Monolith or Compacted Granular Materials Using a Semi-Dynamic Tank Leaching Test, Draft Method 1315.

EPA—U.S. Environmental Protection Agency. 2009d. Leaching Test (Liquid-Solid Partitioning as a Function of Liquid to Solid Ratio) of Constituents in Solid Materials Using a Parallel Batch Extraction Test, Draft Method 1316.

Fechtelkord M. 2000. "Influence of Sodium Ion Dynamics on the 23Na Quadrapolar Interaction in Sodalite: A High-Temperature 23Na MAS NMR Study." *Solid State Nuclear Magnetic Resonance* 18:70-88.

Fetter G, E Ramos, MT Olguin, P Bosch, T Lopez, and S Bulbulian. 1996. "Sorption of 131I- by Hydrotalcites." *Journal of Radioanalytical and Nuclear Chemistry* 221:63-66.

Fiskum S, ST Arm, MS Fountain, MJ Steele, and DL Blanchard. 2006a. *Spherical Resorcinol-Formaldehyde Resin Testing for 137Cs Removal from Simulated and Actual Hanford Waste Tank 241-AP-101 Diluted Feed (Envelope A) Using Small Column Ion Exchange WTP-RPT-134*. Battelle−Pacific Northwest Division, Richland, Washington.

Fiskum S, I Burgeson, OT Farmer, LR Greenwood, CZ Soderquist, MJ Steele, and MP Thomas. 2006b. *Spherical Resorcinol-Formaldehyde Resin Analysis Following Actual Hanford Tank Waste Processing*. PNWD-3752 (WTP-RPT-144 Rev. 0), Battelle-Pacific Northwest Division, Richland, Washington.

Fredrickson JK, JM Zachara, RK Kukkadapu, JP McKinley, SM Heald, C Liu, and AE Plymale. 2004. "Reduction of TcO4- by Sediment-Associated Biogenic Fe(II)." *Geochimica et Cosmochimica Acta* 68:3171-3187.

Fredrickson JK, JM Zachara, AE Plymale, SM Heald, JP McKinley, DW Kennedy, C Liu, and P Nachimuthu. 2009. "Oxidative Dissolution Potential of Biogenic and Abiogenic Tc_{O2} in Subsurface Sediments." *Geochimica et Cosmochimica Acta* 73:2299-2313.

Fried S, AM Friedman, D Cohen, JJ Hines, and RG Strickert. 1978. *The Migration of Long-Lived Radioactive Wastes in Selected Rocks*. ANL-78-46, Argonne National Laboratory, Argonne, Illinois.

Fryxell GE, J Liu, AA Hauser, Z Nie, KF Ferris, SV Mattigod, M Gong, and RT Hallen. 1999a. "Design and Synthesis of Selective Mesoporous Anion Traps." *Chemical Materials* 11:2148-2154.

Fryxell GE, J Liu, and SV Mattigod. 1999b. "Self-Assembled Monolayers on Mesoporous Supports (SAMMS) - an Innovative Environmental Sorbent." Materials Technology: Advanced Performance Materials 14(4):188-191.

Fujihara H, T Murase, T Nishi, K Noshita, T Yoshida, and M Matsuda. 1998. *Low-Temperature Vitrification of Radio-Iodine Using AgI-Ag2O-P2O5 Glass System*. Materials Research Society Symposium. Materials Research Society, Warrendale, Pennsylvania.

Fukumoto M and M Kanzaki. 1998. *Method for Solidifying Waste Containing Radioactive Iodine*. Doryokuro Kakunenryo Kaihatsu Jigyodan. U.S. Patent No. 5,826,203. Abstract accessed October 27, 2009, at http://www.freepatentsonline.com/5826203.html.

Gehner P, RM Lowy, and G Dunford. 2009. *Secondary Waste Treatment Quantity and Composition (WTP Solid Waste Streams.)* RPP-RPT-42519, Rev. A Pacific Northwest National Laboratory, Richland, Washington. Washington River Protection Solutions (WRPS), Richland, Washington.

Gilliam TM, RD Spence, B Evans-Brown, IL Morgan, WD Bostick, and JL Shoemaker. 1988. *Performance Testing of Blast Furnace Slag for Immobilization of Technetium in Grout.* CONF-880903-17, Oak Ridge National Laboratory, Oak Ridge, Tennessee.

Gilliam TM, RD Spence, WD Bostick, and JL Shoemaker. 1990. "Solidification/Stabilization of Technetium in Cement-based Grouts." *Journal of Hazardous Materials* 24:189-197.

Glasser FP. 1997. "Fundamental Aspects of Cement Solidification and Stabilization." *Journal of Hazardous Materials* 52:151-170.

Glasser FP, J Marchand, and E Samson. 2008. "Durability of Concrete - Degradation Phenomena Involving Detrimental Chemical Reactions." *Cement and Concrete Research* 38:226-246.

Gong W, W Lutze, and I Pegg. 2006. *Low-Temperature Solidification of Radioactive and Hazardous Wastes.* U.S. Patent Application No. 20060211908 A.

Gradev GD. 1987. "Sorption of Iodide Ions on Cationic Forms of Clinoptilolite." *Journal of Radioanalytical and Nuclear Chemistry* 116:341-346.

Graydon JW, X Zhang, DW Kirk, and CQ Jia. 2009. "Sorption and Stability of Mercury on Activated Carbon for Emission Control." *Journal of Hazardous Materials* 168:978-982.

Hakem N, B Fourest, R Guillaumont, and N Marmier. 1996. "Sorption of Iodine and Cesium on Some Mineral Oxide Colloids." *Radiochimica Acta* 74:225-230.

Haq Z, GM Bancroft, WS Fyfe, G Bird, and VJ Lopata. 1980. "Sorption of Iodide on Copper." *Environmental Science and Technology* 14:1106-1110.

Herbst AK. 2002. *Testing and Disposal Strategy for Secondary Wastes from Vitrification of Sodium-Bearing Waste at the Idaho Nuclear Technology and Engineering Center*. NEEL/EXT-02-00007. Idaho National Engineering and Environmental Laboratory, Idaho Falls, Idaho.

Huheey JE, EA Keiter, and RL Keiter. 1993. *Inorganic Chemistry: Principles of Structure and Reactivity, Fourth Edition*. HarperCollins College Publishers, New York.

Hund F. 1984. "Nitrit-, Cyanid- und Rhodanid-Sodalith." *Zeitschrift fur Anorganische und Allgemeine Chemie* 511(4):225-230.

Ito K and K Akiba. 1991. "Adsorption of Pertechnetate Ion on Active Carbon from Acids and their Salt Solutions." *Journal of Radioanalytical and Nuclear Chemistry* 153:381-390.

Ito K and T Kanno. 1988. "Sorption Behavior of Carrier-Free Technetium-95m on Minerals, Rocks and Backfill Materials under both Oxidizing and Reducing Conditions." *Journal of Nuclear Science and Technology* 25:534-539.

Jantzen CM. 2002. *Engineering Study of the Hanford Low Activity Waste (LAW) Steam Reforming Process*. WSRC-TR-2002-00317, Rev. 0; SRT-RPP-2002-00163, Rev. 0, Westinghouse Savannah River Company, Savannah River Site, Aiken, South Carolina.

Jantzen CM. 2006. *Fluidized Bed Steam Reformer (FBSR) Product: Monolith Formation and Characterization*. WSRC-STI-2006-00033, Rev. 1, Savannah River National Laboratory, Aiken, South Carolina.

Jantzen CM. 2008. *Mineralization of Radioactive Wastes by Fluidized Bed Steam Reforming (FBSR): Comparison to Vitreous Waste Forms, and Pertinent Durability Testing*. WSRC-STI-2008-00268, Rev. 0, Savannah River National Laboratory, Aiken, South Carolina.

Jantzen CM, TH Lorier, JM Pareizs, and JC Marra. 2007. "Fluidized Bed Steam Reformed (FBSR) Mineral Waste Forms: Characterization and Durability Testing." Presented at the *Material Research Society Symposium Proceedings,* Vol. 985.

Johnson GM, PJ Mead, and MT Weller. 2000. "Synthesis of a Range of Anion-Containing Gallium and Germanium Sodalites." *Microporous and Mesoporous Materials* 38:445-460.

Kang MJ, SW Rhee, and H Moon. 1996. "Sorption of MO4-(M= Tc, Re) on Mg, Al Layered Double Hydroxide by Anion Exchange." *Radiochimica Acta* 75.

Kang MJ, SW Rhee, and Y Do. 1999. "Comparison of Sorption Behavior of I- and TcO4- on Mg/Al Layered Double Hydroxide." *Radiochimica Acta* 85:169-173.

Kaplan DI. 2003. *Estimated Duration of the Subsurface Reducing Environment Produced by the Z-Area Saltstone Disposal Facility (U)*. Westinghouse Savannah River Company LLC, Aiken, South Carolina.

Kaplan DI, RJ Serne, KE Parker, and IV Kutnyakov. 2000a. "Iodide Sorption to Subsurface Sediments and Illitic Minerals." *Environmental Science and Technology* 34:399-405.

Kaplan D, SV Mattigod, KE Parker, and G Iversen. 2000b. *Experimental Work in Support of the 129I-Disposal Special Analysis*. WSRC-TR-2000-00283, Rev 0, Westinghouse Savannah River Company, Savannah River Site, Aiken, South Carolina.

Kaplan DI, T Hang, and SE Aleman. 2005. *Estimated Duration of the Reduction Capacity within a High-Level Waste Tank.* Westinghouse Savannah River Company LLC, Aiken, South Carolina.

Kaplan DI, K Roberts, S Serkiz, and M Siegfried. 2008. *Saltstone and Concrete Interactions: Radionuclide Sorption and Desorption, and Saltstone Reduction Capacity*. Laboratory, Savannah River Nuclear Site. SRNS-NTI-2008-00045, Westinghouse Savannah River Company LLC, Aiken, South Carolina.

Kemner KM, X Feng, J Liu, GE Fryxell, LQ Wang, AY Kim, M Gong, and SV Mattigod. 1999. "Investigation of the Local Chemical Interactions Between Hg and Self-Assembled Monolayers on Mesoporous Supports." *Journal of Synchrotron Radiation* 6:633-635.

Klingsberg C and J Duguid. 1980. *Status of Technology for Isolating High-Level Radioactive Wastes in Geologic Repositories*. DOE/TIC 11207, U.S. Department of Energy, Washington, D.C.

Koci GI. 2005. *Conceptual Design Report for Effluent Treatment Facility Solidification Treatment Unit*. Fluor Hanford, Richland, Washington.

Krumhansl JL. 2003. *A Preliminary Assessment of Tc, I, and Se Getter Development Activities for Hanford Tank Closure Applications Draft Letter Report*. Sandia National Laboratories, Albuquerque, New Mexico.

Krumhansl JL, JD Pless, B Chwirka, and KC Holt. 2006. *Yucca Mountain Project Getter Program Results (Year 1): I-129 and Other Anions of Concern*. SAND2006-3869, Sandia National Laboratories, Albuquerque, New Mexico.

Kunze, V Neck, K Gompper, and T Fanghanel. 1996. "Studies on the Immobilization of Technetium Under near-Field Geochemical Conditions." *Radiochimica Acta* 74:159-163.

Kyritsis K, N Meller, and C Hall. 2009. “Chemistry and Morphology of Hydrogarnets formed in Cement-Based CASH Hydroceramics Cured at 200° to 350°C.” *Journal of the American Ceramic Society* 92:1105-1111.

Langton CA. 1988a. *Challenging Applications for Hydrated and Chemically Reacted Ceramic.* DP-MS-88-163, Savannah River Laboratory, Aiken, South Carolina.

Langton CA. 1988b. “Slag-Based Saltstone Formulations.” In: Material Research Society Symposium Proceedings 112:61-70.

Lasaga AC and A Lüttge. 2001. “Variation of Crystal Dissolution Rate Based on a Dissolution Step Wave Model.” *Science* 291:2400-2404.

Lee SY and EA Bondietti. 1983. “Technetium Behavior in Sulfide and Ferrous Iron Solutions.” *Scientific Basis for Nuclear Waste Management* 15:315-322.

Li J and J Wang. 2006. “Advances in Cement Solidification Technology for Waste Radioactive Ion Exchange Resins: A Review.” *Journal of Hazardous Materials* B135:443-448.

Li JF, ZG Hao, and JL Wang. 2005. “Solidification of Low-Level-Radioactive Resins in ASC-Zeolite Blends.” *Nuclear Engineering and Design* 235:817-820.

Liang LY, BH Gu, and XP Yin. 1996. “Removal of Tc-99 from Contaminated Groundwater with Sorbents and Reductive Materials.” *Separations Technology* 6:111-122.

Lide DR. 2009. *CRC Handbook of Chemistry and Physics, Internet Version 2008-2009*. Taylor and Francis, Boca Raton, Florida.

Lieser KH and CH Bauscher. 1988. “Technetium in the Hydrosphere and in the Geosphere, II. Influence of pH of Complexing Agents and Some Minerals on the Sorption of Technetium.” *Radiochimica Acta* 44/45:125-128.

Liu J, GE Fryxell, SV, Mattigod, M Gong, Z Nie, X Feng, and KN Raymond. 1998. *Self-Assembled Monolayers on Mesoporous Support (SAMMS) Technology for Contaminant Removal and Stabilization*. PNL-12006, Pacific Northwest National Laboratory, Richland, Washington.

Liu W, RD Vidic, and TD Brown. 2000. “Optimization of High Temperature Sulfur Impregnation on Activated Carbon for Permanent Sequestration of Elemental Mercury Vapors.” *Environmental Science and Technology* 34:483-488.

Liu J, GE Fryxell, SV Mattigod, TS Zemanian, Y Shin, and LQ Wang. 2000. “Synthesis and Applications of Functionalized Nanoporous Materials for Specific Adsorption.” *Studies in Surface Science and Catalysis* 129:729-738.

Liu Y, J Terry, and JS Jurisson. 2008. “Pertechnetate Immobilization with Amorphous Iron Sulfide.” *Radiochimica Acta* 96:823-833.

Livens FR, MJ Jones, A Hynes, JM Charnock, FW Mosselmans, C Hennig, H Steele, D Collison, DJ Vaughn, RAD Pattrick, WA Reed, and LN Moyes. 2004. X-Ray Absorption Spectroscopy Studies of Reactions of Technetium, Uranium and Neptunium with Mackinawite." *Journal of Environmental Radioactivity* 74:211-219.

Lockrem LL, GA Cooke, GL Troyer, and JL Person. 2003. *Cast Stone Technology for Treatment and Disposal of K Basin Sludge Demonstration Test Report*. RPP-19163 Rev. 0, CH2M Hill, Richland, Washington.

Lockrem LL. 2005a. *Cast Stone Technology for Treatment and Disposal of Iodine-rich Caustic Waste Demonstration*. Fluor Hanford, Richland, Washington.

Lockrem LL. 2005b. *Hanford Containerized Cast Stone Facility Task 1 - Process Testing and Development, Final Report*. RPP-RPT-26742, Rev. 0, Fluor Hanford, Richland, Washington.

Lockrem LL, GA Cooke, BA Clark, and R Westburg. 2008. *Cast Stone Technology for Treatment & Disposal of Iodine Rich Caustic Waste Demonstration Final Report*. CH2M Hill, Richland, Washington (RPP-RPT-26725), Rev. 0-A; link is to Rev 0, Rev 0-A included all authors).

Lorier TH, JM Pareizs, and CM Jantzen. 2005. *Single-Pass Flow Through (SPFT) Testing of Fluidized-Bed Steam Reforming (FBSR) Waste Forms.* Westinghouse Savannah River Company, Aiken, South Carolina.

Lothenbach B, T Matschei, G Scheiner, and FP Glasser. 2008. "Thermodynamic Modeling of the Effect of Temperature on the Hydration and Porosity of Portland Cement." *Cement and Concrete Research* 38:1-18.

Lukens WW, JJ Bucher, DK Shuh, and NM Edelstein. 2003. *Evolution of Technetium Speciation in Reducing Grout.* University of California, Berkeley, California.

Lukens WW, JJ Bucher, DK Shuh, and NM Edelstein. 2005. "Evolution of Technetium Speciation in Reducing Grout. "Environmental Science and Technology 39:8064-8070.

Luo, Z, et al. 2006, "Stability of Mercury on Three Activated Carbon Sorbents." Fuel Processing Technology 87:679-85.

Lüttge A. 2004. "Crystal Dissolution Kinetics Studied by Vertical Scanning Interferometry (VSI) and Monte Carlo Simulations." In: X-Y Liu, Editor, *Nanoscale Structure and Assembly at Solid-Fluid Interfaces. Vol. I. Interfacial Structures versus Dynamics*. Kluwer Academic Publishers, New York.

Lüttge A, EW Bolton, and AC Lasaga. 1999. "An Interferometric Study of the Dissolution Kinetics of Anorthite: The Role of Reactive Surface Area." *American Journal of Science* 299:652-678.

Mann FM. 2002. *Annual Summary of ILAW Performance Assessment for 2002*. CH2M Hill Hanford Group, Inc., Richland, Washington.

Maset ER, SH Sidhu, A Fisher, A Heydon, PJ Worsfold, AJ Cartwright, and MJ Keith-Roach. 2006. “Effect of Organic Co-Contaminants on Technetium and Rhenium Speciation and Solubility under Reducing Conditions.” *Environmental Science and Technology* 40:5472-5477.

Matsuoka, S, H Nakamura, and T Tamura. 1984, "Stability and Chemical Form of Iodine Sorbed on Silver-Exchanged Zeolite X." J Nuclear Science and Technology 21:862-70.

Mattigod SV, X Feng, GE Fryxell, J Liu, M Gong, C Ghormley, S Baskran, Z Nie, and KT Klasson. 1997. *Mercury Separation from Concentrated Potassium Iodide/Iodine Leachate Using Self-Assembled Mercaptan on Mesoporous Silica Technology*. Pacific Northwest National Laboratory, Richland, Washington.

Mattigod SV, D Kaplan, VL LeGore, RD Orr, HT Schaef, and JS Young. 1998. *Radionuclide Incorporation in Secondary Crystalline Minerals Resulting From Chemical Weathering of Selected Waste Glasses: Progress Report for Subtask 3d*. PNNL-12005, Pacific Northwest National Laboratory, Richland, Washington.

Mattigod SV, KE Parker, GE Fryxell, J Liu, and RJ Serne. 2000. *Evaluation of Novel Getters for Adsorption of Radionuclides from Hanford Groundwater and Waste Glass Leachates Letter Report to CHG*. Pacific Northwest National Laboratory, Richland, Washington.

Mattigod SV, BP McGrail, DE McCready, L Wang, KE Parker, and JS Young. 2006. “Synthesis and Structure of Perrhenate Sodalite.” *Microporous and Mesoporous Materials* 91:139-144.

McGrail BP, JP Icenhower, PF Martin, DR Rector, HT Schaef, EA Rodriguez, and JL Steele. 2000. *Low-Activity Waste Glass Studies: FY2000 Summary Report.* Pacific Northwest National Laboratory, Richland, Washington.

McGrail BP, EM Pierce, HT Schaef, EA Rodriguez, JL Steele, AT Owen, and DW Wellman. 2003a. *Laboratory Testing of Bulk Vitrified and Steam Reformed Low-Activity Waste Forms to Support A Preliminary Risk Assessment for an Integrated Disposal Facility*. Pacific Northwest National Laboratory, Richland, Washington.

McGrail BP, HT Schaef, PF Martin, DH Bacon, EA Rodriguez, DE McCready, AN Primak, and RD Orr. 2003b. *Initial Suitability Evaluation of Steam-Reformed Low-Activity Waste for Direct Land Disposal.* Battelle, Pacific Northwest Division, Richland, Washington.

McKeown DA, AC Buechele, WW Lukens, DK Shuh, and LL Pegg. 2007. “Tc and Re Behavior in Borosilicate Waste Glass Vapor Hydration Tests.” *Environmental Science and Technology* 41:431-436.

Moak DP. 1981. *Waste Package Materials: Screening and Selection*. Battelle Memorial Institute, Columbus, Ohio.

Moore RC. 2003. *Sorption of Tc by Sn(II) Treated Apatite, Draft Letter Report*. Sandia National Laboratories, Albuquerque, New Mexico.

Morgan MT, JG Moore, HE Devaney, GC Rogers, C Williams, and E Newman. 1978. *Disposal of Iodine-129*. Chemical Technology Division, Oak Ridge National Laboratory, Oak Ridge, Tennessee.

Also published in the Proceedings of the Materials Research Society Symposium on Science Underlying Radioactive Waste Management, November 29-December 1, Boston, Massachusetts

Moriyama N, S Dojiri, and H Matsuzuru. 1977. "Leaching of Cs-137 from Ion-Exchange Resin Incorporated in Polyethylene or Cement Composite." *Health Physics* 32:549-552.

Morris K, FR Livens, JM Charnock, JIT Burke, JM McBeth, JDC Begg, C Boothman, and JR Lloyd. 2008. :An X-Ray Absorption Study of the fate of Technetium in Reduced and Reoxidised Sediments and Mineral Phases." *Applied Geochemistry* 23:603-617.

Nash CA and MD Dowley. 2007. *Characterization of Spent Spherical Resorcinol-Formaldehyde Resin*. WSRC-STI-2007-00213, Rev. 0 (SRNL-RPP-2006-00029 Rev. 0). Washington Savannah River Company, Savannah River Site, Aiken, South Carolina.

Neilson RM and P Columbo. 1982. *Solidification of Ion Exchange Resin Wastes.* BNL-51615, Brookhaven National Laboratory, Upton, New York.

Nowak EJ. 1980. *Radionuclide Sorption and Migration Studies of Getters for Backfill Barriers*. SAND79-1110, Sandia National Laboratories, Albuquerque, New Mexico.

NRC—U.S. Nuclear Regulatory Commission. 1991. *Technical Position on Waste Form, Rev. 1*. Final Waste Classification and Waste Form Technical Position Papers, NRC, Washington, DC.

NRC—U.S. Nuclear Regulatory Commission. 2001. *Research Needs for High-Level Waste Stored in Tanks and Bins at U.S. Department of Energy Sites.* National Academy Press, Washington, D.C.

Olson AL, NR Soelberg, DW Marshall, and GL Anderson. 2004. *Fluidized Bed Steam Reforming of Hanford LAW Using THORSM Mineralizing Technology*. INEEL/EXT-04-02564, Idaho National Engineering and Environmental Laboratory, Idaho Falls, Idaho.

Osmanlioglu AE. 2007. "Progress in Cementation of Reactor Resins." *Progress in Nuclear Energy* 49:20-26.

Pabalan RT, FP Glasser, DA Pickett, GR Walter, S Biswas, MR Juckett, LM Sabido, and J L Myers. 2009. Review of Literature and Assessment of Factors Relevant to Performance of Grouted Systems for Radioactive Waste Disposal. Center for Nuclear Waste Regulatory Analyses, San Antonio, TX.

Palmer DA and RE Meyer. 1981. "Adsorption of Technetium on Selected Inorganic Ion-Exchange Materials and on a Range of Naturally Occurring Minerals under Oxic Conditions." *Journal of Inorganic and Nuclear Chemistry* 43, 2979-2984.

Pan LK, BD Chang, and DS Chou. 2001. "Optimization for Solidification of Low-Level-Radioactive Resin Using Taguchi Analysis." *Waste Management* 21:767-772.

Perera DS, MG Blackford, ER Vance, JV Hanna, KS Finnie, and CL Nicholson. 2004. "Geopolymers for the Immobilization of Radioactive Waste." Material Research Society Symposium Proceedings Vol 824.

Perera DS, Z Aly, ER Vance, and M Mizumo. 2005. “Immobilization of Pb in a Geopolymer Matrix.” *Journal of the American Ceramic Society* 88:2586-2588.

Peretyazhko T, JM Zachara, SM Heald, B-H Jeon, RK Kukkadapu, C Liu, D Moore, and CT Resch. 2008a. “Heterogeneous Reduction of Tc(VII) by Fe(II) at the Solid-Water Interface.” *Geochimica et Cosmochimica Acta* 72, 1521-1539.

Peretyazhko T, JM Zachara, SM Heald, RK Kukkadapu, C Liu, AE Plymale, and CT Resch. 2008b. “Reduction of Tc(VII) by Fe(II) Sorbed on Al (hydr)Oxides.” *Environmental Science and Technology* 42:5499-5506.

Phifer MA, MR Millings, and GP Flach. 2006. *Hydraulic Property Data Package for the E-Area and Z-Area Soils, Cementitious Materials, and Waste Zones*. Washington Savannah River Company, Savannah River Site, Aiken, South Carolina.

Pierce EM. 2007. *Accelerated Weathering of Fluidized Bed Steam Reformation Material Under Hydraulically Unsaturated Conditions*. Materials Science and Technology 2007, Detroit, Michigan.

Pierce EM, LR Reed, WJ Shaw, BP McGrail, JP Icenhower, CF Windisch, EA Cordova, and J Broady. 2009. “Experimental determination of the effect of the ratio of B/Al on glass dissolution along the nepheline ($NaAlSiO_4$)-malinkoite ($NaBSiO_4$) join.” *Geochimica et Cosmochimica Acta*. In Press. Dio:10.1016/j.gca.2009.09.006.

Plecas I, A Peric, A Kostadinovic, J Drljaca, and S Glodic. 1992. “Leaching Behavior of 60Co and 137Cs from Spent Ion Exchange Resins in Cement Matrix.” *Cement and Concrete Research* 22:937-940.

Plecas I, R Pavlovic, and S Pavlovic. 2003. “Leaching of ^{60}Co and ^{137}Cs from Spent Ion Exchange Resins in Cement-Bentonite Clay Matrix.” *Bull. Mater. Sci.* 26:699-701.

Plecas I, R Pavlovic, and S Pavlovic. 2004. “Leaching behavior of Co-60 and (CS)-C-137 from spent ion exchange resins in cement-bentonite clay matrix.” *Journal of Nuclear Materials* 327:171-174.

Plecas I, S Dimovic, and I Smiciklas. 2009. “Influence of bentonite and zeolite in cementation of dry radioactive evaporator concentrates.” *Applied Clay Science* 43:9-12.

Rancon D. 1988. “Comparative Study of Radioiodine Behavior in Soils Under Various Experimental and Natural Conditions.” *Radiochimica Acta* 88:187-193.

Randall P and S Chattopadhyay. 2004. “Advances in Encapsulation Technologies for the Management of Mercury-Contaminated Hazardous Wastes.” *Journal of Hazardous Materials* 114:211-223.

Russell RL, MJ Schweiger, JH Westsik, PR Hrma, DE Smith, AB Gallegos, MR Telander, and SG Pitman. 2006. *Low Temperature Waste Immobilization Testing*. Pacific Northwest National Laboratory, Richland, Washington.

Sakuragi T, T Nishimura, Y Nasu, H Asano, K Hoshino, and K Iino. 2008. “Immobilization of Radioactive Iodine Using AgI Vitrification Technique for the TRU Wastes Disposal: Evaluation of

Leaching and Surface Properties." In: W Lee, J Roberts, N Hyatt, and R Grimes, Editors.)*Scientific Basis for Nuclear Waste Management.* Materials Research Society, Warrendale, Pennsylvania.

Sazarashi M, Y Ikeda, R Seki, and H oshikawa. 1994. "Adsorption of I- Ions on Minerals for 129I Waste Management." *Journal of Nuclear Science and Technology* 31:620-622.

Sazarashi M, Y Ikeda, R Seki, H Yoshikawa, and Y Takashima. 1995. "Adsorption Behavior of I Ions on Minerals for Geological Disposal of 129I Wastes." In: Material Research Society Symposium Proceedings 353:1037-1043.

Scheele RD, LL Burger, and KD Wiemers. 1984. *Leach Resistance of Iodine Compounds in Portland Cement, Geochemical Behavior of Disposed Radioactive Waste*. American Chemical Society, Washington, D.C.

Scheele RD, CF Wend, WC Buchmiller, AE Kozelisky, and RL Sell. 2002. *Preliminary Evaluation of Spent Silver Mordenite Disposal Forms Resulting from Gaseous Radioiodine Control at Hanford's Waste Treatment Plant*. PNWD-3225, Battelle−Pacific Northwest Division, Richland, Washington.

Siemer DD. 2002. "Hydroceramics, a 'New' Cementitious Waste Form Material for U.S. Defense-Type Reprocessing Waste." *Materials Research Innovations* 6:96-104.

Silsbee MR, M Avila, BA Clark, GA Cooke, MD Guthrie, GL Koci, RJ Lee, LL Lockrem, and KJ Lueck. 2005. "Effluent Treatment Facility Waste Stream Stabilization Testing." Presented at the RemTech 2005 Symposium, Banff, Alberta, October, 19-21, 2005. CH2M Hill, Richland, Washington. Available at: RPP-RPT-27298-FP (Full Paper).

Singh D and AS Wagh. 1998. *Phosphate Bonded Structural Products from High Volume Wastes*. The University of Chicago, Chicago, Illinois.

Singh D, AS Wagh, JC Cunnane, and JL Mayberry. 1997. "Chemically Bonded Phosphate Ceramics for Low-Level Mixed-Waste Stabilization." *Journal of Environmental Science and Health Part A* 32(2):527-541.

Singh D, AS Wagh, and SY Jeong. 2000. *Method for Producing Chemically Bonded Phosphate Ceramics and for Stabilizing Contaminants Encapsulated Therein Utilizing Reducing Agents*. U.S. Patent No. 6,133,498.

Soelberg NR, DW Marshall, SO Bates, and DD Siemer. 2003. *SRS Tank 48 Steam Reforming Proof-of-Concept Test Results*. INEEL/EXT-03-01118, Idaho National Engineering and Environmental Laboratory, Idaho Falls, Idaho.

Speight JG. 2005. *Lange's Handbook of Chemistry*. McGraw Hill, New York.

Spence RD and C Shi. 2005. *Stabilization and Solidification of Radioactive and Mixed Waste*. CRC Press, Boca Raton, Florida.

Sposito G. 1982. "On the Surface Complexation Model of the Oxide-Aqueous Solution Interface." *Journal of Colloid and Interface Science* 91:329-340.

Srdanov VI, WTA Harrison, TE Gier, GD Stucky, A Popitsch, K Gatterer, D Markgraber, and HP Fritzer. 1994. “Structure and Spectroscopy of Sodalite Containing MnO4- Ions.” *Journal of Physical Chemistry* B 98:4673-4676.

Strachan DM. 1978. *Analysis of the Dissolver Silver Reactors from Hanford’s PUREX Plant*. Rockwell Hanford Operations, Richland, Washington.

Strickert RG, AM Friedman, and S Fried. 1980. “The Sorption of Technetium and Iodine Radioisotopes by Various Minerals.” *Nuclear Technology* 49:253-266.

Taylor P. 1990. *A Review of Methods for Immobilizing Iodine-129 Arising from a Nuclear Fuel Cycle Plant, with Emphasis on Waste-Form Chemistry AECL-10163*. Whiteshell Nuclear Research Establishment, Atomic Energy Canada Ltd., Pinawa, Canada.

THOR. 2009. *Report for Treating Hanford Low-Activity Waste and Waste Treatment Plant Secondary Waste Simulants: Pilot Plant Mineralizing Flowsheet*. THOR Treatment Technologies, LLC, RT-21-002, Denver, Colorado.

Uno M, M Shinohara, K Kurosaki, and S Yamanaka. 2001. “Some Properties of a Lead Vanado-Iodoapatite Pb10(VO4)6I2.” *Journal of Nuclear Materials* 294:119-122.

Uno M, A Kosuga, S Masuo, M Imamura, and S Yamanaka. 2004. Thermal and mechanical properties of AgPb9(VO4)6I and AgBa9(VO4)6I. Journal of Alloys and Compounds 384, 300-302.

Vance, E, and D Agrawal. 1982, "X-Ray Studies of Iodine Sorption in Some Silver Zeolites." J Material Science 17:1889-94.

Vandergraff TT, KV Ticknor, and LM George. 1984. “Reactions Between Technetium in Solution and Iron-Containing Minerals under Oxic and Anoxic Conditions.” In: Geochemical Behavior of Disposed Radioactive Waste, American Chemical Society Symposium Series 246:25-43.

Viani B. 1999. *Assessing Materials ("Getters") to Immobilize or Retard the Transport of Technetium Through Engineered Barrier System at the Potential Yucca Mountain Nuclear Waste Repository*, UCRL-ID-133596, Lawrence Livermore National Laboratory, Livermore, California.

Vora V, A Olson, B Mason, B Evans, and K Ryan. 2009. “Steam Reforming Technology Demonstration for Conversion of Hanford LAW Tank Waste and LAW Recycle Waste into a Leach Resistant Alkali Aluminosilicate Waste Form.” Presented at: *Waste Management Conference ’09*, March 1-5, 2009, Phoenix, Arizona.

WAC. 2000a. “Dangerous Waste Characteristics.” WAC 173-303-090. *Washington State Administrative Code*, Olympia, Washington.

WAC. 2000b. “Land Disposal Restrictions.” WAC 173-303-140. *Washington State Administrative Code*, Olympia, Washington.

Wagh AS. 2004. *Chemically Bonded Phosphate Ceramics: Twenty-First Century Materials with Diverse Applications.* Elsevier, Amsterdam, The Netherlands.

Wagh AS and SY Jeong. 2002. *Chemically Bonded Phosphate Ceramics of Trivalent Oxides of Iron and Manganese*. The University of Chicago, Chicago, Illinois.

Wagh AS and SY Jeong. 2004. F*ormation of Chemically Bonded Ceramics with Magnesium Dihydrogen Phosphate Binder*. The University of Chicago, Chicago, Illinois.

Wagh AS, D Singh, and SY Jeong . 1998. *Method of Waste Stabilization via Chemically Bonded Phosphate Ceramics*. The University of Chicago, Chicago, Illinois.

Wagh AS, D Singh, and SY Jeong. 2000. *Mercury Stabilization in Chemically Bonded Phosphate Ceramics*. Argonne National Laboratory, Argonne, Illinois.

Wagh AS, SY Jeong, D Lohan, and A Elizabeth. 2003. *Chemically Bonded Phosphosilicate Ceramics*. The University of Chicago, United States.

Watson JHP, IW Croudace, PAB James, JM Charnock, and D Ellwood. 2001. "Adsorption of Radioactive Metals by Strongly Magnetic Iron Sulfide Nanoparticles Produced by Sulfate-Reducing Bacteria." *Separations Science and Technology* 36:2571-2607.

Wellman DM, SV Mattigod, KE Parker, SM Heald, C Wang, and GE Fryxell. 2006. "Synthesis of Organically Templated Nanoporous Sn(II)/Sn(IV) Phosphate for Radionuclide and Metal Sequestration." *Inorganic Chemistry* 45:2382-2384.

Wharton MJ, B Atkins, JM Charnock, FR Livens, RAD Pattrick, and D Collison. 2000. "An X-ray Absorption Spectroscopy Study of the Coprecipitation of Tc and Re with Mackinawite (FeS)." *Applied Geochemistry* 15:347-354.

Winkler A, H Bruhl, C Trapp, and WD Bock. 1988. "Mobility of Technetium in Various Rocks and Defined Combinations of Natural Minerals." *Radiochimica Acta* 44/45:183-186.

Winters WI. 1980. *Effect of Hot-Pressing Conditions on the Properties of Iodide Sodalite*. RHO-lD-153, Rockwell International Corporation, Energy Systems Group, Richland, Washington.

Yamasaki N, T Kubota, Y Hoshino, and H Tanuma. 1987. *Method for Fixation of Incinerator Ash or Iodine Sorbent.* Mitsui Engineering & Shipbuilding Co., Ltd.

Yang H, R Lu, RT Downs, and G Costin. 2006. "Goethite, α-FeO(OH), from Single-Crystal Data." *Acta Crystallographica Section E* E62:250-252.

Young JF, RJ Kirkpatrick, TO Mason, and A Brough. 1995. *Glass Science Tutorial: Lecture #8, Introduction to Cementitious Systems for Low-Level Waste Immobilization*. Westinghouse Hanford Company, Richland, Washington.

Yousuf M, A Mollah, J Liang, J and DL Cocke. 1998. "Speciation of Silver in Cementitious Environment." *Journal of Hazardous Materials* 63:163-177.

Zachara JM, SM Heald, BH Jeon, RK Kukkadapu, C Liu, C., JP McKinley, A Dohnalkova, and DA Moore. 2007. "Reduction of Pertechnetate [Tc(VII)] by Aqueous Fe(II) and the Nature of Solid Phase Redox Products." *Geochimica et Cosmochimica Acta* 71:2137-2157.

Zhang J and PL Bishop. 2002. "Stabilization/Solidification (S/S) of Mercury-Containing Wastes Using Reactivated Carbon and Portland Cement." *Journal of Hazardous Materials* 92:199-212.

Zhang PC, JK Krumhansl, and PV Brady. 2000. "Boehmite Sorbs Perrhenate and Pertechnetate." *Radiochimica Acta* 88:369-373.

Zhao H, N Awwad, M Glasser, A Hassan, P Zhang, and R Moore. 2002. "Sorption of Technetium by Hydroxyapatite." In: Symposia Papers Presented Before the Division of Environmental Chemistry, April 7-11, Orlando, Florida. American Chemical Society, Washington D.C. 42(1):81-84

Zhuang H, Z Jishu, and Z Lanying. 1988. "Sorption of Radionuclides Technetium and Iodine on Minerals." *Radiochimica Acta* 44/45 143-145.

Zhuang H, JS Zheng, DY Xia, and ZG Zhu. 1995. "Retardation of Technetium and Iodine by Antimony and Mercury-Containing Minerals." *Radiochimica Acta* 68:245-249.

Appendix A

Solution and Solid Phase Analysis Techniques

Appendix A: Solution and Solid Phase Analysis Techniques

A.1 Solution Analysis Instruments

The solution analysis instruments described below are used to analyze solution samples from waste forms to identify their elemental components and measure the concentration of cationic/anionic constituents for either radioactive or nonradioactive ions. Solutions may also arise from the complete dissolution of solids into solution, usually acids. The solid may first be made soluble by fusing with a molten salt, such as KOH, Na_2O_2, lithium metaborate, etc. These salt mixtures are then dissolved in acid and analyzed. The list below is not meant to be exhaustive, but does reflect a comprehensive list of approaches that can be used to conduct solution phase analysis techniques.

Inductively coupled plasma-optical emission spectroscopy/-mass spectroscopy (ICP-OES/ICP-MS). In optical emission spectroscopy, all elements in a solution sample are thermally excited in the core of an inductively coupled plasma at which the temperature can reach up to about 8000°C and give off light at their characteristic wavelengths. The emitted light is collected by the spectrometer, resolved into a spectrum of its constituent wavelengths, and converted to an elemental concentration by comparison with calibration standards. The ICP-OES is sometimes referred to as ICP-AES (atomic emission spectroscopy). In MS, the plasma is also used to generate ions that can be separated, collected according to their mass-to-charge ratios, and analyzed by the mass analyzer. The ICP-OES/-MS instruments are widely used to analyze concentrations of major, minor, and trace cationic constituents in liquid samples. Although the emission spectra have limitations because of inter-element interferences, and the mass spectra has the interference from the common matrix elements, ICP-OES/-MS can analyze many elements (up to about 70) in a single solution sample from major components to very low detection limits (close to sub ppb) with high accuracy and precision.

Atomic absorption (AA) spectroscopy. AA uses the absorption of light to measure the concentration of gas-phase atoms of constituents in solution samples. A flame, graphite furnace, or plasma is used to atomize the constituent in solution. The light transmitted through the atomized gas phase of an element can be measured by a detector and used to convert to the concentration of the cationic element being measured based on the Beer-Lambert law (Axner 2000, pp. 9506–9595).

Ion chromatograph (IC). An IC is used to measure concentrations of major anions and cations in solution sample analysis up to the parts per billion range. Because ionic species are separated differently due to the type and size of species, ionic species can be separated based on their interaction with a column through a pressurized chromatographic column. As an ion extraction liquid (eluent solution) runs through the column, the absorbed ions begin to separate from the column. The retention time of different species determines the ionic concentrations in the sample represented by the height and the breadth of the peaks in analysis.

pH Measurement. The pH measurement is conducted with a meter that measures the voltage difference between a proton-sensitive glass electrode immersed in sample solution and a reference electrode. Through calibration, the potential difference is converted and displayed as the negative log of proton activity in the sample solution.

A.2 Solid Analysis

The solid analysis instruments described below can be used to identify elements, minerals, solid-phase morphology, chemical composition of solid surfaces, and chemical bonding or interaction as well as oxidation states of elements on solids. The list below is not meant to be exhaustive, but does reflect a comprehensive list of approaches that can be used to conduct solid phase analysis techniques.

X-Ray Diffraction (XRD). XRD analysis is a rapid analytical technique used primarily for phase identification of a crystalline solid material. The technique can provide information about unit cell dimensions for the study of crystal structures and atomic spacing. XRD is based on constructive interference of monochromatic X-rays generated by a cathode ray tube with a crystalline sample. The interaction of the incident rays with the sample produces constructive interference (or diffracted rays) when conditions satisfy Bragg's Law (Moore 1997). These diffracted X-rays are detected, processed, and counted by scanning the sample through a range of angles (usually from ~5° to 70°). Conversion of the diffraction peaks to d-spacings allows identification of the mineral because each mineral has a set of unique d-spacings. Based on the XRD patterns and comparison with standard references, identification of minerals associated with the secondary waste forms can be identified, and the average bulk composition of minerals is also determined semi-quantitatively. In addition, a combination of a small-angle X-ray scattering (SAXS) device with XRD can provide more information regarding particle-size distribution and pore-size distribution of the samples.

X-Ray Fluorescence (XRF). XRF is a nondestructive technique that is used to quantify the elemental composition of solid and liquid samples. XRF measures the emission of characteristic "secondary" (or fluorescent) X-rays from a sample as it is being excited by being bombarded with high-energy X-rays or gamma rays. As photon energy (or an electron) is absorbed, the state of the element changes from the ground state (lowest energy state) to an excited state (highest energy state). The excited state of the element can return to normal ground state with the emission of a photon (fluorescence) or an electron in the outer shell of the orbital. Detection of the intensity and energy of the emission that is characteristic of each element can be used for chemical elemental analysis of the secondary waste form. XRF is capable of detecting elements from Al-U in concentrations from a parts-per-million range to 100%. Through the use of appropriate reference standards, XRF can accurately quantify the elemental composition of both solid and liquid samples (Couture 1993). It can analyze areas as small as 30 μm with sampling depths as great as 10 μm. However, no lighter elements than Al can be measured by XRF.

Microscopes. Microscopes fall into one of two classes distinguished by the method of illumination—optical or electron. An optical microscope is a type of microscope using visible light and a system of lenses to magnify images of small samples. Other microscopes, such as scanning electron microscopy (SEM) and transmission electron microscopy (TEM), use a stream of electrons to form images of samples.

SEM rasters across a sample surface using a focused electron beam to provide high-resolution images of the sample surface. TEM and scanning transmission electron microscopy (STEM) are related techniques that use an electron beam to image a sample surface. With SEM, TEM, and STEM microscopes, high-resolution images of surface morphology and particle-size analysis in the solid waste form can be obtained. Analysis of surface morphology can be used to detect cracks or any fractures that may be developed in the waste forms. Both TEM and STEM have better spatial resolution than SEM, though they require significantly more sample preparation time and effort. However, in addition to achieving outstanding image resolution, TEM can also be used to characterize the crystallographic phase and crystallographic orientation when the attached diffraction mode is used. As with XANES, a special attachment to some TEM microscopes can be added that allows one to look at the electron energy loss fine structure to determine the location and identification of the next nearest neighbors.

XANES. XANES is described in a later section within the XAFS part (UM response).

Fourier Transform Infrared Spectroscopy (FTIR). FTIR provides specific information about chemical bonding and molecular structures, making it useful for analyzing organic materials and certain inorganic materials. Because chemical bonds vibrate at characteristic frequencies, a vibrational spectrum is also characteristic of a given sample, and individual peaks may be associated with the presence of particular structural groups within the sample, which can be used to infer the presence of particular phases or molecular groups. Vibrational spectra can be easily obtained for crystalline or amorphous solids, liquids, or gases, and can be easily applied to systems involving elements of low atomic weight. Because a vibrational spectrum is dependent on the inter-atomic forces, temperature, and composition in a particular sample, it is a sensitive probe of the microscopic structure and bonding within the material. When the chemicals are exposed to infrared radiation, they absorb the radiation at frequencies that match their vibration modes. Measuring the radiation absorption as a function of frequency produces a spectrum that can be also used to identify functional groups and compounds.

Raman Spectroscopy (RS). Similar to FTIR, as one of the vibrational spectroscopies, RS also determines the chemical structure of a sample and identifies the compounds present by measuring molecular vibrations. However, the Raman method yields better spatial resolution and enables the analysis of smaller samples. Raman is a good technique for the qualitative analysis of organic and/or inorganic mixed materials and can also be used for semi-quantitative and quantitative analysis. It can be used to identify inorganic compounds both in the bulk and in individual particles, map the distribution of components in a sample through Raman imaging and depth profiling, investigate the presence of different carbon types and their relative proportions, determine inorganic oxides and their valence state, and measure the stress and crystalline structure in secondary waste forms and other materials.

X-Ray Photoelectron Spectroscopy (XPS). XPS is based on the photoelectric effect. When materials are bombarded with X-rays enough to eject electrons from the inner shell, the difference between the incoming photon energy and electron binding energy is converted to the kinetic energy of the escaping photo-electron (Hochella 1988). XPS is a surface-sensitive technique because it is based on the detection of photoelectrons, which have undergone no inelastic collisions and can only happen near the surface. The depth of analysis is therefore typically between 10 and 50 Å. Because every element has a unique atomic structure and the low-energy X-rays used can only excite a few atomic levels from each element, elements can be identified unambiguously in most cases. A wide-energy-range “survey” scan can be used to identify the elements present in the sample, but it is not used for quantification of elemental composition because it lacks resolution; instead, narrow scans are used for this purpose. A chemical shift is defined as the difference in binding energy between a particular line and the binding energy for the same line in a reference compound. By means of chemical shifts, one can distinguish between two different oxidation states of an element in a given sample or between different coordination environments.

Alternatively, XPS can be used for sputter depth profiling of elemental composition to study the alteration or dissolution of mineral (or waste-form) surfaces.

X-Ray Absorption Spectroscopy (XAS). X-ray photon energy is used to eject a photoelectron from the core shell of an atom in the target material at the time of X-ray absorption. X-ray absorption occurs when an X-ray photon travels through matter. The intensity of the incident X-ray photon decreases by passing through the material, and the absorption coefficient is determined by the thickness of the material and the difference of intensities between incident and transmitted X-ray. As the energy of the photon increases, the absorption coefficient generally decreases until the incident energy reaches the threshold energy at which the absorption coefficient arises abruptly. The threshold energy is the minimum energy required to eject an electron from a core shell of the atomic orbital in the material. This sharp increment in the absorption coefficient is attributed to the photoelectron ejection and is referred to as the absorption edge. The absorption coefficient as a function of incident photon energy is used for XAS analysis. The emitted photoelectron by X-ray absorption is partially backscattering with the neighboring atoms before the ejection occurs (Teo 1986). Multiple scattering of ejected photoelectrons is occurring in X-ray absorption near edge structure (XANES), while a single scattering is mainly occurring in extended X-ray absorption fine structure (EXAFS). Both XANES and EXAFS spectroscopies probe only the local environment because of the low energy of photoelectrons. XAS is element selective and can provide molecular local environmental information about the oxidation state, element identity, and bonding (coordination numbers and bonding distance between the central and the nearest neighboring elements). The advantage of XAS is that most elements (except hydrogen in the periodic table) can be studied in any type of phase (crystalline, amorphous solids, liquids, gases, or mineral-water interface), even at low concentration levels (approximately 1 to 10 ppm). XAS is an *in situ* technique that does not need any special sample preparation like drying or vacuum condition for analysis (Brown et al. 1988, Koningsberger and Prins 1988). The disadvantage is that a high intensity X-ray source from the synchrotron radiation facility is required for complicated data collection and analysis. Even though XAS is a short-range order probe (approximately 4 to 6 Å from the absorber) compared to XRD, it provides remarkably unique information about the local structural environment in most materials so that it complements information from other spectroscopic methods to increase our understanding of the binding and leaching mechanisms of contaminants in secondary waste forms.

Gas Adsorption Analysis. Because the contaminant transport or diffusion process through porous materials is closely related to the specific surface area and the pore structure of the material, these physical characteristics of the secondary waste forms should be determined. The specific surface area is the amount of available surface area per unit weight of the solid material and can be measured at liquid nitrogen temperature (approximately 77 K) to allow any N_2 to sorb at the surface of the solid using the N_2-BET method (Brunauer et al. 1938, Gregg and Sing 1982, Webb and Orr 1997). Pore information, including average pore diameter and pore volume (or area) distribution as a function of pore diameter, can be also obtained from the complete adsorption isotherm using the Barret-Joyner-Halenda method (Barrett et al. 1951).

Vertical Scanning Interferometry (VSI). VSI is an optical light technique in which minute changes in surface height can be detected (nanometer range), and the change in height can be correlated with a dissolution rate (Lasaga and Lüttge 2001, Lüttge 2004, Lüttge et al. 1999). Before a dissolution test is run, a small portion of the test material is coated with a waterproof substance that protects the surface from reaction with water. During the test, the non-protected portion of the surface is subjected to dissolution, and the surface dissolves and retreats in height. After the test, the protective material is removed, and the protected area is used as a reference surface to which the height of the dissolved surface is compared. The difference in height is proportional to the dissolution rate. This technique is especially useful for quantifying dissolution rates of insoluble minerals, such as many of the iron oxides. In traditional dissolution tests, the test specimen is placed in a reactor filled with aqueous solution. Aliquots of solution are periodically collected, and the dissolution rate of the specimen is proportional to the concentration of dissolved elements released from the specimen. Because of the slow release of dissolved material to solution, concentrations of elements in solution that would normally quantify dissolution rates are very low, presenting analytical difficulties. However, by analyzing the change in height between the reference and reactive surface using the VSI technique, dissolution rates of sparingly soluble solids in solution can be easily quantified.

X-Ray Micro Tomography (XMT). Different components of a sample lead to different X-ray absorptions, which results in stronger X-ray absorption for a denser element. A visible-light image is generated by a fluorescent screen and then projected by a microscope optic onto a charge-coupled device (CCD) camera. The shadow projections of the object are recorded with a high-resolution CCD-based camera system. After correction and normalization of the projections, the tomograms can be reconstructed for two- and three-dimensional (2D and 3D) images using the filtered back projection technique. The incoming X-ray energy of the synchrotron radiation is also controlled very precisely with the help of a double-crystal monochromater set below and above the absorption edge of an element to be investigated. In the difference of these two measurements, only the distribution of the particular element becomes visible because the absorption of all other elements stays practically constant across the absorption edge (Tricart 2000). The synchrotron-based XMT apparatus achieves spatial resolutions of 3- to 5-μm and can determine attenuation coefficients to about 5% accuracy for single voxels, while the conventional tomography technique has 10- to 200-μm spatial resolution, depending on the size of the specimen and the X-ray source. Because the brightness differences in the reconstructed tomograpy slice are normally a replica of the materials density distribution, chemical compositions can be distinguished by creating image contrast, and they become element specific. Using this behavior can also lead to the development of a 3D elemental distribution in the sample. The 3D images of the internal microstructure of the composites, the spatial physico-chemical characteristics of the composites, and the pore structure characteristics can be also obtained by XMT.

Nuclear Magnetic Resonance (NMR) Spectroscopy. NMR spectroscopy is a powerful technique used to study the static structure and dynamic behavior of condensed phases because it directly examines the properties of a specific element and often offers significant advantages over diffraction methods and vibrational spectroscopy (Kirkpatrick 1988). The nuclei of many elemental isotopes have a characteristic spin, such as integral spin, fractional spin, and zero spin. In the presence of an external magnetic field, two spin states exist in nuclei, +1/2 and -1/2, and the magnetic field causes the spin system to tip with respect to the applied magnetic field. Irradiation of a sample with a radio-frequency energy corresponding exactly to the spin state separation of a specific set of nuclei will cause excitation of those nuclei in the +1/2 state to the higher -1/2 spin state. An NMR spectrum can be acquired by varying or sweeping the magnetic field over a small range while observing the radio-frequency signal from the sample (Stebbins 1988). The coordination information of species, the bonding arrangement, and the diffusion coefficient of hydrogen can be determined using the NMR spectra, including chemical shift, chemical exchange, and nuclear spin relaxation in the secondary waste forms.

Mössbauer Spectroscopy. Mössbauer spectroscopy involves the resonant emission and absorption of gamma radiation by specific atomic nuclei in solids (Hawthorne 1988). Mössbauer spectroscopy is similar to the NMR spectroscopy because nuclear transitions are related to the NMR chemical shift. In Mössbauer spectroscopy, a solid sample is exposed to a beam of gamma radiation, and a detector measures the intensity of the beam transmitted through the sample. The atoms in the source emitting the gamma rays must be of the same isotope as the atoms in the sample absorbing them. A significant fraction of the emitted gamma rays will not lose energy to recoil and thus will have approximately the right energy to be absorbed by the target atoms. In the resulting spectra, the gamma-ray intensity is plotted as a function of the source velocity. At velocities corresponding to the resonant energy levels of the sample, some of the gamma rays are absorbed, resulting in a drop in the measured intensity and a corresponding dip in the spectrum. The number, positions, and intensities of the peaks provide information about the chemical environment of the absorbing nuclei and can be used to characterize the sample. Because of extremely fine energy resolution, Mössbauer spectroscopy can detect even subtle changes in the nuclear environment of the relevant atoms, identify a particular compound in a phase transformation (e.g., the ratio of Fe^{2+} to Fe^{3+}), and provide the crystallite size and grain structure of a material.

A.3 References

Axner O. 2000. “Laser spectrometric techniques in analytical atomic spectrometry.” In: RA Meyers ed., *Encyclopedia of Analytical Chemistry*, John Wiley & Sons, Inc., New York.

Barrett EP, LG Joyner, and PP Halenda. 1951. “The Determination of Pore Volume and Area Distributions in Porous Substances. I. Computations from Nitrogen Isotherms.” *J. Am. Chem. Soc.* 73:373–380.

Brown GE, G Calas, GA Waychunas, J and Petiau. 1988. “X-ray Absorption Spectroscopy and Its Applications in Mineralogy and Geochemistry.” In: Hawthrone, F. C. (Ed.), *Spectroscopic Methods in Mineralogy and Geology*. Mineralogy Society of America, Washington, D. C.

Brunauer S, PH Emmett, and E Teller. 1938. “Adsorption of Gases in Multimolecular Layers.” *Journal of the American Chemical Society* 60:309–319.

Couture RA, MS Smith, and RF Dymek. 1993. “X-ray fluorescence analysis of silicate rocks using fused glass discs and a side-window Rh source tube: accuracy, precision and reproducibility.” *Chemical Geology* 110:315–328.

Gregg SJ and KSW Sing. 1982. “Adsorption, surface area, and porosity.” 2nd edition. Academic Press, Inc., Orlando, Florida.

Hawthornem FC. 1988. “Mossbauer spectroscopy.” In: *Spectroscopic Methods in Mineralogy and Geology* (ed. FC Hawthorne); Reviews in Mineralogy 18:573–637.

Hochella MF, Jr. 1988. “Auger electron and X-ray photoelectron spectroscopies.” In: *Spectroscopic Methods in Mineralogy and Geology* (ed. FC Hawthorne); Reviews in Mineralogy 18:573-637.

Kirkpatrick RJ. 1988. “MAS NMR spectroscopy of minerals and glasses.” In: *Mineral-water Interface Geochemistry* (Edited. FC Hawthorne), Mineralogical Society of America, 18:431–512.

Koningsberger DC and R Prins. 1988. *X-ray Absorption: Principles, Applications, Techniques of EXAFS, SEXAFS, and XANES*. Wiley, New York.

Moore DM and RC Reynolds, Jr. 1997. *X-Ray diffraction and the Identification and Analysis of Clay Minerals*. 2nd Ed. Oxford University Press, New York.

Stebbins JF. 1988. “NMR spectroscopy and dynamic process in mineralogy and geochemistry.” In: *Mineral-water Interface Geochemistry* (Ed. FC Hawthorne), Mineralogical Society of America, 18:431–512.

Teo BK. 1986. “EXAFS: Basic Principles and Data Analysis.” *Inorganic Chemistry Concepts*. Springer-Verlag, New York.

Tricart JP, M Van Geet, and A Sasov. 2000. “Using Micro-CT for 3D characterisation of geological materials.” *Microscopy and Analysis* 65:31.

Webb PA and C Orr. 1997. *Analytical Methods in Fine Particle Technology*. Micromeritics Instrument Corporation, Norcross, Georga.

Distribution

No of Copies	
EXTERNAL	
Kristin A. Colosi	B1-55
Thomas H. May	B1-55
Maxwell Melvin	B1-55
Billie M. Mauss	H6-60

No. of Copies	
INTERNAL	
E. M. Pierce (2)	K3-62
S.V. Mattigod	K3-62
R. J. Serne	K6-81
W. Um	P7-22
N. Qafoku	K8-96
J. Icenhower	K6-81
R. Scheele	P7-25
J. Westsik (10)	K7-15
K. Cantrell	K6-81
K. M. Krupka	K6-81

Pacific Northwest
NATIONAL LABORATORY

U.S. DEPARTMENT OF
ENERGY

902 Battelle Boulevard
P.O. Box 999
Richland, WA 99352
1-888-375-PNNL (7665)
www.pnl.gov